THE JOURNAL
OF
CHEMICAL PHYSICS

VOLUME 16, NUMBER 9 SEPTEMBER, 1948

Contributions to the Theoretical Treatment of Ammonium. I.

J. I. HORVÁTH*
Institute of Physical Chemistry of the Technical College of Budapest, Hungary
(Received December 31, 1946)

In this paper we determine the electron distribution, the binding energy, and the ionic radius of the positive ammonium molecule ion. The general idea of our method is that the molecule is divided by a spherical surface which contains the protons and it is supposed, in our first approximation, that the charge of protons is distributed uniformly on this surface. Now, we we have inside our sphere a nitrogen nucleus, the charge of which is over compensated by ten electrons and so a N^{3-} ion is formed. The whole formation can be regarded from the outside of the sphere as similar to the Na^+ ion, because the charge of the four protons has been added to the charge of the N nucleus. In a second approximation we pay attention to the fact that the protons are not exactly uniformly distributed on the spherical surface but on the points of a tetrahedron. We have taken into consideration the inhomogeneous field of protons by using the perturbation calculation. The ionic radius of our molecule ion is determined as usual in the statistical theory of atoms. Finally, we check our result with a cycle process. We do not use semi-empirical parameters.

IT is interesting that there exist radicals composed of non-metallic atoms which have the same properties as metals. The most common example is ammonium, which forms salts similar to those of alkali metals. It is obvious that the four protons of the radical penetrate the electron cloud of the nitrogen and it may be presumed that the molecule has, in addition to the closed shell of the positive ammonium radical, one s-electron, just as the alkali metals have.

The theoretical treatment of ammonium is an especially interesting problem, because pure ammonium is experimentally unknown. Consequently, its constants have not been established. We cannot ignore the exceedingly remarkable fact that, on the one hand, ammonium (just as alkali metals do) forms an amalgam, which, though sufficiently liable to decay, can be prepared under high pressure and has the same properties as the amalgams of alkali metals; on the other hand, up till now pure ammonium metal has not been produced.

In the first part of our paper we shall determine the electron distribution, binding energy, nitrogen-proton distance, and ionic radius of the positive ammonium ion; in the second part the wave function of the valence electron, ionization energy of ammonium, and the eigenfrequencies of NH_4^+ will be determined.

I.

In the case of the positive ammonium ion, nitrogen is linked with four hydrogens, while one electron is given to the anion. The four protons are on the surface of a sphere, which has a radius R, and the molecule ion has tetrahedral symmetry.

The theoretical treatment of molecules of such type would be possible generally on grounds of

* At present at the Institute of Physics, Med. Faculty, University of Debrecen, Debrecen, Hungary.

an ionic model,[1] supposing that in the center would be a negative ion with a fourfold charge surrounded by four protons. According to this premise, the binding energy would be derived from the Coulomb and polarization energy. For this, however, the polarizability of the ion should be known very exactly. This is possible in the case of the halogen atoms (for this reason the ionic model is a very good start for the discussion of hydrochloric acid), but in the case of higher negative ions the values of polarizability are practically completely unreliable. Now, in the case of ammonium it must be taken into consideration that the center is a negative ion with triple charge which has to bind four protons. This structure could not be explained electrostatically.

We have used Neugebauer's method[2] for our calculation. Neugebauer has calculated the methane molecule with similar assumptions. The general idea of this method is that the molecule is divided by the surface of a sphere, which contains the protons and has a radius R. Furthermore, it is supposed, in the first approximation, that the charge of the protons is distributed uniformly on this surface. Now we have inside our sphere a nitrogen nucleus with a sevenfold charge, which is overcompensated by the ten electrons to a N^{3-} ion. This is surrounded by the four protons, the charge of which is handled in the first approximation as uniformly distributed on the spherical surface. The whole structure can also be regarded, from the outside of the sphere, as similar to the Na^+ ion, because the charge of the four protons has been added to the charge of the nitrogen nucleus. In a second approximation we pay attention to the fact that this assumption is rough and the protons are really on the points of a tetrahedron. We have taken into consideration the inhomogeneous field of the protons in terms of perturbation calculation, where the energy is produced because the inhomogeneous distribution is small enough for the application of this method, as will be shown in the calculation.

This model forms a transition between the ionic and the covalent interpretation of the chemical bond. It approaches the facts very well and points out the indubitably right view that the chemical bond is brought about by the valence electrons, which are on a common energy level. We do not use Slater and Pauling's theory of valence forces,[3] because the relations of stability are given automatically in case of tetrahedral symmetry.

Let $\rho(r)$ be the density distribution of valence electrons which we wish to normalize so that the number of valence electrons may be correctly given far from the nucleus, that is,[4]

$$\int \rho(r)dv = 8, \tag{1}$$

where dv is the element of volume and the integral, now and always, if not otherwise stated, shall be extended over the whole space. As, on the one hand, the maximum of the density distribution of electrons on the level $1s$ is low inside our tetrahedron, so, on the other hand, the valency electrons bring about the chemical bond. Therefore, we regard the charge of the $1s$ electrons as being united with the nucleus. We have, in this way, neglected the effect of two electrons only and the calculation will be much shorter. However, we mention that this approximation is not to be used in the case of a central atom of higher atomic number.

When determining energy terms we take the mutual effects into consideration as follows: the mutual effect among the protons, between the protons and the nitrogen nucleus, between the protons and electrons, between the nucleus and electrons, and, finally, must take into consideration the mutual effect among electrons.

Electrostatically the mutual effect of protons is given, based on a simple geometrical consideration, by

$$E_1 = 3/(R \cdot \sin\alpha/2) \tag{2}$$

where $\alpha = 109°28'$ is the tetrahedron angle.

As we imagine the electrons on the level $1s$ to be united with the nucleus, the repulsion potential of the nucleus is $4(5/R)$. But the elec-

[1] J. H. De Boer, *Electron Emission and Absorption Phenomena* (Cambridge University Press, Teddington, England, 1935), p. 31.

[2] Th. Neugebauer, Zeits. f. Physik **98**, 638 (1936); Mat. Term. Tud. Ért. Budapest **36**, 450 (1937); **57**, 182 (1938).

[3] J. C. Slater, Phys. Rev. **38**, 1109 (1931); L. Pauling, Phys. Rev. **37**, 1185 (1931).

[4] We use Hartree's atomic units. See D. R. Hartree, Proc. Camb. Phil. Soc. **24**, 91 (1927–28).

trons, which are inside our sphere, shield this effect of the nucleus with one attracting term in the form $-(4/R)\int\rho(r)dv$ (where the integral must be extended over the inside of the sphere). Therefore, the mutual effect between the protons and the nucleus as well as between the protons and the electrons inside our sphere is summed up in the following term:

$$E_2=(4/R)\left\{5-\int\rho(r)dv\right\},\quad r\leqq R. \tag{3}$$

The mutual effect between the protons and the electrons outside our sphere is given simply by

$$E_3=-4\int(\rho(r)/r)dv,\quad r\geqq R, \tag{4}$$

where the integral must be extended now outside the sphere.

The energy term, which corresponds to the attracting effect of the nucleus after uniting the $1s$ electrons with the nucleus, is given by

$$E_4=-5\int(\rho(r)/r)dv. \tag{5}$$

The greatest mutual effect between the electrons is that which follows in consequence of electrostatic forces. At a distance $\mathbf{r}$ from the nucleus, the potential energy is plainly $-\int[\rho(\mathbf{r})/|\mathbf{r}-\mathbf{r}'|]dv$. Therefore, the next energy term is

$$E_5=\tfrac{1}{2}\int\int[\rho(\mathbf{r})\rho(\mathbf{r}')/|\mathbf{r}-\mathbf{r}'|]dv'dv. \tag{6}$$

This term contains the mutual effect of each electron on itself, which we do not correct here, but shall take into consideration later.

As a result of Pauli's exclusion principle[5] we must pay attention to Fermi's kinetic zero-point energy, which is

$$E_6=(3/10)(3\pi^2)^{2/3}\int\rho^{5/3}(r)dv. \tag{7}$$

Then we ought to introduce the exchange energies between the electrons with parallel spin and with an antiparallel one. The first is given by[6]

[5] W. Pauli, Zeits. f. Physik **41**, 81 (1927).

[6] P. A. M. Dirac, Proc. Camb. Phil. Soc. **26**, 376 (1930); F. Bloch, Zeits. f. Physik **57**, 545 (1927). Geiger-Scheel, *Handbuch der Physik* (1933), Vol. 24, p. 485. H. Jensen, Zeits. f. Physik **89**, 713 (1934); **93**, 232 (1935); L. Brillouin, J. de phys. et rad. **5**, 185 (1934).

TABLE I. The values of $A(R)$ and $C(R)$.

R	1.5	1.6	1.7	1.8	1.9	2.0
$A(R)$	4.58870	6.78759	9.99601	14.62811	18.93651	29.89032
$C(R)$	1.42999	1.32085	1.21955	1.13909	1.09742	1.04180

$$E_7=-(3/4)(3/\pi)^{1/3}\int\rho^{4/3}(r)dv. \tag{8}$$

This term also contains the mutual effect of electrons on itself. As is shown by the statistical theory of the atoms,[7] this compensates for our former error.

We write the second exchange energy, called by Wigner correlation energy[8] and employed by Gombás[9] in the statistical theory of atoms in the form

$$E_8=-\int[a\rho^{4/3}(r)/(\rho^{1/3}(r)+b)]dv, \tag{9}$$

where $a=0.05647$ and $b=0.1216$.[10]

Finally we pay attention to the polarization energy which has its foundation in the inhomogeneity of the proton tetrahedron. The same thing happens as in the theory of crystals.[11]

We write the formula of polarization energy in the form

$$E_9=-[H_1^2(ss)-|H_1(ss)|^2]/h\bar{\nu}, \tag{10}$$

where in the denominator there is one energy, instead of the usual difference, one mean frequency, which we calculate so that the polarizability should be given correctly. In the numerator the elements of the matrix are given by

$$H_1^2(ss)=\int\psi^*v^2\psi dv, \text{ and} \tag{11}$$

$$H_1(ss)=\int\psi^*v\psi dv, \tag{12}$$

[7] A. Sommerfeld, *Atombau und Spektrallinien, II* (F. Vieweg & Sohn, Braunschweig, 1939), second edition, pp. 700–702.

[8] E. Wigner, Phys. Rev. **46**, 1002 (1934).

[9] P. Gombás, Zeits. f. Physik **121**, 523 (1943).

[10] In connection with the two latter energy terms I have to mention that in this case they mean only a lesser kind of correction and do not considerably influence the place of the minimum of the energy. But in the case of a molecule having a central atom with higher atomic number (e.g., SiH_4, see in Nature (in press)) they are more important factors.

[11] P. Gombás and Th. Neugebauer, Zeits. f. Physik **92**, 375 (1934); Th. Neugebauer, *ibid.* **95**, 717 (1935) and reference[2].

TABLE II. The energy terms and the total energy as a function of R.

R	E_1	$-E_2$	$-E_3$	$-E_4$	E_5	E_6	$-E_7$	$-E_8$	$-E_9$	$-E$
1.6	2.44956	2.57690	4.36332	36.77885	22.28027	11.24672	3.99087	0.35492	0.11477	12.2308
1.6	2.29646	3.15352	3.87304	36.19630	22.07200	10.07200	3.83082	0.35411	0.08664	**12.5788**
1.7	2.14138	3.43661	3.26172	35.08775	21.53023	9.76558	3.70924	0.35402	0.07089	12.4304
1.8	2.04130	3.65737	2.74001	34.13760	20.91274	9.24820	3.57544	0.35391	0.05937	12.3146
1.9	1.93385	4.13677	2.00165	33.61115	20.52973	9.18355	3.53073	0.35202	0.05111	12.0630
2.0	1.83717	4.22810	1.63172	32.86035	20.03026	8.90180	3.42544	0.34824	0.04417	11.7879

where ψ is the wave function of the molecule-ion, v is the perturbation energy which we will now form into a series of Legendre functions in the usual way:

$$v=\sum_{i=1}^{4}v_i=\sum_{i=1}^{4}\{[1/(R^2+r^2-2Rr\cos\vartheta_i)^{\frac{1}{2}}]-(1/R)\}$$
$$=\sum_{i=1}^{4}\sum_{k=1}^{\infty}P_k(\cos\vartheta_i)(r^k/R^{k+1}),\quad r<R,\quad(13)$$

and

$$v=\sum_{i=1}^{4}v_i=\sum_{i=1}^{4}\{[1/(R^2+r^2-2R+\cos\vartheta_i)^{\frac{1}{2}}]-(1/R)\}$$
$$=\sum_{i=1}^{4}\sum_{k=1}^{\infty}P_k(\cos\vartheta_i)(R^k/r^{k+1})$$
$$+\sum_{i=1}^{4}[(1/r)-(1/R)],\quad r>R.\quad(14)$$

In the last term $1/R$ is constant. Consequently, we can now neglect it and as we have supposed, $1/r$ is united with the charge of the nucleus; therefore, we can write (14):

$$v=\sum_{i=1}^{4}\sum_{k=1}^{\infty}P_k(\cos\vartheta_i)(R^k/r^{k+1}),\quad r>R.\quad(15)$$

In our approximation we confine ourselves to the first term.

Equations (2) to (10) give the energy which is necessary to carry the four protons and the eight electrons from our molecule-ion into infinity.

II.

Our calculations are as follows. As wave function we have functions of N^{3-} inside our sphere and the wave functions of Na^+ outside our sphere which we write with the help of Morse, Young, and Haurwitz's formula.[12] They are given by

$$\psi_{N^{3-}}\quad 1s:\ 9.78447\cdot e^{-6.7r},$$
$$2s:\ 1.20799(r\cdot e^{-1.675r}-1.29134\cdot e^{-6.14165r}),$$
$$2p:\ 0.74559\cdot r\cdot e^{-1.28841r}\cdot\begin{cases}\sqrt{2}\cos\vartheta\\ \sin\vartheta\cdot e^{i\varphi}\\ \sin\vartheta\cdot e^{-i\varphi}\end{cases}\quad(16)$$

and

$$\psi_{Na^+}\quad 1s:\ 19.74699\cdot e^{-10.7r},$$
$$2s:\ 6.92899(r\cdot e^{-3.34375r}$$
$$-0.61030\cdot e^{-10.03125r}),$$
$$2p:\ 8.45082\cdot r\cdot e^{-3.39153r}\cdot\begin{cases}\sqrt{2}\cdot\cos\vartheta\\ \sin\vartheta\cdot e^{i\varphi}\\ \sin\vartheta\cdot e^{-i\varphi}\end{cases}\quad(17)$$

where these functions are orthonormalized *per definitionem*.

After neglecting $1s$ electrons we introduce the electron density defined by

$$\rho(r)=\begin{cases}C(R)\{2|\psi_{N^{3-},2s}|^2\\ \qquad+6|\psi_{N^{3-},2p}|^2\},\quad r\leqq R,\\ C(R)A(R)\{2|\psi_{Na^+,2s}|^2\\ \qquad+6|\psi_{Na^+,2p}|^2\},\quad r\geqq R,\end{cases}\quad(18)$$

where the constants $C(R)$ and $A(R)$ are determined so that the wave functions of N^{3-} and Na^+ may be equal at place R and that this may satisfy the conditions (1), consequently

$$2|\psi_{N^{3-},2s}|^2+6|\psi_{N^{3-},2p}|^2$$
$$=A(R)\{2|\psi_{Na^+,2s}|^2+6|\psi_{Na^+,2p}|^2\}\quad(19)$$

and

$$C(R)\Big\{\int_0^R 4\pi r^2[2|\psi_{N^{3-},2s}|^2+6|\psi_{N^{3-},2p}|^2]dr$$
$$+A(R)\int_R^\infty 4\pi r^2[2|\psi_{Na^+,2s}|^2$$
$$+6|\psi_{Na^+,2p}|^2]dr\Big\}=8.\quad(20)$$

[12] P. M. Morse, L. A. Young, and E. S. Haurwitz, Phys. Rev. **48**, 948 (1934).

The derivatives of the wave functions are not equal in the place R, but that does not matter because it is possible to prove that this does not play a part in the calculation of the energy, as the protons deform the electron cloud in the place R independently of this, and this effect reduces our error.

We sum up the values of $A(R)$ and $C(R)$ as functions of R in Table I.

We remark that in case of a central atom which has more than one closed shell, we must normalize the wave functions of different shells separately, as can be understood without any difficulty.

We have calculated the integrals with the help of Simpson's formula[13]

$$\int_a^{a+pw} f(x)dr=(w/3)\{y_0+4y_1+2y_2+\cdots+4y_{p-1}+y_p\}, \quad (21)$$

where p is an even integer number and y_i is the value of this function $y=f(x)$ in the ith point. The error of this approximation is

$$(p\cdot w^2/180)f^{(4)}(\xi), \quad a\leqq\xi\leqq a+pw. \quad (22)$$

It is very difficult to determine the integral (6). By means of one semiclassical argument by Neugebauer[2] we have written this double integral in the form

$$E_5=\tfrac{1}{2}\int_0^\infty\left\{(1/r')\int_0^{r'}4\pi r^2\rho(r)dr+\int_{r'}^\infty 4\pi r^2(\rho(r)/r)dr\right\}4\pi r'^2\rho(r')dr', \quad (23)$$

which can be calculated by a machine without great difficulty.

The appropriate term of the correlation energy has $\rho^{\frac{1}{3}}(r)$ in its denominator. Consequently, the calculation of the integral would be very lengthy, if carried out exactly, but as we shall make no greater mistake than 1 percent if we multiply b also by the normalizing factor, we use this simplification.

In connection with the polarization energy we make the following remark. It is well-known that

$$\sum_{i=1}^4 P_k(\cos\vartheta_i)=0 \quad (24)$$

if $k=1$, 2 and

$$\int_0^\pi\int_0^{2\pi}\left\{\sum_{i=1}^4 P_3(\cos\vartheta_i)\right\}^2\sin\vartheta d\vartheta d\varphi=(2/7)2\pi\{4+12(11/17)\}. \quad (25)$$

Furthermore, the second term vanishes because

$$\int_0^\pi P_k(\cos\vartheta)\sin\vartheta d\vartheta=0 \quad \text{if} \quad k=1, 2, 3. \quad (26)$$

Therefore, the polarization energy is

$$-(1/h\bar{\nu})\cdot(1/7)\{4+12(11/17)\}\times(1/R^8)\int_0^R 4\pi r^2\rho(r)r^6dr, \quad r\leqq R, \quad (27)$$

inside our sphere and

$$-(1/h\bar{\nu})\cdot(1/7)\{4+12(11/17)\}\times R^6\int_R^\infty 4\pi r^2(\rho(r)/r^8)dr, \quad r\geqq R, \quad (28)$$

outside our sphere.

We shall determine the average frequency—at present unknown—by obtaining the known α-polarizability of Na^+ rightly based on the formula

$$\alpha=[2\cdot P^2(ss)/h\bar{\nu}], \quad (29)$$

where

$$P^2(ss)=\int_0^\infty\int_{-1}^{+1}\int_0^{2\pi} r^2\cos^2\vartheta\rho(r)drd(\cos\vartheta)d\varphi. \quad (30)$$

The polarizability of Na^+ can be seen in well-

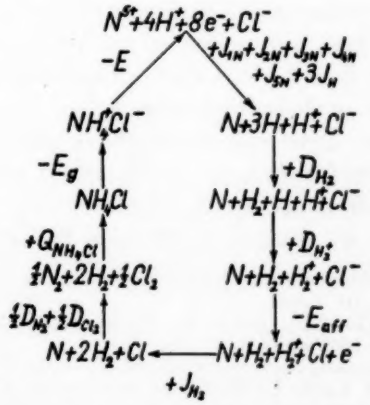

FIG. 1. Cycle for computation of the NH_4^+ energy.

[13] H. Geiger and K. Scheel, *Handbuch der Physik* (Berlin, 1928), Vol. 3, p. 626.

known experimental tables,[14] but in this case we introduce with $h\bar{\nu}$ one semi-empirical constant. We can avoid this by using the theoretical value of Gombás.[15] This value is not very good (agreeing only in magnitude with the experimental value), but can be used because this energy term is only 7 percent of the total energy, and therefore is unimportant.

So we find the total energy as the function of R. Now, based on the "variation principle" we determine its minimum, in this way obtaining the stable state. The value of the energy terms and of the total energy as a function of R is summed up in Table II.

We can see that the minimum is at $R=1.6a_H$, which is 0.845A. The calculated value of energy is $12.56788e^2/a_H=340.34$ ev.

III.

It is not easy to check our result because we have no experimental data. Therefore, we use the following method.

In the statistical theory of the atom the density distribution of electrons does not vanish on the limit of the atom and the ion, but it has there a definite value, which determines also the radius of the ion.[16] In case of a model, which is supplemented by the correlation energy, this value is, according to Gombás,[10]

$$\rho(r_0)=0.003074. \tag{31}$$

In our case this takes place at $3.1a_H$, which is 1.63A. Goldschmidt's crystallographic value[17] of this is 1.43A, so our value is higher by 11.3 percent. This is natural because it is well known that in crystals the ions are very compressed in consequence of electrostatic forces. Therefore, the crystallographic radii are always smaller.

We check our value of the energy with the help of an extended cycle-process of Born and Haber[18] as is shown in Fig. 1.

As we have calculated the energy which is necessary for us to remove the four protons and eight electrons from our molecule ion into infinity, we start with a fivefold ionized nitrogen atom, four protons and eight electrons, and also a chlorine ion. We unit the electrons with the nitrogen atom and three protons, in this way freeing the ionization energy of electrons ($J_{1,N}$, $J_{2,N}$, $J_{3,N}$, $J_{4,N}$, $J_{5,N}$, $3J_H$). We unite two hydrogen atoms into a hydrogen molecule, and in the next step a hydrogen atom and a proton into a hydrogen molecule ion, thus gaining their dissociation energy (D_{H_2}, $D_{H_2^+}$). Now from the negative chlorine ion we take away an electron and add this to the hydrogen molecule ion. For this we must invest the energy E_{aff} corresponding to the electron affinity of chlorine, but this sets free the ionization energy of the hydrogen molecule (J_{H_2}). We change the nitrogen and the chlorine atom into molecules, then we win their dissociation energy (D_{N_2}, D_{Cl_2}). When we unite these molecules into ammonium chloride crystal the heat of formation (Q_{NH_4Cl}) is set free. We supply to the ammonium chloride its lattice energy (E_g) because it dissolves to positive ammonium and negative chlorine ions. Finally we supply ammonium with our calculated energy and are back at our starting point again; we finish our cycle process. The difference with zero is our calculation error.

Our experimental data are as follows: The ionization energies of nitrogen are 14.48, 29.47, 47.40, 72.04, 97.43,[19] $J_H=13.53$,[19] $D_{H_2}=4.72$ (the zero-point energy here is 0.27),[20] $D_{H_2^+}=2.78$ (the zero-point energy is 0.14),[20] $E_{aff}=3.75$,[21] $J_{H_2}=15.235$,[22] $D_{N_2}=11.9$,[23] $D_{Cl_2}=2.46$, $Q_{NH_4Cl}=3.28$,[24] every datum is to be taken in ev.

For the lattice energy of ammonium chloride we have no experimental data. In order to determine this we use the Madelung's formula[25]

$$E_g=545(d/M)^{\frac{1}{3}}, \tag{32}$$

(d is the density of halogene and M is the molecular weight) which is sufficient in case of a crystal of the rock salt type. This data is also written in ev.

In our cycle we must pay attention to the

[14] K. Fajans and G. Joos, Zeits. f. Physik **23**, 1 (1924), $\alpha=0.196\cdot10^{-24}$ cm³.
[15] P. Gombás, Zeits. f. Physik **122**, 497 (1944), $\alpha=0.850\cdot10^{-24}$ cm³.
[16] H. Jensen, Zeits. f. Physik **93**, 232 (1935).
[17] V. M. Goldschmidt, Chem. Berichte **60**, 1263 (1927).
[18] M. Born and C. Landé, Verh. d. D. Phys. Ges. **20**, 210 (1918); F. Haber, *ibid.* **21**, 750 (1919).
[19] I. Náray-Szabó, *Kristálykémia* (Mérnöki Továblképző Intézet, Budapest, 1944).
[20] O. W. Richardson, Proc. Roy. Soc. **152**, 466 (1929).
[21] F. A. Henglein, Zeits. f. anorg. Chemie **123**, 159 (1922).
[22] O. W. Richardson and P. M. Davison, Proc. Roy. Soc. **123**, 466 (1929).
[23] R. T. Birge and H. Sponer, Phys. Rev. **28**, 477 (1926).
[24] V. F. Thomsen, J. prakt. Chem. (2) **21**, 477 (1880).
[25] A. Eucken, *Lehrb. d. phys. Chem.* (Akademische Verlagsgesellschaft M. B. H., Leipzig, 1934), p. 370.

following corrections. The zero-point kinetic energy of nuclei always appears in molecules. Therefore, the calculated dissociation energy has a smaller negative value than the experimental data. In some cases we pay attention to this. In our cycle a positive energy term corresponds to the vibration, which comes from the nine degrees of freedom of our molecule ion. But unfortunately, we have no experimental data for this. This does not cause any great mistake because this error does not exceed 1–2 percent as shown in other molecules.

The energy, which is calculated from our cycle is 423.57 ev, or expressed in atomic units $11.94944e^2/a_H$ while our result was 12.56788 e^2/a_H. The difference is 5.17 percent, which is satisfactory, if we pay attention to the error beyond our control.

THE JOURNAL OF CHEMICAL PHYSICS VOLUME 16, NUMBER 9 SEPTEMBER, 1948

Contributions to the Theoretical Treatment of Ammonium. II.

J. I. Horváth
Institute of Physical Chemistry of the Technical College of Budapest, Hungary
(Received December 31, 1946)

In this second part of our paper we have determined the ionization energy of the ammonium molecule and the eigenfrequencies of the positive ammonium molecule ion. Because we know the electron distribution of the positive radical, we can determine the eigenfunction of the valence electron of ammonium in the same way as is done in cases of alkali metals with larger atomic number. In Section I of Part II we review this method. In Section II we determine the eigenfrequencies of the ammonium molecule ion by Neugebauer's method.

In Part I of this paper[1] we have determined the electron distribution of the positive ammonium ion. The substance of our method was that the molecule is divided by the sphere surface which contains the protons and it is supposed, in our first approximation, that the charge of the protons is distributed uniformly on this surface. Inside our sphere we have a nitrogen nucleus with sevenfold charge, which is overcompensated by the ten electrons and so a N^{3-} ion is formed; outside, as the charge of the protons has been added to the charge of the nucleus, an ion similar to Na^+ comes into existence. In a second approximation we have paid attention to the fact that the protons are not really on the sphere surface but on the points of a tetrahedron. We have taken into consideration the inhomogeneous field of the protons based on perturbation calculation.

In this way we have also determined the binding energy of our molecule ion, the distance between nitrogen nucleus and protons and, finally, its ionic radius. In every case the difference between our result and our check was small enough.

Now we complete our molecule ion with one electron into an ammonium molecule, and later, in Section II, we determine the eigenfrequencies of NH_4^+.

I.

Since, in respect to its chemical properties, the ammonium molecule is quite similar to the alkali metals, we may presume that, in addition to the closed shell of the positive ammonium molecule ion, the ammonium molecule has one *s* electron, just as the alkali metals have. Since the electron distribution of the positive radical is known, we can determine the eigenfunction of the valence electron of ammonium in the same way as in the cases of alkali metals with higher atomic number.

We ought to determine the eigenfunction of the valence electron by solving Schrödinger's equation, but it is well known that it is impos-

[1] From the references of Part I T. Neugebauer's works should be emphasized: Zeits. f. Physik **98**, 638 (1936); Math. Term. Tud. Ért. Budapest **56**, 450 (1937); **57**, 182 (1938).

sible to do this exactly, and so we must use approximate methods. Our method is as follows.

A. The spectrum of the alkali metals (and also the spectrum of ammonium, if a pure ammonium molecule existed at all) is very similar to the spectrum of hydrogen, and it is possible to describe it by changing the quantum state of one electron. The bond of this electron, in comparison with the others, is very weak. Therefore, it is evident that we must pay special attention to it and presume the rest of the electrons to be united with the nucleus to form an ion. By this approximation we reduce our problem to the one-electron problem, but we must take care that the electron is in a central field of forces which originates from the ion.

In our case this is not very difficult because, according to a result of the quantum mechanics, the charge distribution of closed shell has the symmetry of a sphere. Therefore, the potential of the ion has also the symmetry of a sphere, and our Schrödinger equation is separable just as in the case of the hydrogen atom.

Let ψ_i be the wave function of electrons, which are in the closed shell. Introducing the designation $\psi_i v = P_i$, the potential,[2] which comes from the electrons, of distance r from the nucleus is given by

$$v(r) = -(1/r)\int^{r} 4\pi \sum_{i=1}^{8} P_i^2 d\rho - \int_{r}^{\infty} 4\pi (1/\rho) \sum_{i=1}^{8} P_i^2 d\rho. \quad (1)$$

Therefore, the potential of the ion is

$$V(r) = (Z/r) + v(r), \quad (2)$$

where Z is the charge of the nucleus. Let the effective charge of the nucleus be designated by Z^*. Then we can write the total potential of the ion in the form Z^*/r. At great distance from the nucleus the eigenfunction of the electrons in the closed shell can be neglected. Therefore, here the effective charge is equal to the charge of the ion, but at smaller distances, which are just as important for the valence electron, Z^* is a continous function of r. Z^* can be determined *per definitionem* as follows[3]

$$\mathbf{E}(r) = Z^*/r^2 = -\partial V(r)/\partial r = [Z/r^2] - [\partial v(r)/\partial r]. \quad (3)$$

Therefore,

$$Z^* = Z - 4\pi \int_0^r \sum_{i=1}^{8} P_i^2 d\rho. \quad (4)$$

Since we know the distribution of charge, we can give Z^* as function of r.

The value of the energy, determined by the eigenfunction, which is calculated in this way will be smaller than the right value, because we do not take in account the polarizing effect between the valence electron and the electrons of the ion. In our first approximation we can suppose that the electric field of the valence electron is also homogeneous in the ion. Then the corresponding polarization energy is given by

$$(1/2) \cdot \alpha \cdot (1/r^4), \quad (5)$$

where α is the polarizability of our ion.[4] This approximation, especially in our cases, where there is a polarization effect between the valence electron and the protons too, seems to be very rough. In spite of this, for lack of better approximation—which could be calculated without great difficulty—we must use the above one, because, as the applications of Fock's method show, the greater part of this energy is the exchange energy which is due to the mutual effect between the electron cloud and the valence electron. But we remark that, as Gombás and Kónya's result show, it is possible to reach good results also by this approximation.

We must pay attention to Pauli's exclusion principle, as a result of which the valence electron cannot sink to a place which is filled with the electrons of the cloud. In the exact quantum-mechanical discussion this happens by orthonormalization and antisymmetrization of the eigenfunction.

As Gombás[5] does, we conceive Pauli's prin-

[2] Atomic units used were introduced by D. R. Hartree: Proc. Camb. Phil. Soc. **24**, 91 (1927–28).

[3] As with Hartree's method. E.g., it is to be shown by A. Eucken, *Lehrb. d. chem. Physik. I* (Akademische Verlagsgesellschaft, Leipzig, 1938), p. 246.

[4] Remarks regarding polarizability may be seen in Part I. We use now Gombás's value because the error in his result compensated our error to a certain extent.

[5] P. Gombás, Ann. d. Physik (5) **35**, 65 (1939), **36**, 680 (1939), Zeits. f. Physik **116**, 184 (1940); **118**, 164 (1941), Mat. Term. Tud. Ért. Budapest **60**, 373 (1941); P. Gombás and A. Kónya, *ibid.* **61**, 677 (1942).

This energy term in a primitive form quite heuristically

ciple statistically. Let $\rho(r)$ be the density of electrons. Then in one element of volume dv the number of the electrons is $\rho(r)dv$. As a result of Pauli's principle the electrons fill every state up to a maximal energy, which is given by

$$u_{\max}=\tfrac{1}{2}(3\pi^2)^{\frac{1}{3}}\rho^{\frac{1}{3}}=c\cdot\rho^{\frac{1}{3}},\quad c=\tfrac{1}{2}(3\pi^2)^{\frac{1}{3}}. \qquad (6)$$

In our case this means that the electrons of the ion fill every state up to $u_{\max}$ and the valence electron can occupy a state which has larger energy than $u_{\max}$. If the valence electron has this energy *ab ovo*, its place can be found in dv, but when its energy is smaller we must increase it to such an extent that it goes into dv. This added energy may be regarded as corresponding to a repulsion energy, and the electrons of the cloud influence the valence electron, which is only the consequence of Pauli's principle. This cannot be explained by the classical theory.

Let u_0 be the eigenenergy of the valence electron and $\rho_0(r)$ the density of electrons which have smaller value of potential than u_0. In this case we must increase the energy of the valence electron to enable it to take part in the bond of the atom by

$$c(\rho^{\frac{1}{3}}-\rho_0^{\frac{1}{3}}). \qquad (7)$$

The potential of this repulsion force is given by Gombás as

$$-(\rho^{\frac{1}{3}}-\rho_0^{\frac{1}{3}}). \qquad (8)$$

The value of $\rho_0(r)$ is determined by the $s, p, d, \cdots$ states, in which we put our valence electron. In our case the filled states are as follows: $(1s)$,[2] $(2s)$,[2] $(2p)$.[6]

By determining the s states of the valence electron, as in case $l=0$, the lowest state is the $1s$ state; therefore, u_0 is equal to the energy of the $1s$ state. But we have no electrons of lower state. Consequently, $\rho_0(r)\equiv 0$.

In case p $(l=1)$ the lowest level is the state $2p$. Therefore, we must equalize the u_0 to the energy of state $2p$. The $\rho_0(r)$ is the sum of electron density on the level $1s$ and $2s$.

As the NH_4^+ ion has no electrons on the level $d, f, g, \cdots$ these states are unfilled. Consequently, Pauli's principle does not exclude the arrival of a valence electron into this lowest state. Hence our respulsion potential vanishes in this case.

If the eigenfunction which is determined by us would be the exact eigenfunction, this repulsion term would not be acted in our calculation. It is evident that when the exact eigenfunction of the valence electron (which, in consequence of the orthonormalization of the eigenfunctions, has a nodal surface) is to be used, in the term of kinetic energy, the $\Delta\psi$ will be large. In our case, in consequence of the statistical treatment, our eigenfunction gives only an average distribution and the zero place of the eigenfunction dwindles down into the origin. But this does not matter

---

occurs in H. Helmann [Acta Physicochimica U.S.S.R. 1, 913 (1935)], but with the method of Gombás it is easily verifiable by the statistical theory of atoms.

Beside the above-mentioned we may add the following to this. It is well-known that Fermi's kinetic zero-point energy is merely the consequence of Pauli's principle. So Pauli's principle and the orthogonalizing conditions, if the ion possesses a closed electronic shell, can be replaced—with a good approximation—by this change of energy, which may be defined this way.

Let the electronic density of the ion be $\gamma(r)$ and let $\rho(r)$ be—considering the problem quite in general—the density of valency electrons. Supposing that densities are simply superposed, then the changing of the kinetic energy

$$\Delta E=\alpha\int\{(\gamma+\rho)^{5/3}-(\gamma^{5/3}+\rho^{5/3})\}dv,$$

$$\alpha=(3\pi^2/10)(3/\pi)^{2/3}e^2/a_H,$$

where dv is the element of volume. $\gamma(r)$ is a known function and let us consider $\rho(r)$ too a known one, only for a moment.

In order to simplify our calculations let us transform the above expression. Define *that* r_0 radius for which $\gamma(r_0)=\rho(r_0)$. This way space has been divided into two parts: in the first part (v_1) $\gamma(r)>\rho(r)$ and in the other (v_2) $\gamma<\rho$. Now we extend the above expression in terms of power series and neglect the small terms higher in order. Then

$$\Delta E=(5/3)\alpha\int_{v_1}\gamma^{2/3}\rho dv-\alpha\int_{v_1}\rho^{5/3}dv$$

$$+(5/3)\alpha\int_{v}\gamma\rho^{2/3}dv-\alpha\int_{2}\gamma^{5/3}dv.$$

By extending the first integral to the whole volume $(v_1+v_2=v)$ and again substracting the term being added to in this way,

$$\Delta E=(5/3)\alpha\int_{v}\gamma^{2/3}\rho(r)dv-(5/3)\alpha\int_{v_2}\gamma^{2/3}\rho dv$$

$$-\alpha\int_{v_1}\rho^{5/3}dv+(5/3)\alpha\int_{v_2}\gamma\rho^{2/3}dv-\alpha\int_{v_2}\gamma^{5/3}dv.$$

In this expression only the first term plays a considerable part; the others, in comparison with this, are obviously small. This term can be regarded as if the valency electrons were in a field of forces, where the potential is $-(5/3)\alpha\gamma^{2/3}$ in conformity with our Eq. (8).

We have to mention that this method of Gombás, besides giving more than merely the theoretical foundations, contains more than that of Hellmann in the following respect too. Hellmann had disregarded the fact that at different states of the energy of valency electrons different forms of density functions of the closed electronic shells have to be taken into consideration, as we shall describe them above.

[6] A. Kónya, Mat. Term. Tud. Ért. Budapest **60**, 390 (1941); A. Kónya and B. Kozma, Zeits. f. Physik **118**, 153 (1941).

TABLE I. The energy terms as functions of λ.

λ	E_1	E_2	$-E_3$	E_4	$-E$
0.1	0.001	0.00014	0.00607	0.00074	0.00419
0.2	0.004	0.00531	0.04637	0.00989	0.02717
0.3	0.009	0.02664	0.09852	0.02834	**0.03454**
0.4	0.014	0.07212	0.15075	0.05259	0.01004
0.6	0.036	0.24293	0.24321	0.10864	−0.14436
0.8	0.064	0.51038	0.31970	0.16707	−0.42175

because it is very easy to see that this approximation, especially in our case, is very good in the limit of our radical, and p, as Zener[7] has shown, the places of the nodal surface have no great influence on the spectrum of the eigenenergy.

B. In consideration of this we can begin the solution of Schrödinger's equation of the valence electron, which is, in our case,

$$\tfrac{1}{2}\Delta\psi_\sigma+\{E-V(r)\}\psi_\sigma=0, \tag{9}$$

where, by using (4), (5), and (8) we have

$$V(r)=(Z^*/r)-c(\rho^{\frac{1}{3}}-\rho_0^{\frac{1}{3}})+\tfrac{1}{2}\alpha(1/r^4). \tag{10}$$

For our purpose it is convenient to express this equation in the language of a set of polar coordinates r, ϑ, φ, and the equation can evidently be treated by the method of separation of variables if we write the solution in the form

$$\psi_\sigma=R(r)\cdot Y(\vartheta,\varphi). \tag{11}$$

By substituting this result,

$$(r^2/R)\{(d^2R/dr^2)+(2/r)(dR/dr)+2[E-V(r)]R\}$$
$$=-(1/Y)\{(1/\sin\vartheta(\partial/\partial\vartheta)(\sin\vartheta(\partial Y/\partial\vartheta))$$
$$+(1/\sin^2\vartheta)(\partial^2Y/\partial\varphi^2)\}. \tag{12}$$

We make both parts of this equation equal to one constant. Now the exact solution of

$$(1/\sin\vartheta)(\partial/\partial\vartheta)(\sin\vartheta(\partial Y/\partial\vartheta))$$
$$+(1/\sin^2\vartheta)(\partial^2Y/\partial\varphi^2)+\lambda Y=0 \tag{13}$$

can be given, if it is

$$\lambda=l(l+1),\quad l=0,1,\cdots \tag{14}$$

by

$$Y(\vartheta,\varphi)=\{[(l-m)!/(l+m)!][(2l+1)/2]\}^2$$
$$\times P_l^m(\cos\vartheta)e^{im\varphi} \tag{15}$$

where the normalizing factor is determined by the equation

$$\int\psi_\sigma^*\psi_\sigma dv=1, \tag{16}$$

[7] C. Zener, Phys. Rev. (2) **36**, 57 (1930).

respectively, in case of $Y(\vartheta,\varphi)$:

$$\int_0^\pi\int_0^{2\pi}|Y(\vartheta,\varphi)|^2\sin\vartheta d\vartheta d\varphi=1. \tag{17}$$

By using the value λ, we have the equation

$$(d^2R/dr^2)+(2/r)(dR/dr)$$
$$+\{2E-2V(r)+[l(l+1)/r^2]\}R=0 \tag{18}$$

to determine the radial eigenfunction. Formally we can see the term $-\frac{1}{2}[l(l+1)/r^2]$ as a potential[8] and we can write

$$V^*(r)=V(r)-\tfrac{1}{2}[l(l+1)/r^2]. \tag{19}$$

Now we have

$$(d^2R/dr^2)+(2/r)(dR/dr)$$
$$+2\{E-V^*(r)\}R=0 \tag{20}$$

which is similar to that of a one-dimensional problem. Our condition of normalizing is

$$\int_0^\infty r^2R^2dr=1. \tag{21}$$

By using this, because of

$$\int_0^\infty\{(d^2R/dr^2)+(2/r)(dR/dr)\}r^2Rdr$$
$$=-\int_0^\infty r^2(dR/dr)^2dr, \tag{22}$$

the value of energy is given by

$$E=\tfrac{1}{2}\int_0^\infty r^2(dR/dr)^2dr+\int_0^\infty r^2R^2(Z^*/r)dr$$
$$-c\int_0^\infty r^2R^2(\rho^{\frac{1}{3}}-\rho_0^{\frac{1}{3}})dr+\tfrac{1}{2}\alpha\int_0^\infty r^2R^2(1/r^4)dr$$
$$-[l(l+1)/2]\int_0^\infty r^2R^2(1/r^2)dr. \tag{23}$$

Now we write the radial wave function in the form

$$R(r)=A\cdot r^k\cdot e^{-\lambda r}(1+a_1r+a_2r^2+\cdots) \tag{24}$$

and determine the parameters k, λ, a_1, a_2, a_3, $\cdots$ by a variation calculation, with help of the minimum principle. A is a normalizing factor.

[8] In another way this may be found in Kónya's work (see reference 6) too.

When calculating the ψ_σ we must take care that the eigenfunctions of the higher states of valence electrons are orthogonal to the eigenfunctions of its lower states.

C. We want to determine the eigenfunction of the lowest state of the valence electron. Therefore, we can write $R(r)$ in the form

$$R(r)=Ar^k e^{-\lambda r}, \tag{25}$$

where we find

$$A=[(2\lambda)^{2k+3}/\Gamma(2k+3)]^{\frac{1}{2}}. \tag{26}$$

We calculate k as is usual in the case of Slater's method.[9] $k=n^*-1$ where n^* is the effective quantum number which is 3 in our case. If we varied k as well, as the calculations of Gombás[5] and Kónya[6] also show, we should come to an energy value only better by 1–2 percent, which could be neglected in comparison to the other probable errors.

Let us designate the energy terms in (23) in order by E_1, E_2, E_3, E_4, E_5. To avoid the long numerical calculation we approximate the functions Z^* and $\rho^{\frac{1}{2}}$ by

$$B\cdot r^b\cdot e^{-\beta r} \quad \text{and} \quad D\cdot r^d\cdot e^{-\delta r}$$

which, according to Gombás's examination,[10] is satisfactory enough.

In the case of the lowest state it is $\rho_0(r)\equiv 0$. The value of the constants of our approximated functions are

$$\begin{aligned} B&=9.66870, & D&=0.69704,\\ b&=-0.11379, & d&=-0.31531,\\ \beta&=0.45911, & \delta&=0.14512. \end{aligned}$$

Now the energy, as function of λ, is given by Table I. The minimum is at $\lambda=0.3$ and the value of the energy is $0.03454\ e^2/a_H$, which is 0.93966 ev.

A check of our calculation cannot be given because we have no experimental data. We can only remark that the result is very reasonable since the eigenenergy, which is naturally also the ionization energy, is small enough for the instability of ammonium to be understood.

II.

As is well known, the atoms, which compose the molecules, carry out vibration relative to another, and the corresponding lines are in the near ultrared. Since the discovery of Raman's effect, the experimental data proof of these vibrations is obtained easily and with great accuracy, but the theoretical treatment of these vibrations, based on a knowledge of atomic constants, is solved only in cases of some simple molecules. Such a simple case is that of hybrid molecules where the hydrogen atom is simply built. Starting from the ionic model, further simplification is possible because we must pay attention only to the relative place of protons. Kirckwood,[11] Neugebauer,[1] Gombás,[12] Van Vleck,[13] and Dennison[14] have determined the frequencies of the molecules HCl, H_2O, and CH_4.

FIG. 1. A mode of vibration of the NH_4^+ ion.

We further used Neugebauer's method,[1] which was worked out by him in the case of the CH_4 molecule, to determine the frequencies of the positive ammonium molecule ion.

The basis of our treatment is the electron distribution of the ammonium molecule ion, which we have determined in Part I of our paper. In addition to this we must know the binding energy as a function of the $H-N$ distance, which is also given in Part I.

A. The simplest vibration is the totally symmetric eigenvibration by which the protons

FIG. 2. A mode of vibration of the NH_4^+ ion.

[9] J. C. Slater, Phys. Rev. (2) **36**, 57 (1930).
[10] P. Gombás, Zeits. f. Physik **108**, 509 (1938).
[11] J. G. Kirckwood, Physik. Zeits. **33**, 259 (1932).
[12] P. Gombás and T. Neugebauer, Zeits. f. Physik **92**, 357 (1934).
[13] J. H. Van Vleck and R. C. Cross, J. Chem. Phys. **1**, 357 (1935).
[14] D. M. Dennison, Phil. Mag. **1**, 195 (1926).

maintain their tetrahedral symmetry under vibration and only the distance of nitrogen—proton is varied (Fig. 1). The frequency which corresponds to this is given by

$$\nu=(1/2\pi c)(E''/\mu)^{\frac{1}{2}}, \tag{27}$$

where E'' is the second derivate of the energy in respect to R, μ the reduced mass, which is in this case the mass of the four protons, and c is the velocity of light. The result of our calculation is

$$\nu_1=2768\ \text{cm}^{-1}. \tag{28}$$

B. It is more difficult to determine the frequency of the deformation vibration. In the introduction of Part I we mentioned that our method does not contain Slater and Pauling's theory of valence forces. This does not matter in the case of the bond energy owing to the spherical symmetry, but when determining the deformation vibration it is possible that this may cause a great error. In spite of this, as our results show, the calculations are useful also in this approximation.

We shall first determine the frequency brought about by the deformation which occurs when three protons move out of their places on the sphere surface in the direction of the fourth proton (Fig. 2).

The change of the repulsion energy of the protons corresponding to this deformation is as follows

$$E_1=(6/16)\cdot(1/R)\times[(1+\cos^2(\alpha_0/2))/\sin^3(\alpha_0/2)](\Delta\alpha)^2, \tag{29}$$

where now the tetrahedral angle is designated by α_0.

To determine the polarizing energy which is caused by the deformation we proceed as follows: Let ϑ, φ be the angle coordinates of a vector, which has the angles $\alpha_1\alpha_2\alpha_3\alpha_4$ relative to the directions of the tetrahedron, then:

$$\begin{aligned}
\cos\alpha_1&=\cos\beta\cdot\cos\vartheta+\sin\beta\cdot\sin\vartheta\cdot\cos\varphi,\\
\cos\alpha_2&=\cos\beta\cdot\cos\vartheta+\sin\beta\cdot\sin\vartheta\cdot\cos(120^\circ-\varphi),\\
\cos\alpha_3&=\cos\beta\cdot\cos\vartheta+\sin\beta\cdot\sin\vartheta\cdot\cos(240^\circ-\varphi),\\
\cos\alpha_4&=-\cos\vartheta,
\end{aligned} \tag{30}$$

where $\beta=180^\circ-\alpha$. From this it follows that

$$\sum_{i=1}^{4}\cos\alpha_i=\cos\vartheta(3\cos\beta-1), \tag{31}$$

and, therefore, as for a tetrahedron, $\cos\beta=\frac{1}{3}$,

$$\sum_{i=1}^{4}\cos\alpha_i=0. \tag{32}$$

But if the tetrahedron is deformed,

$$\Delta\left(\sum_{i=1}^{4}\cos\alpha_i\right)=-3\cos\vartheta\sin\beta\Delta\beta$$

$$=3\cos\vartheta\sin\beta\Delta\alpha. \tag{33}$$

Because

$$\sin\beta=2\sqrt{2}/3, \tag{34}$$

there follows

$$\int_0^{\pi}\int_0^{2\pi}(3\sin\beta\Delta\alpha)^2\cos^2\vartheta\sin\vartheta d\vartheta d\varphi$$

$$=8(4\pi/3)(\Delta\alpha)^2. \tag{35}$$

When integrating the part which depends on r, we must take into account, as we did in the first part, that the definition of the density inside and outside our sphere is different. By using this,[15]

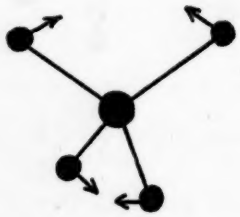

FIG. 3. A mode of vibration of the NH_4^+ ion.

[15] Let us place the series I (13) and (15) into the expressions I (11) and (12), respectively, and let us use polar coordinates. As the distribution of charge has the symmetry of a sphere, on the basis of

$$\int_0^{\pi}P_l(\cos\vartheta)\sin\vartheta d\vartheta=0,\quad \text{if } l\neq 0,$$

the expression I (12) will vanish. By the introduction of the functions $\rho(r)$, defined in (18),

$$H_1^2(ss)=\int_0^{\pi}\int_0^{2\pi}\int_0^{R}\left\{\sum_{i=1}^{4}\sum_{k=1}^{\infty}P_k(\cos\vartheta_i)(r^k/R^{k+1})\right\}^2\times\rho(r)r^2\sin\vartheta d\vartheta d\varphi dr$$

inside our sphere ($r\leqq R$). As we have seen in I (25), in the case of a non-deformed symmetrical tetrahedron the terms containing P_1 and P_2 fall out. But now on the basis of (35) we must take them into consideration. As $\rho(r)$ does not depend on ϑ and φ, we can directly evaluate the integration for this variable as we have done in the case of Eq. (35). And regarding these, Eq. (36) directly follows on the basis of I (10). We obtain Eq. (37) and later the energy terms (56) and (57) in a quite similar way.

$$E_{p1i} = -(8/3)(1/h\bar{\nu})(1/R^4) \times (\Delta\alpha)^2 \int_0^R 4\pi r^2 \rho(r) r^2 dr, \quad r \leqq R \quad (36)$$

is inside our sphere and

$$E_{p1a} = -(8/3)(1/h\bar{\nu})R^2 \times (\Delta\alpha)^2 \int_R^\infty 4\pi r^2 (\rho(r)/r^4) dr, \quad r \geqq R \quad (37)$$

outside our sphere.

To determine the polarizing energy which comes from the second Legendre function, we build the next sum:

$$\sum_{i=1}^{4} P_2(\cos\alpha_i) = \tfrac{3}{2}\{3\cos^2\beta\cos^2\vartheta + \tfrac{3}{2}\sin^2\beta\sin^2\vartheta + \cos^2\vartheta\} - 2 = 0. \quad (38)$$

Therefore,

$$\Delta\left(\sum_{i=1}^{4} P_2(\cos\alpha_i)\right) = \tfrac{3}{2}\{-6\cos\beta\sin\beta\cos^2\vartheta + 3\sin\beta\cos\beta\sin^2\vartheta\}\Delta\beta \quad (39)$$

and because

$$\cos\beta\sin\beta = 2\sqrt{2}/9, \quad (40)$$

$$\Delta\left(\sum_{i=1}^{4} P_2(\cos\alpha_i)\right) = -(\sqrt{2}/3)\{3 - 9\cos^2\vartheta\}\Delta\alpha, \quad (41)$$

and

$$\int_0^\pi \int_0^{2\pi} \left\{\Delta\left(\sum_{i=1}^{4} P_2(\cos\alpha_i)\right)\right\}^2 \sin\vartheta d\vartheta d\varphi = (8/5)4\pi(\Delta\alpha)^2, \quad (42)$$

$$E_{p2i} = -(8/5)(1/h\bar{\nu})(1/R^6) \times (\Delta\alpha)^2 \int_0^R 4\pi r^2 \rho(r) r^4 dr, \quad r \leqq R \quad (43)$$

is inside our sphere and the corresponding one outside our sphere can be neglected.

Dennison called the corresponding infra-red active eigenfrequency ν_3. To determine this we use Eq. (27), where

$$E'' = 0.09023, \quad (44)$$

and the reduced mass is given by

$$1/\mu = (1/3m) + (1/(M+m)\sin\beta), \quad (45)$$

TABLE II. The lines in the region 400–1400 cm^{-1} of same mixtures of NH_4^+.

$H_3C \cdot COO \cdot NH_4$			653	923		1346
$NH_4 \cdot NO_3$						
(liquid)			728	1050		1361
(cryst.)			709	1043		
$(NH_4)_2SO_4$						
(liquid)		454	618	983		
(cryst.)		447	623	974		
$(NH_4)_2S_2O_4$	322	557	836	971	1027	1290
$NH_4 \cdot ClO_4$		462	633	971	1107	1285

where m is the mass of protons and M the mass of nitrogen nucleus. Our result is

$$\nu_3 = 1545 \text{ cm}^{-1}. \quad (46)$$

C. Finally we determine the frequency, which is designated by ν_2. This is a Raman-active line and comes from the deformation, when proton pairs move from their place in the direction of the binding line (Fig. 3).

The change of the repulsion energy of the protons is given now by

$$E_1 = (1/2!)\cdot(1/2R)[(1+\cos^2(\alpha_0/2))/\sin^3(\alpha_0/2)] \cdot \tfrac{1}{4}\{2(2\Delta\beta)^2 + 4(\Delta\beta)^2\}. \quad (47)$$

To determine the polarizing energy following the deformation, we introduce polar coordinates. For the axis we choose a line, the direction of which halves the angle formed by the vibrating pairs. Again we use for this a straight line which has the coordinates ϑ, φ, crosses the origin, and has the angles $\alpha_1\alpha_2\alpha_3\alpha_4$ with the direction of tetrahedron. Then

$$\begin{aligned}
\cos\alpha_1 &= \cos(\alpha/2)\cdot\cos\vartheta + \sin\alpha/2\cdot\sin\vartheta\cdot\cos\varphi,\\
\cos\alpha_2 &= \cos(\alpha/2)\cdot\cos\vartheta + \sin\alpha/2\cdot\sin\vartheta\cdot\cos(\pi+\varphi),\\
\cos\alpha_3 &= \cos(\alpha/2)\cdot\cos(\pi-\vartheta) + \sin(\alpha/2)\cdot\sin(\pi-\vartheta)\cdot\cos(\pi/2+\varphi),\\
\cos\alpha_4 &= \cos(\alpha/2)\cdot\cos(\pi-\vartheta) + \sin(\alpha/2)\cdot\sin(\pi-\vartheta)\cdot\cos(3\cdot\pi/2+\varphi).
\end{aligned} \quad (48)$$

We deform the angle $\alpha/2$ by $\Delta\alpha$ and have

$$\sum_{i=1}^{4} P_2(\cos\alpha_i) = \sum_{i=1}^{4} \cos\alpha_i = 0 \quad (49)$$

and

$$\Delta\left(\sum_{i=1}^{4} \cos\alpha_i\right) = 0. \quad (50)$$

Owing to this deformation the terms corresponding to the first Legendre function play no

role. This must also be so, because this vibration is not infra-red active.

In the case of second Legendre functions it is

$$\sum_{i=1}^{4} P_2(\cos\alpha_i) = \tfrac{3}{2}\{4\cos^2(\alpha/2)\cos^2\vartheta + 2\sin^2(\alpha/2)\sin^2\vartheta\} - 2 = 0, \quad (51)$$

because

$$\sin^2(\alpha/2) = \tfrac{3}{2} \quad (52)$$

and

$$\cos^2(\alpha/2) = \tfrac{1}{3}. \quad (53)$$

Therefore, we have by the deformation

$$\Delta\left(\sum_{i=1}^{4} P_2(\cos\alpha_i)\right) = 2\sqrt{2}\{1 - 3\cos^2\vartheta\}\Delta\alpha, \quad (53)$$

and, finally,

$$\int_0^{\pi}\int_0^{2\pi} \{\Delta(P_2(\cos\alpha_i))\}^2 \sin\vartheta d\vartheta d\varphi = 32\pi(12/16)(\Delta\alpha)^2. \quad (54)$$

Similar to our former case,

$$E_{p_2 i} = -(32/5)(1/h\bar{\nu})(1/R^6) \times (\Delta\alpha)^2 \int_0^R 4\pi r^2 \rho(r) r^2 dr, \quad r \leqq R \quad (55)$$

inside, and

$$E_{p_2 a} = -(32/5)(1/h\bar{\nu})R^4 \times (\Delta\alpha)^2 \int_R^{\infty} 4\pi r^2 (\rho(r)/r^6) dr, \quad r \geqq R \quad (56)$$

outside our sphere. Applying these equations we arrive at

$$1/\mu = (1/2m) + (1/2m), \quad (57)$$

where m is the mass of protons. Therefore, our result is

$$\nu_2 = 741.47 \text{ cm}^{-1}. \quad (58)$$

D. As the infra-red and Raman lines of the pure ammonium molecule ion are not known, we make the control of our results as follows.

According to Neugebauer's calculation we may expect an agreement with the experimental value in magnitude only. Therefore, in Table II we give from Kohlrausch's book,[16] the lines (in the region 400–1400 cm^{-1}) of same mixtures which contain ammonium.

In three cases we find satisfactory agreement and we may suppose that those three lines correspond to the ammonium ion. Taking the mean values of the third and sixth columns, we obtain the lines 650 and 1320 cm^{-1}. Comparing this with our results (58) and (46), respectively, we have only the deviation of 9.85 and 17.24 percent, respectively, which, taking into consideration our approximation, is very good agreement.

To the frequency which is given by Eq. (28), we find a line only in the Raman spectrum of ammonium acetate (2947 cm^{-1}). This would be satisfactory, but we have no proof that this really originates from ammonium.

The fact that the lines given in Table II correspond to the deformation vibration is very easily seen.

Herewith I wish to express my sincere thanks to the Board of Education for granting me a scholarship for research work. Thanks are also due to Professor I. Náray-Szabó and to Privatdocent T. Neugebauer who, by their kind interest and discussions, have done much to help me in my work.

[16] K. W. F. Kohlrausch, *Der Smekal-Raman Effec* (Struktur und eigenschaften der Materie. XII. J. Springer, Berlin, 1931).

THE JOURNAL OF CHEMICAL PHYSICS VOLUME 16, NUMBER 9 SEPTEMBER, 1948

Diamagnetic Susceptibilities of Shared Electrons

TAI-YUAN YANG
Department of Physics, National Yin-ze University, King-Hwa, Chekiang, China
(Received March 3, 1948)

By regarding the two shared electrons of a covalent bond as forming a doubly charged negative ion, and the molecule as consisting of positive and negative ions, one may, in some cases, assign diamagnetic susceptibilities to the constituent parts of the molecule. The values thus found are in good agreement with the experimental results.

1. INTRODUCTION

TO study the structures of covalent compounds by means of their diamagnetism, the author has assumed that the electrons shared by two atoms move in certain orbits under the influence of their centers of force and form an electron group in such a way as to render the atoms sharing these electrons positively charged.

Since, in this paper, the number of shared electrons we study is limited to two, the electron groups thus formed may be represented by a single symbol $\ominus$, and, for convenience, we consider $\ominus$ as an ion with two negative charges.

It is obvious that the assumption stated above gives the covalent idea an extraordinary meaning and we can thus explain the structures of molecules of covalent compounds in the same way as we have done in the case of electrovalent compounds.

Using the above assumption and utilizing the ionic diamagnetic susceptibilities of some kinds of ions obtained by Angus's modification of Slater's method[1] the author has derived the ionic diamagnetic susceptibility of $\ominus$ and calculated the molecular diamagnetic susceptibilities of a large number of compounds. The values thus found are in complete accord with experimental results. And we have, in this way, enlarged the scope of the magnetochemical investigations.

It is noted that the old structural formula for representing the constitution of a molecule together with the assumption stated above leads us to the neutralization of ions in the molecule.

The susceptibilities used are all given relative to the usual standard $\chi_{H_2O} = -7.2$ (throughout this paper the susceptibilities have been multiplied by 10^7).

2. DERIVATION OF DIAMAGNETIC SUSCEPTIBILITY OF $\ominus$ ION

The diamagnetic susceptibility of the $\ominus$ ion has been derived from the molecular diamagnetic susceptibility of water on the assumption that water is a covalent compound; for, according to my assumption made at the beginning of the introduction, this molecule is formed by the neutralization of $2H^{+1}+2\ominus+O^{+2}$ and, from the experimental value of the molecular diamagnetic susceptibility of water -129.6, we have

$$2\chi_{H^{+1}}+2\chi_{\ominus}+\chi_{O^{+2}}=-129.6.$$

Assuming the susceptibility of H^{+1} to be zero and using Angus's value $\chi_{O^{+2}}=-32.1$,[1] we find

$$\chi_{\ominus}=-48.8. \qquad (1)$$

Of course, this is not the only way to obtain this value. The rigorous verifications (direct or indirect) of this value given in various sections not only justify our assumption concerning the structure of water but also lead us to believing that the $\ominus$ ion occurring in whatever molecules possesses the same diamagnetic susceptibilities.

3. STRUCTURES AND DIAMAGNETIC SUSCEPTIBILITIES OF METHANE SERIES

It is generally accepted that the compounds of methane series are covalent compounds. And, according to my structural theory, the first three members of this series may be represented by Fig. 1, (a), (b), and (c), respectively.

Since the proton H^{+1} and its shared ion $\ominus$ may be considered as forming a group i.e., $(\ominus H^{+1})^{-1}$, Fig. 1 may be replaced by Fig. 2 where the

[1] W. R. Angus, Proc. Roy. Soc. **A136**, 569 (1932).

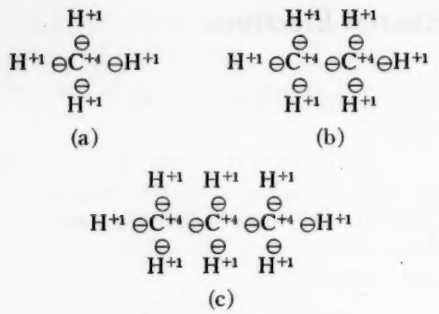

FIG. 1. (a), (b), and (c).

simple symbol G (call G-group) is used instead of $(\ominus H^{+1})^{-1}$.

Now, if we use the symbol M_1* to represent the structure (a) or (a′), and suppose that a proton is removed from it, the remaining part may be represented by M_1^{-1}, but when a G-group is supposed to be removed from (a′) of Fig. 2, the remaining part is represented by M_1^{+1}. From these two symbols M_1^{-1} and M_1^{+1}, the meaning of the general symbols M_n^{-1} and M_n^{+1} for a molecule M_n is obvious.

From Fig. 1, it is seen that when a proton in (a) is replaced by M_1^{+1}, the resulted molecule is (b) and, similarly, when a proton in (b) is replaced by M_1^{+1}, the resulted structure is (c). We have, in this way, obtained the structures of all molecules of methane series (the structures of isomerides are out of consideration).

We are now in a position to study the molecular diamagnetic susceptibilities of this series. Since $\chi_{H^{+1}}=0$, the loss of protons from any molecule does not affect its susceptibility and, according to my structural theory, the following relation holds:

$$\chi_{M_{n+1}}=\chi_{M_n^{-1}}+\chi_{M_1^{+1}}$$

or

$$\chi_{M_{n+1}}=\chi_{M_n}+\chi_{M_1^{+1}}, \qquad (2)$$

since $\chi_{M_n^{-1}}=\chi_{M_n}$. On the other hand, Pascal has shown experimentally that

$$\chi_{M_{n+1}}=\chi_{M_n}-118.6.$$

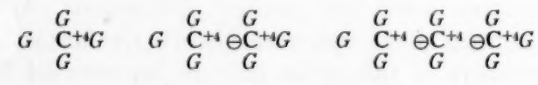

FIG. 2. (a′), (b′), and (c′).

* Similarly, the symbols M_2, M_3, $\cdots$, M_n are used to represent, respectively, the structures of the second, third, $\cdots$, nth molecule of methane series.

Hence we have

$$\chi_{M_1^{+1}}=-118.6. \qquad (3)$$

Using this value as well as the value given in (1), we can calculate the molecular diamagnetic susceptibility of methane as follows:

$$\chi_{M_1}=\chi_{M_1^{+1}}+\chi_G=-(118.6+48.8)=-167.4,$$

on noticing that $\chi_G=\chi_\theta=-48.8$.

By means of this value, we can deduce from (2) the molecular diamagnetic susceptibilities of all molecules of methane series:

Calculated	Observed (Pascal)
$\chi_{M_1}=-167.4$	
$\chi_{M_2}=-286.0$	
$\chi_{M_3}=-404.6$	
$\chi_{M_4}=-523.2$	
$\chi_{M_5}=-641.8$	(4)
$\chi_{M_6}=-760.4$	-764.2
$\chi_{M_7}=-879.0$	
$\chi_{M_8}=-997.6$	-995.5
$\chi_{M_9}=-1116.2$	
$\chi_{M_{10}}=-1234.8$	-1245.0

The agreement between the calculated and the observed values is excellent, and we have, thus, verified both the values $\chi_{M_1^{+1}}=-118.6$ and $\chi_\theta=-48.8$ and the structures of methane series.

It is noticed that all these values are a little lower than those calculated by Pascal. This is due to the fact that the first value $\chi_{M_1}=-167.4$ is a little lower than that calculated by Pascal:

$$\chi_{M_1}=4\chi_H+\chi_C=-(4\times 29.3+60)=-177.2.$$

We shall see later that the calculated values given in (4) will be more agreeable with the experimental results than those calculated by Pascal.

4. STRUCTURES OF ALKYL SULPHIDES $(C_nH_{2n+1})_2S$

In my structural theory, the molecules of alkyl sulphides,

$$CH_3SCH_3, \quad C_2H_5SC_2H_5, \quad C_3H_7SC_3H_7, \quad \cdots,$$

should be formed by the neutralizations, respectively, of

$$2M_1^{-1}+S^{+2}, \quad 2M_2^{-1}+S^{+2}, \quad 2M_3^{-1}+S^{+2}, \quad \cdots,$$

Using the first three values of (4) and Angus's value[1] $\chi_{S^{+2}}=-109.9$, we can calculate the

TABLE I.

Name	Formula	Neutralization of ions	$-\chi_m$	$-\chi_{(NO_2)^{+1}}$
Tetranitromethane	$C(NO_2)_4$	$M_1^{-4*}+4(NO_2)^{+1}$	436.8	67.4
Nitroethane	$C_2H_5NO_2$	$M_2^{-1}+(NO_2)^{+1}$	354.2	68.2
Orthonitrotoluene	$CH_3\cdot C_6H_4\cdot NO_2$	$B^{-2_{1,2}}+M_1^{+1}+(NO_2)^{+1}$	729.6	63.0
Nitrobenzene	$C_6H_5\cdot NO_2$	$B^{-1}+(NO_2)^{+1}$	615.4	67.4
1:3-Dinitrobenzene	$C_6H_4\cdot(NO_2)_2$	$B^{-2_{1,3}}+2(NO_2)^{+1}$	669.0	60.5
1:3:5-Trinitrobenzene	$C_6H_3\cdot(NO_2)_3$	$B^{-3_{1,3,5}}+3(NO_2)^{+1}$	750.7	67.6

* The methane molecule after losing its four protons.

molecular diamagnetic susceptibilities of these molecules:

Calculated	Observed (Pascal)
$\chi_1=-(2\times167.4+109.9)=-444.7$	-449.3
$\chi_2=-(2\times286.0+109.9)=-681.9$	-678.7
$\chi_3=-(2\times404.6+109.9)=-919.1$	-917.8

The agreement between the calculated and the observed values is surprisingly good. We have thus, on the one hand, verified the values -167.4, -286.0, -404.6 and the structures of alkyl sulphides on the other. It should be noted that we have, in this way, verified indirectly the values (1) and (3) from which the calculated values (4) have been obtained.

5. DERIVATION OF MAGNETIC SUSCEPTIBILITY OF NITRO-GROUP (NO_2)

The aim of the derivation is to show that the calculated values given in (4) are extremely consistent with the molecular diamagnetic susceptibility of benzene -548, the mean value obtained from the values observed by different workers.

Before doing so, let us give a short account of the structure of benzene. If we assume its structure to be represented by Fig. 3** and use the symbol B to designate it, then when a proton

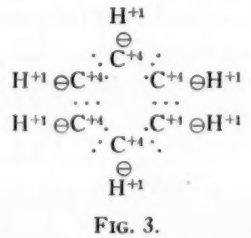

FIG. 3.

H^{+1} is removed from B, the structure of the remaining part may be represented by B^{-1}. On the other hand, when a G-group is supposed to be removed from it, the remaining structure is represented by B^{+1}. But when more than one proton or G-group is removed from B, a more complicated symbol for representing the structure of the remaining part is needed. Let us suppose 3 protons or 3 G-groups in the position 1, 3, 5 to be removed from B, the symbol for representing the remaining structure, in the first case, is $B^{-3_{1,3,5}}$ and, in the second, $B^{+3_{1,3,5}}$. The meaning of the other symbols such as $B^{-2_{1,2}}$, $B^{-3_{1,2,4}}$, etc., is evident. Knowing this, one will meet no difficulty in studying the neutralizations of ions in the molecules of benzene derivatives. Since the mean value of the molecular diamagnetic susceptibility of benzene is $\chi_B=-548$ and since the loss of protons from B does not affect its diamagnetic susceptibility, we have $\chi_{B^{-n}}=-548$, where n denoting the number of protons lost.

To derive the magnetic susceptibility of the group (NO_2), let us consider the structures of molecules contained in the first column of Table I. If we assume the group to be singly positively charged, i.e., $(NO_2)^{+1}$ (here the question whether the atoms in the group are in covalent combination or in electrovalent combination is out of consideration), the neutralizations of the ions in these molecules should be such as shown in the third column. The fourth column gives the molecular diamagnetic susceptibilities observed by Pascal; while in the last column are contained the derived values of $\chi_{(NO_2)^{+1}}$. The derivations are easily carried out and need no illustrations.

The close agreement among the derived values indicates that the calculated values given in (4) are consistent with the observed value $\chi_B=-548$. The results also show that our assumption that the group (NO_2) is singly positively charged is

** The structure was obtained from Thomson's formula for benzene and, in this paper, the three-electron groups existing between the carbon atoms do not enter into consideration.

TABLE II.

Name	Formula	Neutralization of ions	Calculated	Experimental
Phenol	C_6H_5OH	$B^{+1}+(OH)^{-1}$	611.7	610.0
Resorcinol	$C_6H_4(OH)_2$	$B^{+2_{1,3}}+2(OH)^{-1}$	675.4	672.0
Phloroglucinol	$C_6H_3(OH)_3$	$B^{+3_{1,3,5}}+3(OH)^{-1}$	739.1	733.4
Anisole	$C_6H_5\cdot O\cdot CH_3$	$B^{+1}+(O^{-2}M_1^{+1})^{-1}$	719.5	726.0
Phenetole	$C_6H_5O\cdot C_2H_5$	$B^{+1}+(O^{-2}M_2^{+1})^{-1}$	838.1	844.8
Guaiacol	$C_6H_4(OH)(OCH_3)$	$B^{+2}+(O^{-2}M_1^{+1})^{-1}+(OH)^{-1}$	783.2	791.0
Paranitrophenol	$C_6H_4(OH)(NO_2)$	$B^{+2_{1,4}}+(\ominus NO_2)^{-1}+(OH)^{-1}$	677.4	670.0
2:4-Dinitrophenol	$C_6H_3(OH)(NO_2)_2$	$B^{-3_{1,2,4}}+2(\ominus NO_2)^{-1}+(OH)^{-1}$	743.1	731.5

justifiable. From these derived values, we find the mean value:

$$\chi_{(NO_2)^{+1}} = -65.7. \qquad (5)$$

This value will be used in the next section.

6. MOLECULES CONTAINING NEGATIVELY CHARGED OXYGEN ATOMS VERIFICATION OF ANGUS'S VALUE $\chi_{O^{-2}} = -112.5$

We have seen that the oxygen atom in a water molecule is positively charged. We are now going to prove that the oxygen atoms in some kinds of molecules such as those contained in the first column of Table II are negatively charged. The procedure is to assume the oxygen atoms*** in these molecules to be doubly negatively charged i.e., O^{-2} and, then, to give O^{-2} a susceptibility -112.5 obtained theoretically by Angus[1] in evaluating the molecular diamagnetic susceptibilities of these molecules. The old structural formulas give us the neutralizations of ions as shown in the third column. The forth and the last column contain the calculated and the experimental (Pascal) values of the molecular diamagnetic susceptibilities.

To arrive at the calculated values, one should take notice of the following points:

(1) No attention has been directed to the question of isomerides.

(2) Since $\chi_B = -548$, we have

$$\begin{aligned} \chi_{B^{+1}} &= \chi_B - \chi_G = -(548-48.8) = -499.2, \\ \chi_{B^{+2}} &= \chi_B - 2\chi_G = -(548-2\times 48.8) = -450.4, \\ \chi_{B^{+3}} &= \chi_B - 3\chi_G = -(548-3\times 48.8) = -401.6. \end{aligned} \qquad (6)$$

(3) When M_1^{+1} or M_2^{+1} combines with O^{-2}, their diamagnetic susceptibilities are respectively (see sections 8 and 9)

$$\chi_{M_1^{+1}} = -107.8$$

and

$$\chi_{M_2^{+1}} = -(107.8+118.6) = -226.4.$$

(4) $(\ominus NO_2)^{-1}$ represents the combination of $\ominus$ and $(NO_2)^{+1}$, and its susceptibility is therefore

$$\chi_{(\ominus NO_2)^{-1}} = -(48.8+65.7) = -114.5.$$

The agreement between the calculated and the experimental values is extremely close. We have thus confirmed our assumption that the oxygen atoms in these molecules are doubly negatively charged. Finally, it should be noted that Angus's value $\chi_{O^{-2}} = -112.5$ can be verified here only by assuming the value $\chi_\theta = -48.8$ to be true.

7. DERIVATION OF MAGNETIC SUSCEPTIBILITY OF CARBONYL GROUP (CO) AND STRUCTURES OF AMIDES

The susceptibility of the group (CO) can be derived from the molecular diamagnetic susceptibilities of ketones and aldehydes contained in the first column of Table III on the assumption that the group is doubly positively charged, i.e., $(CO)^{+2}$ (here the question whether the atoms in the group are in covalent combination or in electrovalent combination is out of consideration). It will be seen that the derivation is based on the value given in (1) and the calculated values given in (4). The neutralizations of ions in ketones and aldehydes should be such as indicated in the third column of Table III. The fourth column gives the molecular diamagnetic susceptibilities observed by Pascal and the last column, the derived values of $\chi_{(CO)^{+2}}$. The method of arriving at the derived values may be illustrated by acetone. Since the neutralization of this molecule is $M_1^{-1}+(CO)^{+2}+M_1^{-1}$, using the first value of (4) we find

$$\chi_{(CO)^{+2}} = -(337-2\times 167.4) = -2.2.$$

The other derived values may be found in a similar way remembering that $\chi_{M_n^{-1}} = \chi_{M_n}$.

The constancy of the derived values shows that the value (1) is consistent with the cal-

*** Except those contained in the nitro-group (NO_2).

TABLE III.

Name	Formula	Neutralization of ions	$-\chi_m$	$-\chi_{(CO)^{+2}}$
Acetone	$CH_3 \cdot CO \cdot CH_3$	$M_1^{-1}+(CO)^{+2}+M_1^{-1}$	337.0	2.2
Methylethylketone	$CH_3 \cdot CO \cdot C_2H_5$	$M_1^{-1}+(CO)^{+2}+M_2^{-1}$	456.0	2.6
Methylpropylketone	$CH_3 \cdot CO \cdot C_3H_7$	$M_1^{-1}+(CO)^{+2}+M_3^{-1}$	575.0	3.0
Methylbutylketone	$CH_3 \cdot CO \cdot C_4H_9$	$M_1^{-1}+(CO)^{+2}+M_4^{-1}$	691.2	0.6
Methylhexylketone	$CH_3 \cdot CO \cdot C_6H_{13}$	$M_1^{-1}+(CO)^{+2}+M_6^{-1}$	933.0	5.2
Acetaldehyde	$CH_3 \cdot CHO$	$M_1^{-1}+(CO)^{+2}+G$	220.8	4.6
Propionaldehyde	$C_2H_5 \cdot CHO$	$M_2^{-1}+(CO)^{+2}+G$	339.8	5.0
Butyraldehyde	$C_3H_7 \cdot CHO$	$M_3^{-1}+(CO)^{+2}+G$	457.9	4.5
Heptaldehyde	$C_6H_{13} \cdot CHO$	$M_6^{-1}+(CO)^{+2}+G$	815.0	5.8

culated values (4) and this implies that the value (3) $\chi_{M_1^{+1}} = -118.6$ is accurate. From the derived values we find the mean value:

$$\chi_{(CO)^{+2}} = -3.7. \quad (7)$$

This value will be used in the calculations of molecular diamagnetic susceptibilities of amides. For doing so, we shall, first of all, consider the structure of the group $(CONH_2)$. Since ammonia is generally accepted as a covalent compound, the neutralization of ions in NH_3 should be $N^{+3}+3\ominus+3H^{+1}$. Using Angus's value $\chi_{N^{+3}} = -20.9$,[1] we find for the molecular diamagnetic susceptibility of NH_3,

$$\chi_{NH_3} = \chi_{N^{+3}}+3\chi_\theta+3\chi_{H^{+1}} = -(20.9+3\times 48.8) = -167.3. \quad (8)$$

This is in good agreement with the experimental result -170.5 (Gray). If we now assume the group $(CONH_2)$ to be a combination of the ions $(CO)^{+2}+(N^{+3}+3\ominus+2H^{+1})^{-1}$ or simply $(CO)^{+2}+(NH_2)^{-1}$ and represent it by the symbol $(CONH_2)^{+1}$, then its diamagnetic susceptibility may be found from (7) and (8),

$$\chi_i = \chi_{(CO)^{+2}}+\chi_{(NH_2)^{-1}} = -(3.7+167.3) = -171.0 \quad (9)$$

since $\chi_{(NH_2)^{-1}} = \chi_{NH_3}$.

This value will be used in the calculations of molecular diamagnetic susceptibilities of amides. From the old structural formulas for the molecules contained in the second column of Table IV, we can immediately obtain the neutralizations of ions shown in the third column. Since the calculations of the molecular diamagnetic susceptibilities of all these molecules except dimethyloxamide are easily carried out, only the method for obtaining the susceptibility of this molecule is necessary to give here. When one of the two protons in the $(CONH_2)^{+1}$ group is replaced by M_1^{+1}, the diamagnetic susceptibility of the resulted group $(CONHCH_3)^{+1}$ should be

$$\chi_i = \chi_{(CONH_2)^{+1}}-\chi_{H^{+1}}+\chi_{M_1^{+1}} = -(171+118.6) = -289.6$$

and from this follows immediately the molecular diamagnetic susceptibility of dimethyloxamide:

$$\chi_m = \chi_\theta+2\chi_i = -(48.8+2\times 289.6) = -628.0.$$

The excellent agreement between the calculated and the experimental (Pascal) values given in the fourth and the last column affords verification of the value (9) on the one hand and confirmation of the structures of amides on the other.

8. DERIVATION OF MAGNETIC SUSCEPTIBILITY OF $(CH_2OH)_2$ GROUP

This can be done by considering the structures of the molecules shown in the second column of

TABLE IV.

Name	Formula	Neutralization of ions	$-\chi_m$ Calculated	$-\chi_m$ Experimental
Formamide	$H \cdot CONH_2$	$G+(CONH_2)^{+1}$	219.8	218.9
Acetamide	$CH_3 \cdot CONH_2$	$M_1^{-1}+(CONH_2)^{+1}$	338.4	340.8
Benzamide	$C_6H_5 \cdot CONH_2$	$B^{-1}+(CONH_2)^{+1}$	719.0	723.0
Oxamide	$CONH_2CONH_2$	$\ominus+2(CONH_2)^{+1}$	390.8	389.8
Phthalamide	$C_6H_4(CONH_2)_2$	$B^{-2}+2(CONH_2)^{+1}$	890.0	913.0
Dimethyloxamide	$COHCH_3 \cdot COHCH_3$	$\ominus+2[(CO)^{+2}(NHCH_3)^{-1}]^{+1}$	628.0	630.7
Urea	$NH_2 \cdot CONH_2$	$(NH_2)^{-1}+(CONH_2)^{+1}$	338.3	336.0

TABLE V.

Name	Formula	Neutralization of ions	$-\chi_m$	$-\chi_{(CH_2OH)^{+1}}$
Methyl alcohol	$H\cdot CH_2OH$	$G+(CH_2OH)^{+1}$	218.9	170.1
Ethyl alcohol	CH_3CH_2OH	$M_1^{-1}+(CH_2OH)^{+1}$	342.7	175.3
n-Propyl alcohol	$C_2H_5CH_2OH$	$M_2^{-1}+(CH_2OH)^{+1}$	459.8	173.8
n-Octyl alcohol	$C_7H_{15}CH_2OH$	$M_7^{-1}+(CH_2OH)^{+1}$	1048.3	169.3
Glycol	$CH_2OH\cdot CH_2OH$	$\ominus+2(CH_2OH)^{+1}$	386.9	169.1

Table V. In my structural theory the group should be a combination of the ions $C^{+4}+2\ominus+2H^{+1}+(O^{-2}+H^{+1})^{-1}$ and consequently may be represented by $(CH_2OH)^{+1}$ and the molecules may, therefore, be formed by the neutralizations of ions shown in the third column. The fourth column gives the molecular diamagnetic susceptibilities observed by Pascal, and the last column, the derived values of $\chi_{(CH_2OH)^{+1}}$.

The derivations are easily carried out and need no illustrations. The mean value of the derived values is

$$\chi_{(CH_2OH)^{+1}}=-171.5. \qquad (10)$$

The close agreement among the derived values shows that the value (1) and the calculated values (4) are consistent. We shall see that the value (10) is exact and can be used to explain some observed facts by assuming that the value $\chi_{O^{-2}}=-112.5$ is true.

We know that the molecular diamagnetic susceptibility of methyl alcohol can be calculated by the relation:

$$\chi_m=\chi_G+\chi_{(CH_2OH)^{+1}}=-(48.8+171.5)=-220.3. \qquad (11)$$

But, if we consider the neutralization of ions in this molecule as $(CH_3)^{+1}+(OH)^{-1}$ or $M_1^{+1}+(OH)^{-1}$, we have

$$\chi_{M_1^{+1}}+\chi_{(OH)^{-1}}=-220.3$$

and

$$\chi_{M_1^{+1}}=-107.8 \qquad (12)$$

since $\chi_{(OH)^{-1}}=-112.5$. This shows that when M_1^{+1} combines with $(OH)^{-1}$, its diamagnetic susceptibility changes from -118.6 to 107.8, i.e., decreases by -10.8. This result is extremely remarkable and accords completely with experimental results which we shall describe in the next section.

Besides, we have seen in this derivation that if we write $C_nH_{2n+1}\cdot CH_2OH$ as the general formula for alcohols, then when the series is ascended from methyl alcohol, the increment of diamagnetic susceptibility for every member of this series may be considered the same, i.e., -118.6.

9. PARAMAGNETIC PROPERTY OF CARBON ION C^{+4}

In the preceding sections we have obtained the following results:

$$\chi_{M_1^{+1}}=-118.6, \quad \chi_{(CH_2OH)^{+1}}=-171.5.$$

Since these results can be considered as firmly established and the values $\chi_G=\chi_\theta=-48.8$ and $\chi_{O^{-2}}=-112.5$ have been well verified, we can from them derive the ionic susceptibility of the carbon ion C^{+4}. Thus from

$$\chi_{M_1^{+1}}=\chi_{C^{+4}}+3\chi_G=-118.6$$

and

$$\chi_{(CH_2OH)^{+1}}=\chi_{C^{+4}}+2\chi_G+\chi_{(OH)^{-1}}=-171.5$$

we find

$$\chi_{C_1^{+4}}=+27.8 \quad \text{and} \quad \chi_{C_2^{+4}}=+38.6, \qquad (13)$$

where C_1^{+4} and C_2^{+4} denote the carbon ion C^{+4} in M_1^{+1} and $(CH_2OH)^{+1}$, respectively. We are thus led to the natural conclusion that the carbon ions C^{+4} possess paramagnetic properties and their paramagnetic susceptibilities are different as they are in different types of molecules.

To interpret these facts, the author assumes that the two electrons contained in the *K*-shell of C^{+4} can exist in different excited states in which their resultant magnetic moment does not vanish, and the different paramagnetic susceptibilities of C^{+4} correspond respectively to these different excited states, and that in cases where the two electrons return to normal state the ion becomes diamagnetic; it is only in these cases that the formula for evaluating the ionic diamagnetic susceptibilities is applicable.

Now the question arises: if a carbon ion C^{+4} could exist in a series of excited states, what would be the corresponding paramagnetic susceptibilities? To solve this question completely, a paramagnetic theory for the positive ions of this sort is needed. It is sure that the values given in (13) are two of these corresponding paramagnetic susceptibilities. For the present, our important task is to investigate whether the results given in (13) can be in conformity with some other observed facts. We shall show that we have such cases.

Angus and Hill[2] in their systematic investigation on the diamagnetic susceptibilities of the (CH_2) group and isomerides showed that the diamagnetic increment for the conversion of an acid into its methyl ester was -107. This result may be considered completely the same as I have found at the end of the last section and can be fully explained as follows: When the proton in the group (COOH) is replaced by M_1^{+1}, the carbon ion C^{+4} in M_1^{+1} changes its excited state, in other words, jumps from a lower state defined by the paramagnetic susceptibility $+27.8$ to a higher state defined by the paramagnetic susceptibility $+38.6$, and the increase of paramagnetic susceptibility from $+27.8$ to $+38.6$ of C^{+4} in M_1^{+1} when touching to O^{-2} causes the decrease of diamagnetic susceptibility of M_1^{+1} from -118.6 to -107.8 as indicated at the end of the last section.

They also noted that for esters the value of χ_{CH_2} was the same irrespective of whether the series is ascended through R or R′ in RCOOR′. This fact together with what we have described at the end of the last section suggest that when M_n^{+1} combines with O^{-2}, among the n positive carbon ions C^{+4} in M_n^{+1}, only the one which touches it directly changes its paramagnetic state from $+27.8$ to $+38.6$.

This is an important remark which can be used to explain the difficulty described by Angus and Hill.[2] Putting $n=0$ in the general formula $(CH_2)_nHOH$ for alcohols to obtain the final member of this series, the relation $\chi_m=n\chi_{CH_2}+b$ becomes $\chi_m=\chi_{HOH}=-95$. This value is considerably different from the value -129.6 for water.

It seems to me that this difficulty can be explained perfectly by the remark just mentioned. If we write $C_nH_{2n+1}\cdot OH$ as the general formula for alcohols, the neutralization of ions in each molecule of this series is $M_n^{+1}+(OH)^{-1}$, and among the n ions C^{+4} in M_n^{+1} only the one which touches the group $(OH)^{-1}$ directly possesses a paramagnetic susceptibility $+38.6$. This tells us that the relation $\chi_m=n\chi_{CH_2}+b$ should be replaced by

$$\chi_m=(n-1)\chi_{CH_2}-107.8+b. \qquad (14)$$

Putting $n=0$, we have

$$b=\chi_{HOH}+\chi_{CH_2}+107.8. \qquad (15)$$

The value of b defined in this way would represent the molecular diamagnetic susceptibility of water and would be equal to -112.5 if water were an electrovalent compound. But, as we have seen water is necessarily a covalent compound, it is therefore, still unreasonable to expect the value b even obtained from (15) to be agreeable with the value -129.6 for water.

It is a pleasure to express my appreciation and indebtedness to Professor W. R. Angus, for his helpful criticisms, and to Professor S. Wen for his invaluable help and kind interest during the preparation of this work.

[2] Angus and Hill, Trans. Faraday Soc. **39**, 185 (1943).

THE JOURNAL OF CHEMICAL PHYSICS VOLUME 16, NUMBER 9 SEPTEMBER, 1948

Note on an Equation of State for Linear Macromolecules in Monolayers*

S. J. SINGER**
Gates and Crellin Laboratories, California Institute of Technology, Pasadena, California
(Received April 15, 1948)

An equation of state for monolayers of large threadlike molecules based on the highly idealized quasi-lattice model is presented, and applied with fair success to the small number of experimental data available. Although protein molecules in monolayers may be highly organized structures, the theory can be applied to them at moderate film pressures without requiring unreasonable values for their molecular parameters. By analogy with the three-dimensional case, the theory requires improvement in order to apply to the low pressure regions, where experimental differences between protein and polymer films should become more marked.

IN recent years considerable interest has centered about the experimental study of monomolecular films of large molecules. The structure of cellulose and its derivatives,[1] and of synthetic high polymers[2–4] have been investigated by this technique. A greater number of papers have been published dealing with monolayers of protein molecules, in the determination of their size and structure[5–7] and in the nature of their reactions.[8] In this paper we will present an equation of state for macromolecular monolayers derived on the basis of a highly idealized model, which should have significance for the films of synthetic polymers, but whose application to those of proteins is rendered uncertain by the nature of the model.

The investigations cited show that in true monomolecular films, polymer and protein molecules alike lie flat and unfolded at the interphase. It is interesting that films of both polymers and proteins are highly compressible, and exhibit comparable force-area relations, though in three-dimensional solution the protein is generally much more rigid and compact than the polymer molecule. However, while the latter might be expected to exist as a more or less randomly coiled thread on the surface, loosely anchored to the aqueous substrate by polar groups distributed along the thread, the protein molecule may unfold into a more or less well knit sheet on the surface, retaining a considerable degree of internal hydrogen bonding. If this is so, application of this random-coil theory to protein films becomes ambiguous. Nevertheless, as will be shown below, upon comparing theory with experiment for protein films, no startling discrepancies arise.

Our model of the surface at the interphase is a two-dimensional quasi-lattice in which the linear macromolecule may move about, taking on a great number of energetically equivalent configurations, and our calculations are exactly analogous to those of Huggins[9] and Flory[10] describing the thermodynamic behavior of three-dimensional solutions of polymers. The total surface of area σ is composed of N_0 cells of area σ_0 each. In this first approximation, we neglect energies of interaction between solvent and polymer molecules, whether situated in or out of the interphase, and it is therefore immaterial whether we consider the surface occupied by solvent plus polymer molecules, or holes plus polymer molecules, or by all three. Consider that there are, finally, N large molecules on the surface, each with x identical submolecules (monomer units), and n remaining sites for holes or solvent molecules, the areas occupied by a single submolecule and a solvent molecule being

* Contribution No. 1198 from the Gates and Crellin Laboratories of the California Institute of Technology.
** Abbott Research Fellow, 1947–48.
[1] N. K. Adam, Trans. Faraday Soc. 29, 90 (1933).
[2] W. D. Harkins, E. F. Carman, and H. E. Reis, Jr., J. Chem. Phys. 3, 692 (1935).
[3] F. T. Wall and M. Zelikoff, J. Am. Chem. Soc. 68, 726 (1946).
[4] D. J. Crisp, J. Coll. Sci. 1, 49, 161 (1946).
[5] I. Langmuir and V. J. Schaefer, Chem. Rev. 24, 181 (1939).
[6] H. B. Bull, J. Am. Chem. Soc. 67, 4, 8, 10 (1945); 68, 745 (1946).
[7] J. Gaustella, J. chim. phys. 42, 71 (1945).
[8] A. Rothen, J. Biol. Chem. 168, 75 (1947).
[9] (a) M. L. Huggins, J. Phys. Chem. 46, 151 (1942); (b) M. L. Huggins, Ann. N. Y. Acad. Sci. 43, 1 (1942).
[10] P. J. Flory, J. Chem. Phys. 10, 51 (1942).

the same, σ_0. We count the number of different ways we can place the polymer submolecules in the lattice, adding one polymer molecule at a time. Proceeding by the method of Huggins,[9b] we find that total number of different configurations, Φ, to be:

$$\Phi=\frac{\prod \nu_{i,j}}{N!\beta^N};\quad \prod \nu_{i,j}=\prod_{i=1}^{N}\frac{N_0 z y^{x-2}(1-f_{i,j})^x}{\left(1-\frac{2(x-1)}{xz}f_{i,j}\right)^{x-1}}. \quad (1)$$

Here $\nu_{i,j}$ is the number of sites available to the jth submolecule of the ith polymer molecule; z is the coordination number of the lattice; $y=\nu_{1,3}\cong z-1$; $f_{i,j}$ is the fraction of sites already occupied when the jth submolecule of the ith polymer molecule is added to the lattice, and β is the symmetry number of the polymer chain. For $x\geqslant 10$, we can write

$$f_{ij}=f_0+\frac{(i-1)x(1-f_0)}{N_0}, \quad (2)$$

where f_0 is some small constant. For $x<10$, $f_0\sim 0$. We take logarithms of both sides of Eq. (1), replace summations by integrals, factorials by their Stirling approximations, and utilizing Eq. (2), arrive at an equation for the change in the surface entropy, ΔS_s, produced by placing the N polymer molecules in the lattice:

$$\begin{aligned}\Delta S_s=k\ln\Phi=k\Bigg\{&N\ln\left(\frac{zy^{x-2}}{\beta}\right)+(N+n)\ln N_0\\&-N\ln N-n\ln n-2N+xN\ln(1-f_0)\\&-(x-1)N\ln\left[1-\frac{2(x-1)f_0}{xz'}\right]\\&-(x-1)\left[\frac{z'n}{2x}+\left(\frac{z'}{2}-1\right)N\right]\\&\times\ln\left[\frac{N_0}{n+(1-2/z')xN}\right]\Bigg\}. \quad (3)\end{aligned}$$

In this equation

$$z'=\frac{zx}{(x-1)(1-f_0)}-\frac{2f_0}{(1-f_0)},$$

for practical purposes, a constant.

The film pressure, π, is given by $\pi=\gamma_W-\gamma_F$, the surface tension of water minus the surface tension of the water covered with the film. $\pi=(\partial\Delta F_s/\partial\sigma)_{N,T}=-T(\partial\Delta S_s/\partial\sigma)_{N,T}$, where ΔF_s is the surface free energy change, since we are neglecting the variation in the surface enthalpy. Substituting into Eq. (3), the relations $n=N_0-xN$, and $N_0=\sigma/\sigma_0$, and performing the indicated operations, we find

$$\pi=\frac{kT}{\sigma_0}\left\{\frac{(x-1)z'}{2x}\ln\left(1-\frac{2xN\sigma_0}{\sigma z'}\right)-\ln\left(1-\frac{xN\sigma_0}{\sigma}\right)\right\}. \quad (4)$$

For $(xN\sigma_0/\sigma)\ll 1$, this reduces to the perfect gas law, $\pi=NkT/\sigma$. If we let $kT/\sigma_0=\pi_0$, $\sigma/N=A$, the observed area per molecule, and $x\sigma_0=A_0$, the condensed area per molecule, Eq. (4) is modified to a reduced equation of state:

$$\frac{\pi}{\pi_0}=\left[\frac{(x-1)z'}{2x}\ln\left(1-\frac{2}{z'}\frac{A_0}{A}\right)-\ln\left(1-\frac{A_0}{A}\right)\right]. \quad (4')$$

Aside from the imperfections of the quasi-lattice model, two approximations are seriously to be considered: (a) the neglect of energies of interactions, and (b) the assumption that, on adding a polymer molecule to the lattice, the segments of those polymer molecules already placed in the lattice are randomly situated among occupied sites. Since no extensive investigations have as yet been made of the temperature dependence of the pressure-area curves of monolayers of macromolecules, the effect of the first of these approximations is not known. It will be better satisfied in dilute than in concentrated surface solutions. Attempts have been made to improve the second approximation,[11] but no satisfactory theory covering the entire concentration range has yet been obtained. In very dilute solutions, deviations of theory from experiment will arise from this source. In addition, one might think it possible that the molecules occupy more than one molecular thickness in the third dimension, instead of being restricted to coil in two dimensions only, but this effect would provide for greater compressibility of the

[11] P. J. Flory, J. Chem. Phys. 13, 453 (1945).

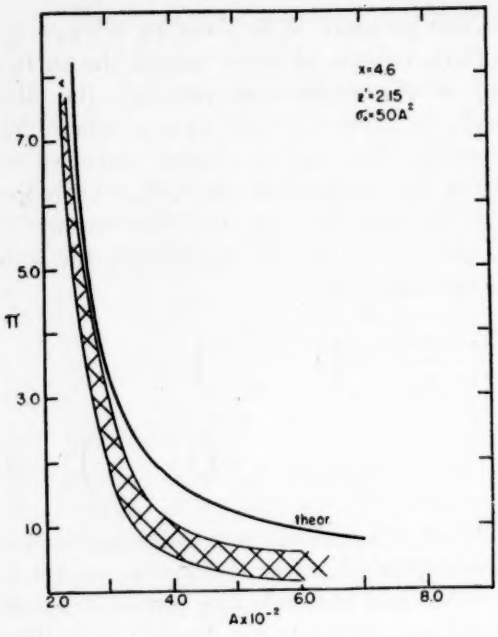

Fig. 1.

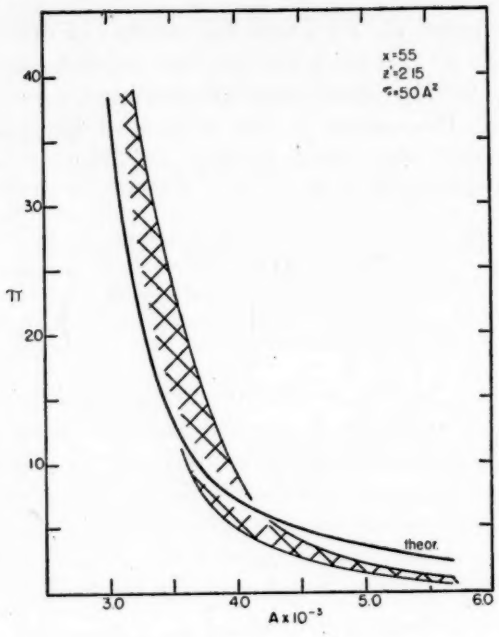

Fig. 3.

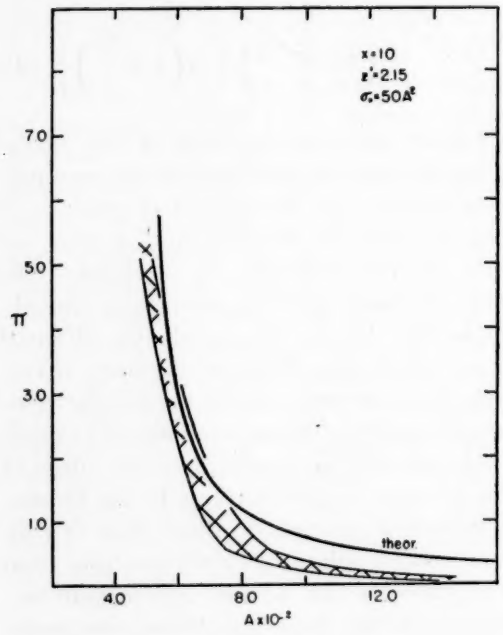

Fig. 2.

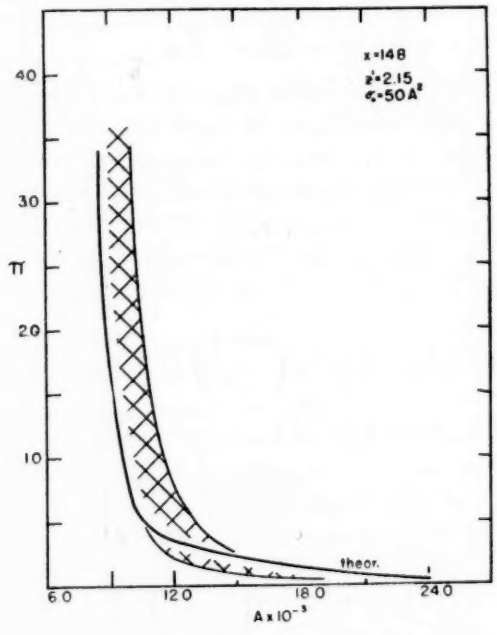

Fig. 4.

FIGS. 1–4. Comparison of theoretical and experimental force-area relations for ω-hydroxy decanoic acid polymers.[2] Cross-hatched areas represent the variations in the experimental curves in going from 0.01 *N* NaOH to 0.01 *N* HCl as substrate.

films, whereas the theory as it stands already appears to err in that direction.

We may now proceed to compare the theory with experiment qualitatively. Equation (4′) permits one to evaluate the effect of molecular weight on pressure-area relations for homologous series of polymers. For a variety of polymer series, it has been found[1,2,4] that at moderate pressures the area per molecule is practically a linear function of molecular weight, or, i.e., that

the area per unit of polymer is nearly independent of molecular weight. From Eq. (4′) it is clear that for $x>10$, and for moderate film pressure, the relation between π/π_0 and A/A_0 is practically independent of molecular weight, in accord with the experimental fact. Moreover, the small dependence of the reduced pressure-area relation on molecular weight predicted by Eq. (4′) is such that the curves for lower molecular weight species lie slightly above those of their higher molecular weight homologues. This has been found to be so by Adams,[1] with some nitrocellulose spread on 2*N* NaOH, and by Harkins *et al.*[2] with a series of ω-hydroxy decanoic acid polymers spread on dilute acid and base.

Quantitative comparison of theory with experiment requires knowledge of three parameters, z', x, and σ_0. Of the studies on synthetic polymers, that of Harkins *et al.* is the only one amenable to such a calculation. The number average molecular weights of the various ω-hydroxy decanoic acid polymers investigated range from 780 to 25,200, x varying from 4.6 to 148. A reasonable value of σ_0 for the $(CH_2)_9COO$ unit is about 50A², while for z', a value between 2 and 4 is to be expected. In Figs. 1 to 4 are plotted the theoretical and experimental curves for four of these polymers, using $z'=2.15$ and $\sigma_0=50$A². The cross-hatched areas represent the variation in the pressure-area relations caused by changing the *p*H of the substrate. Concerning the fraction of lowest molecular weight, the value of $x=4.6$ is below that required by the use of certain approximations in the theory, but even so, the same values of the parameters yield the proper order of magnitude for the relation. However, the data seem to indicate that irrespective of molecular weight a lower value of z' is required in the low pressure region than in the high.

In attempting to interpret the data obtained with protein monolayers, certain experimental difficulties should first be realized. Various investigators do not agree on their experimental results, possibly because of difficulties in attaining equilibrium, or from the considerably increased solubility of some spread proteins upon increase of film pressure, or for a variety of other reasons.

Moreover, as we have mentioned above, the structure of the protein molecule in a film may be considerably different from a random coil because of intramolecular hydrogen bonding. Further complications might arise from the possibility of the side chains on the polypeptide backbone changing their orientation on compression of the film. Qualitatively, however, the pressure-area curves for proteins so far investigated resemble one another considerably, and are quite similar to those observed with polymers. In particular, there is no indication that phase changes of the kind appearing in films of low molecular weight compounds[12] occur with protein films.

As an example, we have attempted to fit the data of Bull[6] on egg albumin monolayers spread on 35 percent ammonium sulfate solution. Using $z'=2.10$ and $\sigma_0=14.5$A², we obtain the curve shown in Fig. 5 for the high pressure region. The value of $\sigma_0=14.5$A² is slightly lower than that found by Bull, 15.1–15.6A², from the area corresponding to the minimum in the compressibility *versus* area relation (compressibility $=-\partial A/A\partial\pi$), and by Palmer and Galvin,[13] 15.4A²,

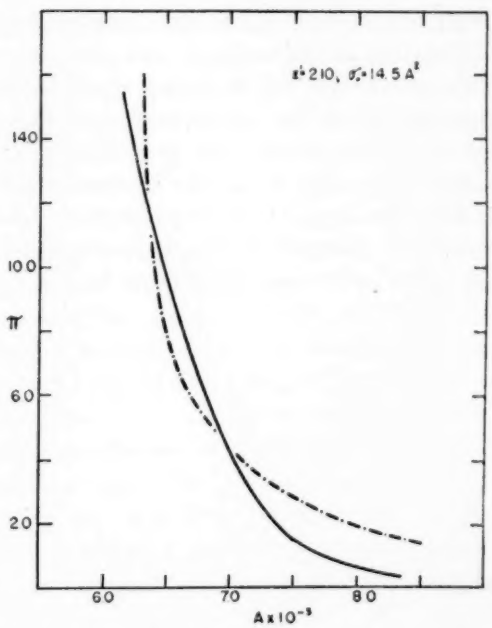

FIG. 5. Comparison of theoretical and experimental force-area relations in the high pressure region for egg albumin[6] spread on 35 percent $(NH_4)_2SO_4$. The solid line represents the experimental curve.

[12] W. D. Harkins, in J. Alexander, *Colloid Chemistry* (Reinhold Publishing Corporation, New York, 1944), Vol. V, p. 22.

[13] K. J. Palmer and J. A. Galvin, J. Am. Chem. Soc. 65, 2187 (1943).

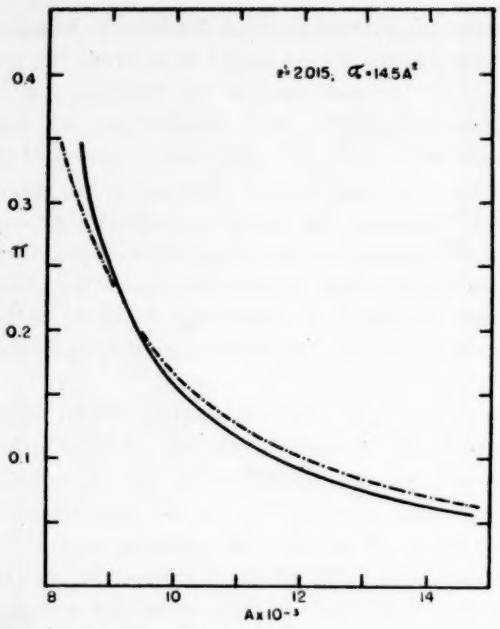

FIG. 6. Same as Fig. 5 in the low pressure region.

from x-ray data on fibers of egg albumin. Bull's value, however, is expected to be somewhat larger than ours. A minimum in the film compressibility is an indication of film collapse, and the area per molecule at collapse will be larger than A_0. The correspondence of the theoretical and experimental curves is not as good as with the polymers. To fit the data in the low pressure region, below 0.5 dynes cm^{-1}, a lower value of z', 2.015, is required, as is shown in Fig. 6. The need for a revised value of z' also appears to be the case with the ω-hydroxy decanoic acid polymers. A similar effect is noted in the case of three-dimensional polymer solutions,[11] a smaller coordination number being required in dilute than in concentrated solutions. Probably, then, a similar cause is responsible, namely, the fact that in dilute solutions the approximation of randomly occupied sites does not hold as well as in more concentrated ones. That is, the distribution of occupied sites becomes markedly discontinuous when the molecules are, on the average, far from each other. If necessary, an approximate theory for the low pressure, or "gaseous film," region corresponding to that of Flory[11] for dilute three-dimensional solutions could be readily developed. The lack of data in the low pressure regions, however, makes this hardly worth while at present. It should be realized, however, that if experimental problems can be overcome, the low pressure region will yield valuable information concerning not only the molecular weight,[6] but particularly the structure of macromolecular films. If protein molecules form fairly well knit structures on the interphase as compared to those of polymers, it is in this region that marked differences in the pressure-area relations will appear, the proteins behaving more nearly as ideal two-dimensional gases than polymers at comparable low pressures.

The author wishes to express his sincere gratitude to Professor J. G. Kirkwood for his many helpful suggestions.

THE JOURNAL OF CHEMICAL PHYSICS VOLUME 16, NUMBER 9 SEPTEMBER, 1948

Polarized Infra-Red Radiation as an Aid to the Structural Analysis of Long-Chain Polymers. I.

A. ELLIOTT, E. J. AMBROSE, AND R. B. TEMPLE
Courtauld's Limited, Maidenhead, Berkshire, England

(Received March 29, 1948)

An experimental procedure is described for measuring dichroism in the infra-red spectrum of oriented materials. Oriented films of polythene, polyvinyl alcohol, polyvinyl chloride, polyvinyl acetate, and Nylon have been examined in the region 3600–700 cm^{-1}, and the species (parallel or perpendicular) of many bands has been identified. The bearing of these results on current ideas concerning the structure of these polymers is discussed. A general result is that frequencies involving the motion of hydrogen atoms show rather low dichroism. On the other hand, very high dichroism has been found in some frequencies in which the motion is believed to be confined to other atoms.

INTRODUCTION

WHEN unpolarized radiation, which contains electric vector components vibrating in an infinite number of planes perpendicular to the direction of propagation, is passed through a purely random spatial arrangement of molecules such as we find in a gas, a liquid, or an amorphous solid, there is an equal probability of interaction between the radiation and all the possible modes of vibration of the molecules. Consequently, all the permitted frequencies will be absorbed. If, however, we consider the case of a substance in which the molecules are uniformly oriented, as in a perfect crystal, this is no longer true, and the intensity of absorption should be a function of the angle between the direction of change of the dipole moment and the plane in which the electric vector is vibrating. To take an extreme case, the absorption coefficient should be zero for those vibrations in which the moment changes parallel to the direction of the incident radiation. Intensity changes of this kind, depending on the orientation of a crystal relative to unpolarized radiation, have been recorded by Barnes[1] in the case of quartz, by Plyler[2] for ice, and very recently by Glatt and Ellis in films of oriented paraffins,[3] but such preferential absorption has received surprisingly little attention, although combined with the results of x-ray analysis it might prove a valuable aid to vibrational analysis.

Even more detailed information about the nature of the vibrational frequencies should be forthcoming from absorption spectra obtained with plane-polarized radiation, particularly where the crystal structure has already been determined by x-ray analysis, but here too investigations have until recently been confined almost entirely to studies of relatively simple salts and minerals.[4] The first recorded attempt to apply the technique to the study of polymers was made by Thompson,[5] who, however, obtained only inconclusive results in an attempt to discover the nature of the polythene band at 720 cm^{-1}. Recently, Glatt and Ellis[3] have made some measurements on oriented films of polythene and some high molecular weight paraffin waxes, but their investigations have been confined to the overtone region between 0.6 and 2.7 mu. Nevertheless, the results obtained are of considerable interest. Using a new type of transmission polarizer,[6] we have been able to study a number of polymers in the fundamental region up to 14 mu; the results, though not yet complete, are now presented for the four compounds, polythene, polyvinyl-alcohol, polyvinyl-chloride, polyvinyl-acetate, together with preliminary results ob-

[1] R. B. Barnes, Phys. Rev. **39**, 562 (1932).
[2] E. K. Plyler, J. Opt. Soc. Am. **9**, 545 (1924).
[3] L. Glatt and J. W. Ellis, J. Chem. Phys. **17**, 880 (1947).
[4] C. Schaeffer and F. Matossi, *Das Ultrarote Spektrum* (Verlag Julius Springer, Berlin, 1930); J. W. Ellis and J. Bath, J. Chem. Phys. **6**, 221, 723 (1938), **5**, 862 (1939), Phys. Rev. **77**, 1098 (1939); J. Mann and H. W. Thompson, Nature **160**, 17 (1947), D. A. Crookes, *ibid.*; G. B. B. M. Sutherland, and A. Vallance-Jones, Nature **160**, 567 (1947).
[5] H. W. Thompson and P. Torkington, Proc. Roy. Soc. **184A**, 3 (1945).
[6] A. Elliott and J. Ambrose, Nature **179**, 641 (1947); A. Elliott, J. Ambrose, and R. B. Temple, J. Opt. Soc. Am. **38**, 212, (1948).

tained on two more, namely, polyisobutene and Nylon.

EXPERIMENTAL

The production of highly oriented and sufficiently thin layers of these polymers presents considerable practical difficulties which have so far been only partly overcome. Under carefully controlled conditions, it is possible to obtain substances which crystallize readily from solution or from the melt, in the form of thin layers which exhibit considerable double refraction when viewed between crossed Polaroids, and which must therefore be highly oriented. Such methods are generally inapplicable to long-chain polymers, many of which remain in a disordered state when cooled below their melting point. The molecules of such substances can be at least partially oriented by stretching or rolling. Stretching tends to produce orientation in the plane of the film parallel to the direction of stretch, whereas rolling may, in certain cases, produce three-dimensional orientation.[7] The chief difficulty is to obtain oriented films which are thin enough to give adequate transmission. For the very strongly absorbing materials it is not possible to stretch films of the requisite thinness, and a method which we have found satisfactory is to roll the material between jeweller's rolls, either in the form of a "sandwich" between two pieces of silver chloride (which is transparent over the whole of the rocksalt region) or cast on a piece of lead foil, from which it is later stripped. The thickness of the films is conveniently measured by an optical lever.

The degree of orientation produced in the crystalline region of the material can be determined from x-ray photographs by the method of Hermans and Platzek,[8] which involves measuring the spread of the polar arcs. We suggest that information on the degree of orientation can be obtained by measuring the quantity

$$\frac{\log I_0/I_\pi}{\log I_0/I_\sigma},$$

where I_0 represents the intensity of the incident radiation and the subscripts π, σ refer to the cases where the E-vector is, respectively, parallel and perpendicular to the direction of stretching of the polymer. Such a measurement must, of course, be carried out on a band which is known to be associated with a change of dipole moment exclusively parallel or perpendicular to the chain axis of the polymer. This quantity is known as the "dichroic ratio." In the case where the change of dipole is parallel to the chain axis, it can be shown that

$$\frac{\log I_0/I_\pi}{\log I_0/I_\sigma} = 2\cot^2\theta,$$

and, similarly, for a change of dipole perpendicular to the axis

$$\frac{\log I/I_\pi}{\log I_0/I_\sigma} = \frac{2\sin^2\theta}{2-\sin^2\theta},$$

where θ is the semi-angle of a cone described about the axis of stretching. θ represents the average direction of orientation of the molecular chains in the material, this method of representation being first used by Hermans and Platzek in determining the degree of orientation from refractive index measurements.

The spectrometer used is a Perkin-Elmer model 12A,[9] with a 60° rocksalt prism in a Wadsworth-Littrow mounting. It has been modified by the introduction of a Hilger-Schwarz vacuum-type compensated thermocouple and suitable condensing mirror. This spectrometer is used in conjunction with a General-Motors contact-modulated amplifier,[10] feeding a photographic recorder of our own design, which has a full-scale sensitivity of 70 microamperes. A full description of this recorder has appeared elsewhere.[11] The polarizer slides into a slot just in front of the entrance slit of the spectrometer. Although attempts have been made to dry the air in the body of the spectrometer in order to minimize atmospheric absorption, it has not proved possible to reduce the intensities of the strongest water lines at 6 mu below about 20 percent and to make it possible to measure the

[7] C. W. Bunn and E. V. Garner, Proc. Roy. Soc. **189A**, 39 (1947).
[8] P. H. Hermans and P. Platzek, Kolloid Zeits. **88**, 68 (1939).
[9] R. B. Barnes, R. S. McDonald, Van Zandt Williams, and R. F. Kinnaird, J. App. Phys. **16**, 77 (1945).
[10] M. D. Liston, C. E. Quinn, W. E. Sargent, and G. G. Scott, Rev. Sci. Inst. **15**, 194 (1946).
[11] A. Elliott and J. Ambrose, J. Sci. Inst. **24**, 324 (1947).

percentage absorption of bands in the water vapor region, the system is designed to record the atmospheric absorption simultaneously with that of the specimen. For this purpose, the specimen is mounted on a small rocker arm, pivoted just behind the polarizer, which is moved in and out of the beam at regular intervals by an electromagnetic mechanism actuated by the prism drive. The oscillations of the meter are recorded continuously and provide a simultaneous record of the background absorption as well as that of the material being examined. To convert these records to percentage absorption or optical-density curves, it is, of course, necessary to measure up the trace at all points at which we are interested, but the labor involved has been greatly reduced by the use of suitable scales, marked on india rubber, which are stretched to suit the size of the spectrum being measured. Above about 3.5 mu a Pyrex shutter is used to correct for scattered radiation.

RESULTS AND DISCUSSION

A. Polythene

Previous investigations of the spectrum at 3 mu were carried out with unpolarized radiation by Fox and Martin,[12] using a grating spectrometer, while Thompson and Torkington[5] studied the longer wave-length regions with the aid of fluorite, rocksalt, and sylvine prisms. The overtone region from 0.6 to 2.7 mu has recently been investigated by Glatt and Ellis,[3] using plane-polarized radiation. Figure 1 shows the spectrum of oriented polythene films which were prepared by melting between Pyrex plates and quenching with cold water; this gave a clear transparent film. The films were oriented by stretching to breaking point at room temperature. From x-ray measurements the crystallites were contained within a cone of semi-angle 46° around the direction of stretching in the specimen examined.

A striking feature of the polythene spectrum is its simplicity. The spectra of very long chain polymers are often considerably less complicated than those of the parent monomers and simpler related substances, and it is obvious that some

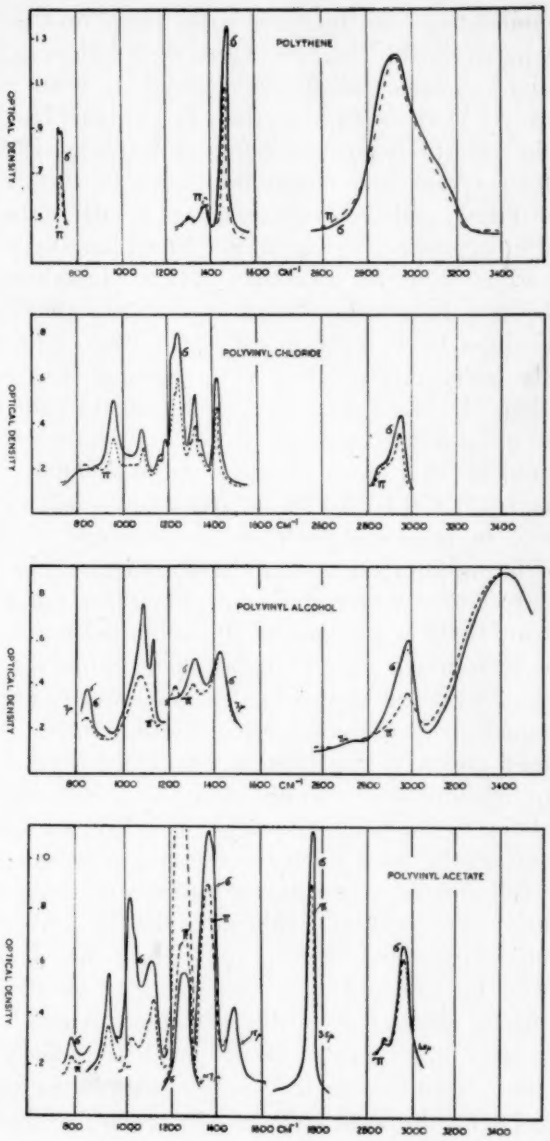

FIG. 1.

factor or factors operate to limit the numer of vibrations which can interact with the radiation. One possible explanation is that the effect of the end groups is much reduced, but a more important limiting factor is probably to be found in the phase relationships which must exist between different parts of the molecule if absorption is to take place.[13] It is generally considered that a given vibration can only give rise to absorption if it produces a change of dipole

[12] J. J. Fox and A. E. Martin, Proc. Roy. Soc. **157A**, 961 (1940).

[13] S. E. Whitcomb, H. H. Nielsen, and L. H. Thomas, J. Chem. Phys. **8**, 143 (1940).

moment for the molecule *as a whole*, and in a long chain this can only be so if the changes in dipole moment arising in neighboring units are nearly in the same direction. For parallel bands the vibrations must therefore be in phase, while for perpendicular modes they must be 180° out of phase, and these requirements greatly reduce the total of active vibrations. For a long hydrocarbon chain, the most general normal mode will be one in which the phase of the vibration changes by a constant angle from one unit to the next, corresponding to the passage of waves along the chain, to be reflected from the ends to form standing waves. In such a chain it is evident that both symmetrical and antisymmetrical C−H stretching frequencies will give rise to perpendicular-type bands, while C−H deformation modes will include both parallel and perpendicular vibrations. For example, a parallel band could be produced if all the hydrogen atoms were to move parallel to the chain in one direction, while all the carbon atoms moved simultaneously in the other. Such a vibration has not been observed in polythene, and it is interesting to inquire how it could occur in a very long chain. If the chain were bent or coiled to a large extent, the total change of dipole would be very small and the absorption coefficient correspondingly low. On the other hand, the greatest intensity would be expected when the chains were fully extended and oriented with the direction of the change of dipole moment parallel to that of the *E*-vector of the incident radiation. Since amorphous and unoriented long-chain polymers do possess strong absorption bands, it is apparent that the chains do not, in fact, vibrate as whole units but in sections, probably as a result of interference with the neighboring chains.

As a result of x-ray investigations,[14] it is known that there are two molecules in the unit cell of polythene in which the chains are parallel but with the fully extended zigzags mutually at right angles. On stretching, the crystallites become oriented with the chains parallel to the direction of stretch. The C−H bonds are thus in planes perpendicular to the chain axis, and the stretching vibrations should therefore show maximum absorption when the *E*-vector is vibrating perpendicular to the axis. This is seen to be so in Fig. 1, although the dichroism is less marked than with the deformation band in the region of 1400 cm^{-1}. The C−H stretching vibrations include both methylene and methyl group vibrations, and it will be shown later that this could (at least in part) account for the small degree of dichroism observed. The symmetrical methylene deformation should also be confined to the plane at right angles to the chain axis and has therefore been correlated with the strong band at 1475 cm^{-1} which shows marked perpendicular dichroism. This is not in agreement with the assignment proposed by Whitcomb, Nielsen, and Thomas in their mathematical treatment of an infinite hydrocarbon chain.[13] These authors attributed the 1475-cm^{-1} band to a fundamental mode in which the hydrogen atoms vibrate in phase against all the carbon atoms in a direction parallel to the chain axis. This explanation has already been criticized by Glatt and Ellis.[3]

The weak band at 1375 cm^{-1} has been attributed by Thompson and Torkington to the presence of methyl groups, which were first detected in polythenes by Fox and Martin.[12] Previously it had been thought that polythene consisted of simple chains of CH_2 groups. 1375 cm^{-1} is exactly the frequency normally attributed to the symmetrical deformation of a methyl group. If the methyl groups were attached directly to the main polythene chain, the dipole change associated with its symmetrical deformation would be expected to occur in a direction perpendicular to the chain. It is found, however, that this frequency exhibits parallel orientation. The most plausible explanation of this is that the methyl groups are end groups attached to side chains of sufficient length to orient parallel to the main chains. This would show itself in reduced dichroism of the CH_2 stretching frequency, on which the methyl group stretching frequencies are superimposed. The methyl groups on the side chains presumably arise when the radical participates in a chain transfer with the polymer already produced. This results in the formation of an active center in the polymer molecule from which a side chain grows, and this probably terminates in a methyl group. More information about the symmetrical defor-

[14] C. W. Bunn, Trans. Faraday Soc. **37**, 482 (1939).

mation of the methyl group was obtained from measurements made with poly-isobutene. The particular specimen of this substance available could not be maintained in the stretched state for more than a few minutes, but the absorption at 1380 cm^{-1} resulting from the methyl groups was found to be more intense in the perpendicular direction. This molecule is thought to have a spiral structure with the *Me* groups projecting at an angle of 63° to the axis,[15] and the dichroism observed is small because of this inclination.

Solid polythene shows a doublet band at about 728 cm^{-1}, which is replaced by a single shallower band on melting.[5] Sutherland and Sheppard have recently compared the spectra of a long-chain paraffin and that of the fully deuterated analog[16] and have shown that this band, which is found in all paraffins containing the group CH_3, $(CH_2)_n$ where $n \geqslant 3$, is a deformation mode of the CH_2 groups. Examination with polarized radiation gives the following results. The perpendicular position gives the sharp doublet, as found by Thompson and Torkington, but with parallel radiation only a single broad and much less intense band appears, one component of the doublet being entirely absent or at least very much weaker. We can attribute the component which disappears to the rocking of the CH_2 groups *across* the chain, since the other possible modes are either known to be of too great a magnitude or else would produce a dipole change in the wrong direction. The nature of the other component is obscure. Since it is reminiscent of the single band which occurs in the molten polymer, it may be due to the amorphous regions of the material. The phenomenon requires further experimental investigation.

B. Polyvinyl Alcohol

This was high solubility material known as "Du Pont de Nemours RH 349." Films of suitable thickness were cast from aqueous solution on glass plates and oriented by stretching in a current of warm air. Thicknesses of the order of 7 microns were found suitable. Most of the results were obtained with films which had not been exhaustively dried, but later experiments were made with a film that had been dried in a vacuum over phosphorus pentoxide, to discover whether any marked changes in the spectrum accompany the removal of water. The spectrum of this substance has already been recorded by Thompson and Torkington,[17] but the use of polarized radiation reveals some interesting new features. (See Fig. 1.)

The C−H stretching frequency at 2975 cm^{-1} shows the expected perpendicular orientation to a considerable extent, in contrast to the very strong −OH valency band at about 3400 cm^{-1} which appears completely unoriented. Furthermore, the breadth of the latter suggests that considerable hydrogen bonding is taking place. That this band is not the result of absorbed water is shown by the examination of the thoroughly dried film in which the breadth and intensity of the band remain unchanged. Hydrogen bonding is in accordance with the structure proposed for the crystalline material by Mooney,[18] although it must be admitted that this structure has been criticized by Bunn.[19] The hydrogen atoms are believed to be bonded to the oxygen atoms of neighboring molecules, the angle between the axis and the O−H−O bond being about 60°. The O−H−O bonds of adjacent groups are not parallel but inclined at 60° to the chain axis in opposite senses. It will readily be seen that the effect of this is to produce a lower dichroic ratio than for a perpendicular bond. Although the low value obtained for the dichroic ratio is in agreement with the structure suggested by Mooney, the *breadth* of the −OH band is not easily reconciled with an exact crystalline structure, which we should expect to give rise to a sharp band at a frequency lower than that associated with an hydroxyl group not subjected to hydrogen bonding.[20] If, however, the oxygen atoms did not always lie on the same side of the chain, as suggested by Bunn,[21] the degree of hydrogen bonding might vary and give rise to a broad band.

[15] R. Brill and F. Halle, Naturwiss. **26**, 12 (1938); C. S. Fuller, C. J. Frosch, and N. R. Pape, J. Am. Chem. Soc. **62**, 1905 (1940).
[16] G. B. B. M. Sutherland and N. Sheppard, Nature **159**, 739 (1947).
[17] H. W. Thompson and P. Torkington, Trans. Faraday Soc. **41**, 246 (1945).
[18] R. C. L. Mooney, J. Am. Chem. Soc. **63**, 2828 (1941).
[19] C. W. Bunn, *Recent Advances in Colloid Science* (Interscience Publishers, Inc., New York, 1946), Vol. III.
[20] J. J. Fox and A. E. Martin, Proc. Roy. Soc. **175A**, 208 (1920).
[21] C. W. Bunn and H. S. Peiser, Nature **159**, 161 (1947).

The strong band at 1450 cm^{-1} has been assigned to a deformation of the methylene group by Thompson and Torkington. This is not borne out by the complete absence of dichroism, and it seems probable that it is, in fact, a deformation mode of the $-OH$ group, the motion of which largely concerns the H atom. The Raman spectra of a number of alcohols contain a line at approximately this frequency. In addition, the intensity of this band appears much greater than might be expected for a methylene vibration. It is possible, however, that the two frequencies are coincident. The perpendicular band at 1340 cm^{-1} may also be due to a hydrogen deformation mode.

The two bands near 1100 are of considerable interest. Comparison with the spectrum of polyvinyl chloride (see below) leads to the belief that they are connected with the presence of the oxygen atoms. The most striking feature is the apparent disappearance of the component at 1146 cm^{-1} when parallel radiation is used. This recalls the polythene band at 728 cm^{-1} already discussed, also an overtone band at 4216 cm^{-1} reported by Glatt and Ellis.[3] Because of the uncertainty of the level of the background between absorption bands, and because of imperfect resolution, it is not possible to be certain that the band has completely disappeared; the dichroic ratio is certainly higher, possibly much higher, than 8:1 in polyvinyl alcohol. No other band in the spectrum of this substance shows such a high degree of orientation. The dichroic ratio for the C−H stretching frequency, for example, was 2:1, the same as for the band at 1100 cm^{-1}. An x-ray photograph showed that the crystalline material was highly oriented, with the crystallites contained in a cone of semi-angle 11°. The dichroic ratio calculated for this degree of orientation is 25:1, so that the effect observed at 1146 cm^{-1} is not unexpected. The general low value obtained from the other bands needs explanation, however.

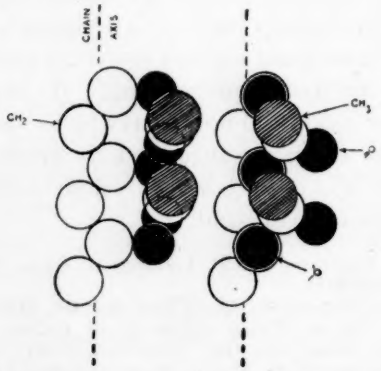

FIG. 2.

C. Polyvinyl Acetate

It is interesting to compare the spectrum of polyvinyl alcohol with that of the corresponding acetate, from which it is prepared by hydrolysis. The polyvinyl acetate examined was a sample of "Gelva-60," kindly supplied by Shawinigan Electrochemicals, Ltd., and had an approximate molecular weight of 180,000 (measured by viscosity). Films were cast from benzene solution and the material oriented by stretching in a current of warm air. The spectrum obtained is shown in Fig. 1 and agrees generally with that already recorded by Thompson and Torkington,[17] although the results obtained with polarized radiation present some interesting features.

The three most intense bands in the spectrum are, in order of intensity, those at 1740, 1240, and 1375 cm^{-1}, respectively. The first and the last show the same degree of perpendicular dichroism (dichroic ratio $\sigma/\pi=1.26$), while the band at 1240 cm^{-1} shows parallel dichroism ($\pi/\sigma=1.3$). All three of these bands were considered by Thompson and Torkington to arise from the vibrations of the acetate group, that at 1740 cm^{-1} from the stretching of the carbonyl radical, the band at 1375 from the symmetrical deformation of the methyl groups, and that at 1240 cm^{-1} to be connected with a mode of vibration of the C·O·CO·C skeleton.[22] These assignments are supported by our polarization measurements, which point to a structure in which the acetate groups are oriented relative to the chain as shown in the Fig. 2. In this figure, all the acetate groups are shown on one side of the chain for simplicity. A random distribution would, however, be equally compatible with the infra-red spectrum. It will be seen from the figure that both the C:O stretching vibration and the

[22] H. W. Thompson and P. Torkington, J. Chem. Soc., 640 (1945).

symmetrical CH_3 deformational vibration should show predominately perpendicular character. In the skeleton $R_1-C^1-O^2-R_2$, where R_2 represent the main chain, we may expect to find two frequencies which are mainly controlled by the stretching of the two C−O bonds 1 and 2. It was suggested by Thompson that the 1240 cm^{-1} band in acetates is to be associated with bond 1, while that arising from bond 2 is to be found in the region from 1000–1100 cm^{-1}. The results we have obtained with polyvinyl alcohol and acetate appear to confirm this assignment. Reference has already been made to the polyvinyl alcohol band at 1146 cm^{-1}, which shows a very high degree of perpendicular orientation and it will be seen that a high dichroic ratio is, also exhibited by the acetate band at 1025 cm^{-1}, which is also highly perpendicular in character. The 1240 band, on the other hand, showing parallel orientation, is peculiar to the acetate (the very weak parallel band which occurs in the alcohol, merely suggesting, as Thompson remarks, the presence of a small residue of unhydrolyzed material). The facts, therefore, suggest very strongly that the strong perpendicular bands in the region of 1000–1150 cm^{-1} in the two materials arise mainly from the stretching of bond number two in the above formula, while the parallel acetate band at 1240 is due to bond number one. There are a few further points to be noted about the spectrum. The band at 2930 arising from the stretching of the C−H bonds shows only slight perpendicular orientation. That at 1475 cm^{-1}, which is presumably caused by a hydrogen deformation mode, appears to be completely unoriented. Both facts can be explained by assuming the superposition of two or more frequencies of opposite configuration. In the former we have unresolved methylene and methyl group frequencies, and if the methyl groups are arranged very nearly perpendicular to the chain axis as suggested, the asymmetric CH_3 stretching mode should have a parallel component which may compensate for the other perpendicular modes. Similarly, we may attribute the absence of dichroism at 1475 cm^{-1} to superposition of the antisymmetrical methylene and methyl group frequencies.

TABLE I.

ν	$D_\pi/D_\sigma=\log\frac{I_0}{I_\pi}\Big/\log\frac{I_0}{I_\sigma}$
2950 cm^{-1}	0.73
1435	0.72
1260	0.70
Mean	0.72

D. Polyvinyl Chloride

This was an unplasticized specimen whose previous history is unknown, but since the spectrum appears to agree with that previously recorded by Thompson and Torkington,[17,23] this is unimportant. As will be seen from Fig. 1, the spectrum obtained with π-radiation is an almost exact replica of that in the σ-direction, with the band intensities slightly reduced. The two exceptions are a band at 1200 cm^{-1}, which appears to be unoriented, and a very weak band at 840 cm^{-1}. Only a few bands in the spectrum can be identified with particular modes. The very strong perpendicular vibration at 1260 cm^{-1} which has no corresponding band in polyvinyl alcohol and which is the strongest band in the spectrum, presumably involves the chlorine atoms. It is probably connected with the rocking of the hydrogen atoms on the −CHCl− groups. The band at 1450 is obviously due to the normal deformation of the CH_2 groups.

Although the dichroic ratio of the polyvinyl chloride bands is practically constant (except for the weak bands noted above), it should be remarked that probably hydrogen atoms, not chlorine atoms, are concerned in the corresponding vibrations. It may therefore be that the particular dichroic ratio (average value $D_\pi/D_\sigma=0.72$, see below) shown corresponds to the average orientation of the C−H bonds. The value of the average orientation angle θ corresponding to a dichroic ratio of 0.72 is 44°. It is quite possible that the band characteristic of the C−Cl stretching frequency, which is outside the region we have investigated, would show a different amount of dichroism. This will be investigated later.

[23] H. W. Thompson and P. Torkington, Proc. Roy. Soc. **184A**, 21 (1945).

E. Nylon

Some preliminary results have been obtained with three specimens of "Nylon," a commercial specimen of "Nylon-66," a material prepared in this laboratory by the method of Chambert,[24] and an interpolymer of unknown constitution obtained from Du Pont de Nemours.

The Nylon type of polymer is interesting because this class of molecules is built up by the introduction of a simple polypeptide link into a straight hydrocarbon chain. The spectrum of Nylon-66 has already been investigated by Thompson and Torkington, using unpolarized radiation.[17] The absorption arising from the peptide link appears to be much stronger than that caused by the hydrocarbon chain. This is to be expected, of course, because of the highly polar nature of the atoms forming it.

Some interesting results have been obtained with polarized radiation, although the interpretation is at present not completely satisfactory. All three Nylons have bands in the regions of 3290, 3080, 2900, 1650, and 1550 cm^{-1}; below 1500 cm^{-1} there are differences in the spectra. Two perpendicular bands at 2922 and 2875 cm^{-1} can be assigned to the symmetrical and antisymmetrical CH_2 valency vibrations, respectively. The stronger and rather broader perpendicular band at about 3290 cm^{-1} is certainly due to the N−H valency vibration. Measurements made by Richards and Thompson[25] on solid *N*-mono-substituted amides, and on the same compounds at widely different concentrations in chloroform, indicate that "free" N−H groups, have a valency vibration of about 3430 cm^{-1}, while when the conditions are most favorable for hydrogen bonding (i.e., in the solid), a single band appears at about 3270 cm^{-1}. In concentrated solutions both bands appear simultaneously. The presence of a single fairly broad band at 3290 cm^{-1} in Nylon therefore indicates that the degree of hydrogen bonding taking place is very considerable, and probably nearly complete.

Further evidence for the existence of hydrogen bonding is afforded by the bands in the region from 1500–1700 cm^{-1}, which appear to be characteristic of the peptide link. Measurements made with unpolarized radiation on a natural polyglutamic acid and on a similar synthetic polymer prepared by Hanby, Waley, and Watson,[26] show that almost identical frequencies occur in both free acids and their silver salts. Similar results have been observed by Darmon and Sutherland, in the case of a denatured keratin and a keratin-type synthetic polypeptide.[27] There is a strong perpendicular band at 1650 cm^{-1} which has been assigned to the stretching mode of the C:O link. This value is considerably lower than that found in the esters and ketones[22] and in *N*-mono-substituted amides in very dilute solution in dioxane,[25] but a similar shift towards low frequencies occurs in the latter compounds in the solid state. This indicates that the double-bond character has been reduced through the formation of hydrogen bridges, and the similar low value in Nylon is further evidence for the presence of the same phenomenon. All three Nylons show a strong parallel band at 1550 cm^{-1}. This has been identified with an N−H deformational vibration by Richards and Thompson, who showed that a corresponding frequency is observed in the spectra of unsubstituted and *N*-mono-substituted amides, but not in those of the *NN*-di-substituted compounds. The vibration appears to take place in a plane parallel to the axis of the molecule. According to Bunn and Garner,[7] the carbon, oxygen, and nitrogen atoms linked by hydrogen bonds between parallel chains lie in an approximate straight line. Assuming a normal disposition of the valency bonds about the nitrogen atom, it is therefore clear that the hydrogen atom must lie to one side of the plane containing the carbon, nitrogen, and oxygen atoms, and this may favor the parallel deformation of the N−H bond. The very weak band found at 3080 cm^{-1} is possibly the overtone of this N−H deformation, and if this is so, it is interesting to note that it appears to have changed its species to a perpendicular type band.

Quite striking differences were observed in the

[24] F. Chambert, Bull. Soc. Chim. **14**, 283 (1947).
[25] R. E. Richards and H. W. Thompson, J. Chem. Soc., 1248 (1947).
[26] W. E. Hanby, S. G. Waley, and J. Watson, Nature **161**, 132 (1948).
[27] S. E. Darmon and G. B. B. M. Sutherland, J. Am. Chem. Soc. **69**, 2074 (1947).

spectra of two films of the interpolymer, one of which had been rolled and the other stretched. These differences must arise from the different types of orientation produced in the two cases. In the stretched film only unidirectional orientation of the chains is produced parallel to the direction of stretch. In the rolled material, the first effect of the compressional force is to produce a planar orientation of the plate-like Nylon crystals, with the 010 planes parallel to the sheet, directional orientation being produced by further rolling. The C:O bonds are thought to lie only slightly out of the 010 planes,[7] and it was found that whereas the corresponding band showed no apparent dichroism in the case of the stretched specimen, quite high perpendicular dichroism was observed in the spectrum of the rolled material. In the stretched Nylon, many of the C:O bonds will lie out of the plane of the sheet and therefore also out of the plane of vibration of the incident light. In an imperfectly oriented specimen, the component of the change of dipole moment resolved into the plane of vibration of the incident light can have a component parallel to the direction of stretching.

In fact, where the C:O bond lies in a plane perpendicular to the plane of the sheet, the component resolved in the plane of the sheet is parallel to the axis of stretch. This effect tends to reduce the amount of dichroism exhibited by a perpendicular band. On the other hand, when the C:O bonds are lying in the plane of the sheet as in the rolled specimen, a small degree of orientation of the bonds will produce an appreciable amount of dichroism. The infra-red data are therefore in agreement with Bunn and Garners' views concerning the disposition of the C:O bonds.

As already stated, the spectra of the three substances are not identical below 1500 cm^{-1}, although the interpretation of these differences is not yet apparent. The material prepared by the method of Chambert showed very sharp absorption bands, which indicates that the crystal structure is very uniform. An x-ray powder photograph of the same material showed nine diffraction rings, also indicative of a high degree of crystallinity.

The presence of peptide links in a hydrocarbon chain at fairly long intervals may make it possible for portions of the chain to vibrate as nearly independent units which are unaffected by the phase relationships which prevent the occurrence of parallel chain vibrations in molecules such as polythene. There are, in fact, two strong parallel vibrations in the spectrum of the Nylon copolymer: a doublet at about 1130 and a single band at about 930 cm^{-1}. It would be interesting to determine whether similar parallel vibrations also occur in a continuous polypeptide chain.

CONCLUSION

The results obtained so far indicate that the spectra obtained with the aid of polarized radiation can yield interesting information about the orientation of particular bonds in high polymers. Since the method is particularly suitable to the study of carbon-hydrogen bonds, it may yield complementary evidence to that obtained from x-ray analysis. One of the more puzzling results is that in all cases studied so far, the C−H bonds appear to exhibit much less than the expected degree of orientation. This phenomenon, which has already been noted by Glatt and Ellis,[3] may in some cases be due to the imperfect resolution of overlapping bands. In other cases, however, the effect is undoubtedly genuine. An x-ray photograph of one specimen of polyvinyl-alcohol, for example, showed a very high degree of orientation which was accompanied by very high dichroism of the C−O stretching frequency but only moderate dichroism of the C−H frequencies. As the above workers have found in the case of the overtones of polythene, the effect is much greater than imperfect alignment of the polarizer and the use of a converging beam of radiation can account for. It may therefore be that the degree of orientation varies considerably for different parts of the molecule, and that the low dichroism exhibited by the C−H bonds means that in the crystalline state the hydrogen atoms are considerably displaced from their expected positions. Although this explanation may hold for a material such as polyvinyl acetate, in which large side groups render the formation of stretched chains difficult, in other cases an alternative explanation may be that put forward by Glatt and Ellis, who suggest

that the coupling of a large number of CH_2 groups, which must occur in a hydrogen chain, may produce a change of dipole moment which has a component parallel to the chain axis.

If it were possible to produce planar orientation in addition to that produced by stretching, more information could be obtained about the directions of the various bonds in the crystallites. Since it is known that rolling produces planar orientation in Nylon-66, this seems a suitable material for future study, in order to develop the technique, and it is hoped to extend the treatment to other polymers. The use of completely crystalline substances also offers attractive possibilities, and here again Nylon-66 seems suitable for experiment, since crystals of it can be grown by the controlled polymerization of hexamethylene diammonium adipate.[24] It is also important to re-investigate several of the polymers already described under the higher resolving power obtainable with a lithium fluoride prism, and work on these lines is now proceeding. Since this increase of resolving power is particularly marked in the 3-mu region, it is intended to make use of it to obtain more definite information about the orientation of methylene and methyl groups.

We wish to acknowledge our indebtedness to Dr. F. Happey, for taking the x-ray photographs, to Dr. C. H. Bamford, M. J. Crank and Dr. M. J. S. Dewar for helpful discussions, and to the Directors of Courtaulds Limited, for permission to publish this account.

THE JOURNAL OF CHEMICAL PHYSICS VOLUME 16, NUMBER 9 SEPTEMBER, 1948

On the Photo-Chemistry of Some Ions in Solution

L. FARKAS AND F. S. KLEIN*
Department of Physical Chemistry, Hebrew University, Jerusalem, Palestine
(Received April 28, 1948)

The absorption spectra of chlorate, bromate, iodate, and hypobromite ions and of hypobromous acid were measured.

The decomposition of bromate ion was investigated in the light of a mercury arc in the spectral region: 1900A to 2600A. The quantum yield of the decomposition is 0.19. The main decomposition reaction leads to the formation of hypobromite and molecular oxygen. The irradiation of hypobromite ions leads to the formation of bromide and bromate ions in a ratio of about 4 to 1 and to the evolution of oxygen. The decomposition of chlorate ion and iodate ion is analogous to that of bromate. It is assumed that in all these cases the primary process of light absorption consists of the transfer of an electron to the hydration layer. In the case of halate ions, the photo-chemical reaction can be formulated as a decomposition of the complex $(XO_3^- \cdot H_2O)$ to $XO^- + H_2O + O_2$; in the case of the hypobromite, as the decomposition of $(XO^- \cdot H_2O)$ to $X^- + H_2O + O$. In the latter case the oxygen atoms formed are responsible for the formation of bromate.

INTRODUCTION

THE photo-chemical decomposition of ions in aqueous solution was the subject of a number of investigations.[1-4] Farkas and Farkas[2] have suggested that the primary process of light absorption consists of the transfer of an electron from the absorbing ion to one of the water molecules** in the hydration layer. If we assume that during this process the water molecules in the hydration layer remain oriented and retain their potential energy, the long wave-length limit of the absorption for an anion is given by the equation

$$h\nu_0 = E_- + H_- - E_{H_2O}, \qquad (1)$$

where E_- is the electron affinity of the anion in

* This paper is part of a thesis submitted to the Senate of the Hebrew University by F. S. Klein in fulfillment of the requirements for the degree of Ph.D.

[1] E. Rabinowitsch, Rev. Mod. Phys. **14**, 112 (1942).
[2] A. Farkas and L. Farkas, Trans. Faraday Soc. **34**, 1113 (1938).
[3] J. Weiss, Trans. Faraday Soc. **37**, 467 (1941).
[4] L. J. Heidt, J. Chem. Phys. **10**, 297 (1942).

** Professor J. Franck recently suggested that the primary light absorption process consists of the transfer of the electron to a "conduction band" of the hydration layer. According to his view, the electron is not attached to an individual molecule, but is spread over all the oriented water molecules (private communication).

the gaseous state, H_- its hydration energy, and E_{H_2O} the energy gained when the electron is attached to the oriented water molecule. E_{H_2O} is therefore related to the electron affinity of water.

In the present communication the absorption spectra and the photo-chemical decomposition of some halate and hypohalite ions were investigated with the view to extending our experimental material in this field.

EXPERIMENTAL

The *absorption spectra* of the various ions were investigated with a small Hilger spectrograph. A hydrogen discharge lamp was used as a continuous light source. Exposures were made with solutions at various concentrations in a silica cell of 10-mm thickness with plane-parallel windows, on Agfa or Ilford plates, which were sensitized with a solution of mineral oil in light petrol. The transmittance of the exposed plates at different wave-lengths was determined by a "Moll" recording microphotometer. With the aid of appropriate intensity marks, the molecular extinction coefficients $\epsilon = [\log_{10}(I_0/I)]/cd$ (c = conc. in mols per liter, d = thickness of absorbing solution in cm) were calculated in dependence of the wave-lengths according to the usual procedure.

As *light source*, a mercury lamp similar to that described by L. Farkas,[5] was used. Figure 1 schematically illustrates the experimental arrangement. The diameter of the innermost tube (A) is 20 mm. The arc of 20-cm length operates on 35 v and 11.5 amp.

Distilled water, circulated through the first concentric tube (B) by an air-lift pump (L), is used for cooling. The temperature of the distilled water is controlled by the thermoregulator (R) and the cooler (S) through which ice water circulates by means of the pump (P). This pump is set in motion and shut off by the thermoregulator R and a suitable relay. Thus the temperature of the reaction vessel (C) can be kept constant to within ±0.2°C in the range of 15° to 38°C.

The second (C) and third (D) concentric-cylindrical vessels of volumes 113 ml and 195 ml, respectively, are fitted with inlets and outlets of standard taper joints. The upper outlet of vessel (C) is connected with a gas collecting system, built on the principle of a Töpler pump. Water serves as the compressing liquid, and the amount of evolved gas can be measured with an accuracy of ±1 percent in a graduated burette. Generally, a time lag occurs in the evolution of the gas, which is due to supersaturation of the irradiated solution with the gas formed. The outer vessel (E) serves to maintain a constant temperature within the reaction vessels (C) and (D).

The quantum output of the arc was measured before and after each irradiation experiment: Vessel (C) was filled with distilled water (or reference solution), and generally after 30

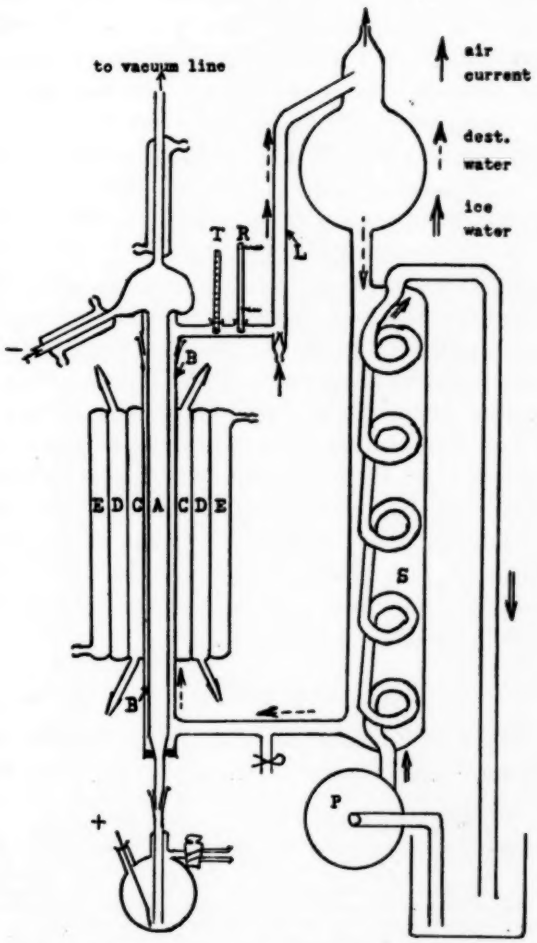

FIG. 1. View of mercury lamp and cooling system.

A	arc tube	*L*	air lift pump
B	dest. water cooler	*P*	circulation pump
C	reaction vessel *I*	*R*	thermoregulator
D	reaction vessel *II*	*S*	ice water cooler
E	cooler	*T*	thermometer

[5] L. Farkas, Zeits. f. physik. Chemie **B83**, 23 (1933).

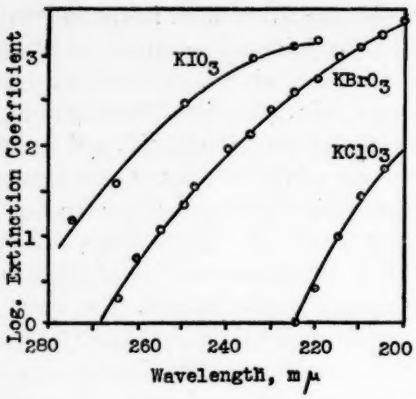

FIG. 2. Curve giving the log extinction coefficient ϵ as a function of the wave-length for chlorate, bromate, and iodate ions in aqueous solution.

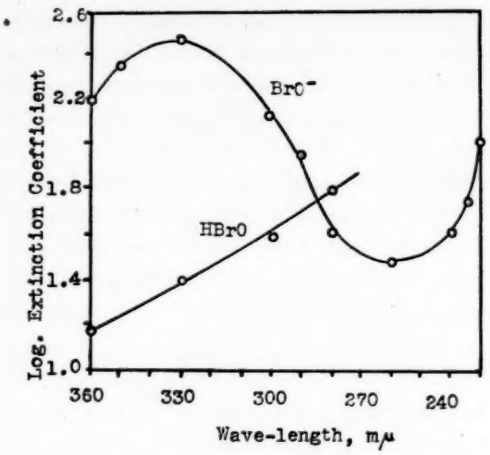

FIG. 3. Curve giving the log extinction coefficient ϵ as a function of the wave-length for hypobromite ion and hypobromous acid in aqueous solution.

minutes of irradiation the extent of decomposition of 1 *M* chloroacetic acid in vessel (*D*) was determined by titrating, according to Volhard, the chloride ions produced. For the calculation of the number of quanta absorbed, Smith and Leighton's[6] value for the quantum yield of 0.35 at 30°C was accepted. The total light intensity of the arc in the region of 1900A to 2600A corresponds to about 10^{19} quanta sec.$^{-1}$. The light intensity of the arc first decreased rapidly (10 percent in the first three hours) and then more slowly (18 percent in the next ten hours). This was caused by the formation of a metallic silicon coating on the walls of tube (*A*). After 30 hours of use, the total decrease amounted to about 50 percent, and then the tube was taken out for cleaning. The silicon could be removed by heating the inner tube in a current of air. Because of uncontrollable changes in the light intensity, the quantum output was estimated with an error of ± 5 percent.

ANALYTICAL

The concentration of bromate, or the sum of bromate and hypobromite, was determined by adding an excess of potassium iodide to the acidified solution and titrating with 0.1 *N* sodium thiosulfate. Iodate, hypochlorite, hypobromite, and hypoiodite were estimated according to Chapin.[7] The chlorate was determined by adding an excess of ferrous sulfate to the acidified solution, heating the mixture, and titrating the residual ferrous ion according to Zimmermann-Reinhardt.

The gas evolved from the solution was analyzed for oxygen, hydrogen, and bromine.

The light absorbed by the irradiated solution was measured according to the method described by Farkas.[5]

TABLE I. Hydrogen content of the evolved gas.

Expt.	Volume (ml)	Gain in weight (μg)	Percent hydrogen content
258	76.6 gas	225	0.35
259	70.0 gas	246	0.40
blank	25.0 air	9	—

[6] R. N. Smith, W. G. Leighton, and P. A. Leighton, J. Am. Chem. Soc. **61**, 2299 (1939).

RESULTS

The Absorption Spectra

The light absorption by chlorate, bromate, and iodate ions is given in Fig. 2. The absorption curves of these ions are similar to those of other ions (I^-, Br^-, OH^-) which have been interpreted as electron transfer spectra. The increase of the extinction coefficient with decreasing wavelength is less steep in the present cases than that observed in the case of the halide and hydroxyl ions. The "absorption limits" corresponding to $\epsilon = 1$ are for:

ClO_3^-: 2250A, BrO_3^-: 2700A, and IO_3^-: 2900A.

The absorption curve of hypobromite ion, given in Fig. 3, shows a strong resemblance to

[7] R. Chapin, J. Am. Chem. Soc. **56**, 2211 (1934).

TABLE II. Dependence of the photo-decomposition of bromate on irradiation time (initial concentration of $KBrO_3$: 0.0925M; 30°C).

Expt.	Irrad. time (min.)	Bromate ions decompos.	Hypobromite formed	Oxygen molec. formed	Quanta absorb. by sol.	Quantum yield Φ	Percent convers. of bromate	Percent hypobromite yield	Percent oxygen yield
		per second $\times 10^{-18}$							
122	7.5	1.51	1.10	1.75	8.42	0.18	11	73	102
121	15	1.43	1.04	1.44	8.27	0.17	20	73	(89)
123	30	1.19	0.56	1.52	8.13	0.15	33	47	100
120	60	1.11	0.22	1.50	8.28	0.13	62	20	96
119	120	0.81	0.01	1.21	7.54	0.11	91	0.6	98

that of nitrate ion.[1] The spectrum of undissociated hypobromous acid is also given in Fig. 3.

The Photo-Decomposition of the Bromate Ion

When dilute (0.002 M to 0.2 M) potassium bromate solutions are irradiated, they evolve gas, and the concentration of bromate decreases. Chemical analysis shows that hypobromite and bromide ions are formed. The absence of bromite in the irradiated solution was shown in a special experiment. In Fig. 4 the concentration changes of these three ions during a typical run are given. Since the hypobromite concentration passes through a maximum and the bromide concentration increases steadily, it is evident that hypobromite is an intermediate product of the decomposition. Furthermore, since the initial rate of decomposition of bromate ($-\Delta BrO_3^-/\Delta t$) and the initial rate of the hypobromite formation ($\Delta BrO^-/\Delta t$) are equal, the main processes taking place during the irradiation can be represented by:

$$BrO_3^- + h\nu \rightarrow BrO^- + O_2, \quad (2)$$

and

$$BrO^- + h\nu \rightarrow Br^- + \tfrac{1}{2}O_2. \quad (3)$$

The evolved gas contains 99.2 to 99.5 percent oxygen, accompanied by a small amount of hydrogen. In two experiments the hydrogen content was quantitatively determined in an apparatus similar to that used for the microcombustion of organic compounds. The gas, dried over magnesium perchlorate, passed first through an electrically heated capillary tube filled with palladinized asbestos. The water formed was absorbed in a tube filled with mag-

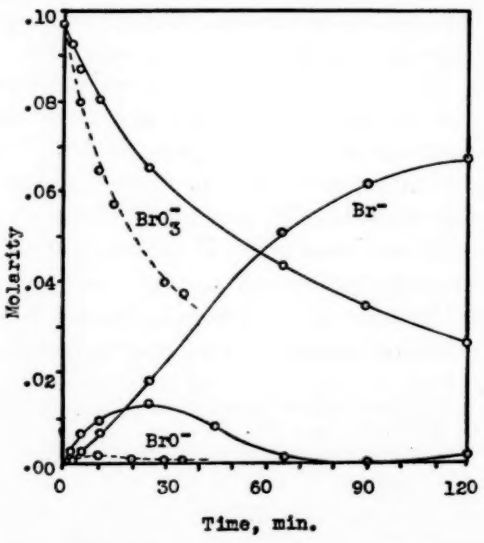

FIG. 4. Photo-decomposition of bromate. Change of concentration of bromate, hypobromite, and bromide with time.

——— ammonium ions absent.
- - - - - - ammonium ions present.

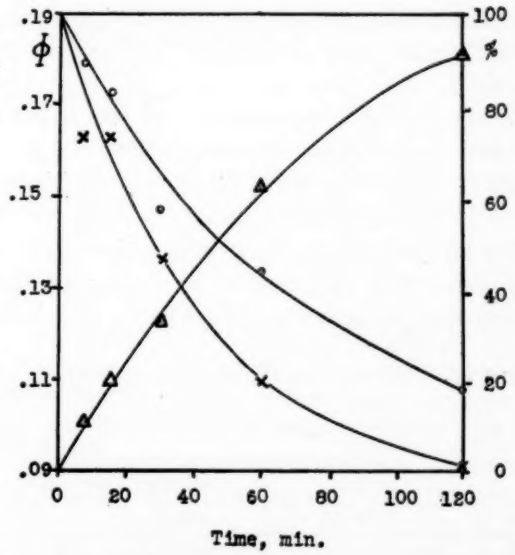

FIG. 5. Photo-decomposition of bromate. Dependence of quantum yield Φ(○), hypobromite yield (×), and bromate conversion (△) on time.

TABLE III. Dependence of the photo-decomposition of bromate on the initial concentration (30-min. irradiation; 30°C).

Expt.	Initial bromate conc. mole/l.	Bromate ions decompos. (per second $\times 10^{-18}$)	Hypobromite formed (per second $\times 10^{-18}$)	Oxygen molec. formed (per second $\times 10^{-18}$)	Quanta absorb. by sol. (per second $\times 10^{-18}$)	Quantum yield Φ	Percent convers. of bromate	Percent hypobromite yield	Percent oxygen yield
59	0.1847	1.45	0.73	—	9.26	0.17	20	50	—
75	0.0874	1.03	0.46	0.67	5.92	0.17	31	45	98
76	0.0106	0.24	0.02	0.24	2.43	0.10	57	7	77
77	0.0021	0.07	0.01	0.04	1.5	0.05	76	—	48

nesium perchlorate, and the tube was then weighed on a Kuhlman microbalance. The results of Table I show that in the photo-decomposition of the bromate, hydrogen is formed by a side reaction. In Tables II to VI, where the results of some experiments on the bromate decomposition are summarized, hydrogen formation is neglected.

The quantum yield of process (2) was measured at different lengths of irradiation time (cf. Table II). In Fig. 5 the true quantum yield Φ_0 was determined by extrapolating the measured quantum yield Φ to "zero" time. It is 0.19 at 30°C. The dependence of Φ on time is caused by the decrease of the absorption of the photochemically active radiation by the bromate, and the accumulation of light absorbing hypobromite (and bromide) in the couse of the experiment.

The hypobromite yield (i.e., the number of hypobromite ions formed per bromate ions decomposed) also decreases during the irradiation, since hypobromite undergoes further decomposition.

If the initial concentration of the bromate solution is gradually decreased from 0.2 *M* to 0.002 *M* (cr. Table III) and the time of irradiation is kept constant, the dependence of the quantum yield and the hypobromite yield on the conversion of bromate is similar to their dependence on time (shown in Fig. 5). This is due to the same effects as mentioned in the case of time dependence.

Change of the temperature within the range of 13.5° to 36°C does not affect the quantum yield and the value of the conversion showing the absence of rate determining secondary processes occurring in the dark.

The influence of the wave-length on the decomposition was not investigated. However, some experiments were made with various filter solutions in vessel *C* while the bromate solution was in vessel *D*. The results are given in Table IV. Since 50 percent acetic acid absorbs all light of wave-length shorter than 2300A, it follows that at least 65 percent of the bromate decomposition is caused by the light in the spectral region of 2300A to 2600A. It is also seen that chloracetic acid absorbs almost all the photochemically active light.

Since every bromate ion gives on decomposition one molecule of oxygen and every hypobromite ion gives half a molecule, the number of oxygen molecules, n_{O_2}, evolved should be equal to: $\frac{3}{2}n_{BrO_3^-} - \frac{1}{2}n_{BrO^-}$. The ratio of these two quantities is given in column 10 (cf. Tables II to VI) as oxygen yield. In most experiments it is approximately 100 percent. Deviations from this value are due to errors in the measurements, if supersaturation occurs.

The influence of the following factors on the photo-decomposition of bromate was studied:

TABLE IV. Dependence of the photo-decomposition of bromate on the spectral region; experiments with various light filters (30-min. irradiation; 30°C).

Exp.	Filter sol.	Initial bromate conc. mole/l.	Bromate ions decomp. (per second $\times 10^{-18}$)	Hypobrom. form. (per second $\times 10^{-18}$)	Oxygen molec. form. (per second $\times 10^{-18}$)	Quant. abs'd by sol. (per second $\times 10^{-18}$)	Quant. yield Φ	Percent conv. of bromate	Percent hypobromite yield	Percent oxygen yield
205	H_2O	0.0952	1.08	0.66	1.33	9.00	0.12	17.5	61	103
206	CH_3COOH, 50%	0.0936	0.70	0.32	0.91	3.80	0.18	11.5	46	101
209	$CH_2ClCOOH$, 2*M*	0.940	0.02	0.01	0.04	0.20	0.11	0.4	55	(140)

TABLE V. Dependence of the photo-decomposition of bromate on the *p*H (30-min. irradiation; 30°C).

Exp.	Initial brom. conc. mole/l.	Bromate in sol. of	Bromate ions decomp.	Hypo-brom. formed	Oxygen molec. formed	Quant. abs'd by sol.	Quant. yield Φ	Percent conv. of bromate	Percent hypo-brom. yield	Percent oxygen yield
			per second $\times 10^{-18}$							
192	0.0922	H_2SO_4, 4*M*	1.72	0.30	2.20	10.74	0.16	49	17	91
109	0.0947	H_2SO_4, 0.05*M*	1.55	0.24	1.96	11.0	0.14	43	16	(89)
124	0.0867	$HBrO_3$, 0.1*M*	1.33	0.22 (0.40)*	1.61	8.14	0.16	40	16 (46)*	95
179	0.0915	NaOH, 4*M*	1.69	0.16	2.18	9.02	0.19	49	10	89

* Corrected for losses of bromine in the oxygen evolved.

(a) The addition of either hypobromite or bromide, or both, had no influence on the primary photo-reaction; the over-all quantum yield decreases, however, since part of the photo-active radiation is absorbed by the added ions.

(b) The addition of 0.02 *M* to 4.0 *M* potassium hydroxide has no influence on either the value of the quantum yield or on the nature of the reaction products. In the acid range, when 0.1 *M* bromic acid or mixtures of sulfuric acid and potassium bromate are irradiated, the decomposition is accompanied by secondary reactions forming elementary bromine in accordance with the equations:

$$HBrO + HBr \rightarrow Br_2 + H_2O,$$
$$HBrO_3 + 5\,HBr \rightarrow 3\,Br_2 + 3\,H_2O.$$

Part of the elementary bromine is carried off with the oxygen evolved. The second reaction gives an apparent increase in bromate conversion. The results of some experiments are summarized in Table V. The quantum yield is not much effected by the change of the *p*H.

It should be mentioned that in case the bromate solution is acidified with hydrochloric acid, a thermal reaction takes place in which chlorine and hypobromous acid are formed;[8] due to these, the light absorption changes considerably as time goes on. Consequently, both the quantum yield and the conversion are much lower than under the conditions of the experiments in Table V.

(c) Certain cations in the bromate solution may effect the secondary reactions. Thus, if potassium bromate is irradiated in the presence of ammonium ion, the hypobromite formed reacts according to the equation:

$$3\,BrO^- + 2\,NH_4^+ \rightarrow N_2 + 3\,Br^- + 2\,H^+ + 3\,H_2O,$$

[8] Unpublished results of this laboratory.

and its concentration is, therefore, low during the photo-decomposition. The active radiation in the spectral range of 2300A to 2600A is absorbed by bromate alone and consequently the rate of decomposition in this case is 60 percent to 100 percent greater than in the absence of ammonium ion (cf. Fig. 4).

The photo-decomposition of silver bromate has some special features, too. Aside from the fact that all the bromide is precipitated as silver bromide, elementary silver is also formed, and it is not possible to detect any hypobromite in the solution. This reaction was not investigated in sufficient detail in order to decide as to whether elementary silver is a primary product of the photo-decomposition of silver bromate or whether it is formed from secondary products.

The Photo-Decomposition of Hypobromite Ion

The decomposition of potassium hypobromite was studied only in alkaline solutions, since in acid solution it decomposes thermally according to:

$$HBrO + Br^- + H^+ \rightarrow Br_2 + H_2O$$

and in neutral solution, the dark reaction,

$$3\,BrO^- \rightarrow BrO_3^- + 2\,Br^-,$$

is very fast.

Upon irradiation of an alkaline hypobromite solution, oxygen, bromate, and bromide ions are formed. In Fig. 6, the concentration changes of these ions during an experiment are given. While the bromate curve passes through a flat maximum, the hypobromite curve falls steeply toward zero. The comparison of the initial decomposition rate of hypobromite ($-\Delta BrO^-/\Delta t$) with the initial rate of formation of bromate ($\Delta BrO_3^-/\Delta t$) shows a ratio of $-\Delta BrO^-/\Delta BrO_3^- \geq 4$.

TABLE VI. Photo-decomposition of various halate ions (30-min. irradiation; 30°C).

Exp.	Halate ion	Init. halate conc. mole/l.	Halate ions decomp. (per second $\times 10^{-18}$)	Hypo-halite formed (per second $\times 10^{-18}$)	Oxygen molec. formed (per second $\times 10^{-18}$)	Quant. abs'd by sol. (per second $\times 10^{-18}$)	Quant. yield Φ	Percent conv. of halate	Percent hypo-halite yield	Percent oxygen yield
168	ClO_3^-	0.1006	0.217	0.00	0.254	0.85	0.26	6.0	0.0	78
116	BrO_3^-	0.0930	1.64	0.58	2.18	9.06	0.18	46	35	100
197	IO_3^-	0.0997	0.196	0.02	0.234	(8.22)	(0.02)	5.0	11	83

The quantum efficiency Φ of the hypobromite decomposition was determined only for that spectral region which is absorbed by chloroacetic acid was found to be about 0.4.

The Photo-Decomposition of Chlorate and Iodate Ion

The primary photo-decomposition of these two ions is similar to that of the bromate (cf. Table VI).

Since the absorption limit of the chlorate is at a shorter wave-length, the total number of quanta is about twelve times smaller than that in the case of the bromate, and the conversion is correspondingly low. The quantum yield of the chlorate decomposition is about the same as that of the bromate. Careful determinations could not dectect any hypochlorite. Evidently the hypochlorite formed by the photo-decomposition of the chlorate ions decomposes immediately under the influence of the strong radiation in the spectral range 2500A to 2600A, which in this case is absorbed by the hypochlorite alone. The yield of chloride ions is, therefore, 100 percent. Perchlorate is not formed.

Though the absorption by the iodate ion begins at a longer wave-length, the photo-decomposition is comparatively slow because of the fact that the hypoiodite produced is unstable and iodine is set free. Iodine absorbs the active radiation strongly and thereby retards the iodate decomposition.

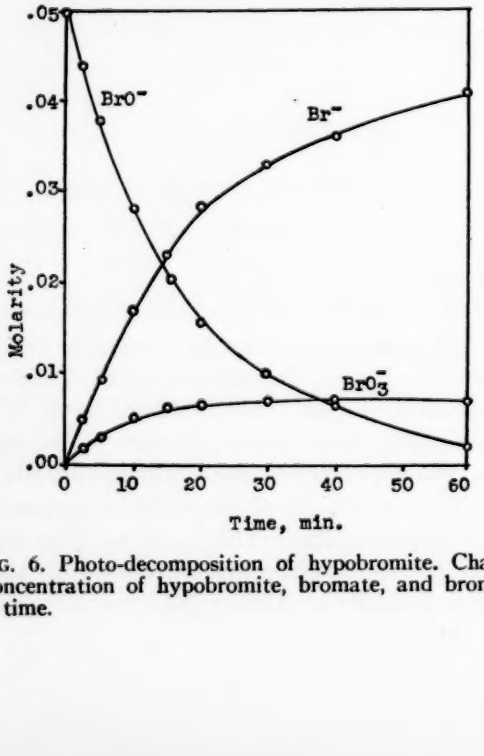

FIG. 6. Photo-decomposition of hypobromite. Change of concentration of hypobromite, bromate, and bromide with time.

DISCUSSION

If we assume that the absorption spectra of the halate ions given in Fig. 2 are electron transfer spectra, the energy corresponding to the absorption frequency should be given by Eq. (1). Only in the case of chlorate ion are experimental data available which allow to check the validity of this relation.

The value for $E_{ClO_3^-}+H_{ClO_3^-}$ is obtained from the following equations:

$$\tfrac{1}{2}\,H_2(g)+\tfrac{1}{2}\,Cl_2(g)+\tfrac{3}{2}\,O_2(g)+(aq)\rightarrow H^+(aq)+ClO_3^-(aq)+20.75\text{ kcal.},$$

$$H^+(aq)+\text{electron}\rightarrow\tfrac{1}{2}\,H_2(g)+90.1\text{ kcal.},$$

$$ClO_3(g)\rightarrow\tfrac{1}{2}\,Cl_2(g)+\tfrac{3}{2}\,O_2(g)+37\text{ kcal.}$$

. . . . . .

$$ClO_3(g)+\text{electron}+(aq)\rightarrow ClO_3^-(aq)+147.85\text{ kcal.}$$

The sum of E_-+H_- thus calculated for a number of monovalent anions from the latest thermodynamic data, is listed in Table VII, together with the above value for the chlorate ion. From the absorption limit of these anions with relation (1), E_{H_2O} can be calculated. The deviation from the mean value of 22.5 kcal. is not very great,*** and in view of the inaccuracy to which the deter-

*** Farkas and Farkas (see reference 2) calculated 18 kcal. for EH_2O since they used a somewhat lower figure for the heat of reaction of $H^+(aq)+$electron.

mination of the absorption limit is amenable, it seems that E_{H_2O} is essentially independent of the nature of the anion.

In the case of bromate and iodate ions, by assuming $E_{H_2O}=22$ kcal., and using known values for the heats of formation of BrO_3^-(aq) and IO_3^-(aq) from the elements (102 kcal. and 145 kcal., respectively), the heats of formation of the hypothetical compounds BrO_3 and IO_3 may be calculated. With $h\nu_{BrO_3^-}=106$ kcal. and with $h\nu_{IO_3^-}=99$ kcal., $\Delta Hf^0_{BrO_3^-}$ is $+23$ kcal. and $\Delta Hf^0_{IO_3^-}$ is -28 kcal. Because of the lack of any thermochemical data concerning the oxides of bromine, the former figure is only of theoretical interest; the latter may be related to the heat of formation of $I_2O_5(c)$, $\Delta Hf^0_{I_2O_5}=-42.0$ kcal.

The primary process of the absorption of the three halate ions is given by:

$$XO_3^-(H_2O)+h\nu_0\rightarrow XO_3+H_2O^-. \qquad (4)$$

In the case of the halide ions, when, after the light absorption, the electron returns to its initial state, the energy liberated is dissipated as heat. On the other hand, in the case of the halate ions, the energy gained by the reverse process of (4) may induce a decomposition according to

$$(XO_3^-\cdot H_2O)\rightarrow XO^-+O_2+H_2O. \qquad (5)$$

The thermal decomposition of chlorate and bromate into oxygen and hypohalite ion is exothermic, the heat of reaction being 5 kcal. and 10 kcal., respectively. The corresponding reaction with iodate possibly occurs as well, since the heat liberated in process (5) considerably exceeds the heat of reaction of -34.5 kcal. The "self"-decomposition of the complex $(XO_3^-\cdot H_2O)$ is most probably the reason for the far higher quantum yield in the present cases as compared with that of the halide ions.

A further possibility for a photo-chemical change is the process in which the electron jumps from its intermediate state in the hydration layer to a positive ion. In the case of the halide ions, hydrogen ions mainly serve as electron acceptors and if their concentration is increased, the quantum yield of the hydrogen evolution also increases. The presence of hydrogen in the gas obtained in the photo-decomposition of bromate in the pH range 6 to 8 indicates that an analogous process occurs according to

$$(BrO_3^-H_2O)+h\nu_0\rightarrow BrO_3+H_2O^-\xrightarrow{+H^+} BrO_3+H+H_2O. \qquad (6)$$

TABLE VII. Comparison of ionic energies (Eq. 1) to experimental values.

Ion	A	$h\nu_0$ kcal.	H_-+E_- kcal.	E_{H_2O} kcal.
Cl^-	2060	137.5	159	21.5
Br^-	2310	122.8	145.7	22.9
I^-	2720	104.2	128.9	24.7
OH^-	2200	129	155	26.0
SH^-	2750	103	121	18.0
ClO_3^-	2250	126	148	22.0

The corresponding quantum yield is less than 0.001, but not much lower than the quantum yield of the hydrogen evolution in neutral or slightly alkaline solutions of iodides.

The ultimate products of the secondary reactions accompanying (6) are in the case of BrO_3, necessarily Br^-, O_2, and hypobromite, and it is not difficult to give various reaction schemes which will lead to these products.

A process similar to (5) in the case of hypobromite may lead to its decomposition according to

$$(BrO^-\cdot H_2O)+\rightarrow H_2O+Br^-+O, \qquad (7)$$

though the dissociation of BrO^- into Br^- and O requires about 52 kcal. If we postulate the following secondary reactions

$$O+BrO^-\rightarrow Br^-+O_2, \qquad (8)$$

$$O+BrO^-\rightarrow BrO_2^-, \qquad (9)$$

$$BrO_2^-+BrO^-\rightarrow Br^-+BrO_3^-, \qquad (10)$$

the formation of bromate during the photo-decomposition of hypobromite is readily explained. The relative probabilities of (8) and (9) will determine the ratio $-\Delta BrO^-/\Delta BrO_3^-$ which in the experiments was about 4.

It may be mentioned that the photo-decomposition of hypochlorite apparently involves similar reactions, since in this case, too, besides chloride and molecular oxygen, chlorate is formed in an appreciable quantity.[9]

[9] A. J. Allmand and W. W. Webb, Zeits. f. physik. Chemie **A131**, 189 (1928).

THE JOURNAL OF CHEMICAL PHYSICS VOLUME 16, NUMBER 9 SEPTEMBER, 1948

The Absorption Spectrum of Diborane*

W. C. PRICE
Ryerson Physical Laboratory, University of Chicago, Chicago 37, Illinois
(Received May 7, 1948)

The absorption spectrum of diborane has been investigated in the infra-red from 1–25μ and in the vacuum ultraviolet down to 1000A. The rotational structure obtained for certain of the infra-red bands rules out the ethane-type structure but agrees very well with the interpretation of the electron diffraction results in terms of a bridge model. The ultraviolet spectrum indicates a simple electronic structure and a first ionization potential about 11–12 volts.

INTRODUCTION

IN a recent review of the evidence bearing on the problem of the structure of diborane Professor R. S. Mulliken[1] stressed the fact that while there was a growing weight of experimental data favoring the bridge model as against the ethane-type structure, it was desirable that some unambiguous direct evidence should be forthcoming so that a clear-cut decision could be made between the two. This has now been obtained in the present work as a result of the examination of the infra-red spectrum of diborane under greater resolving power than had hitherto been used. The rotational structures of some of the perpendicular bands have been resolved, and these have been found to show the alternation of intensity to be expected from a bridge model but which cannot possibly be associated with a structure of the ethane type in either the eclipsed or staggered form. A very close analogy of the band structures and envelopes observed in diborane with those of certain ethylene bands is evident. In particular, those bands of ethylene and diborane (bridge model) in which the CH_2 and the terminal BH_2 groups undergo the same bending and stretching moments exhibit a striking similarity in their band envelopes. This indicates that the degree of departure from a symmetrical top is much the same for both molecules. The assignments seem to fit in well with a normal coordinate treatment of the bridge model due to Bell and Longuet-Higgins,[2] though there are some minor discrepancies.

* Work done under Office of Naval Research Contract N6ori-20, T.O. IX at the University of Chicago during the author's leave of absence from Imperial Chemical Industries (Billingham Division), England.

[1] R. S. Mulliken, Chem. Rev. **41**, 207 (1947).

[2] R. P. Bell and H. C. Longuet-Higgins, Proc. Roy. Soc. **183**, 357 (1945).

EXPERIMENTAL

A specimen of diborane of high purity prepared by Dr. G. W. Schaeffer of the chemistry department was used. It was fractionally distilled from liquid air in the usual gas-handling apparatus into the absorption cell which was of glass with windows of rock salt or potassium bromide. The cell length was 10 cm and runs were made at pressures varying from a few tenths of a mm up to 70 cm. The instrument employed was a Perkin-Elmer recording spectrometer fitted with lithium fluoride, sodium chloride, and potassium bromide prisms. Its performance can be judged by the fact that it was capable of resolving the rotational structure of the 4.2μ band of carbon dioxide without difficulty.

RESULTS

Apart from the greater detail observed in the bands as a result of the higher resolving power, the general features of the spectrum obtained were essentially similar to those reported by Stitt.[3] There are some minor differences in the wave-lengths of the weaker bands but the most important discrepancy is our failure to reproduce the band structure reported by Stitt in the 25μ region although our prisms and aperture were several times greater than his.

The general view of the spectrum is given in Fig. 1. Higher resolution pictures of the bands around 2600, 1175, and 974 wave numbers are shown in Figs. 2a and 2b. Table I gives the frequencies of the band centers and their assignments. Table II contains the Raman data of Anderson and Burg[4] with the assignments of

[3] F. Stitt, J. Chem. Phys. **9**, 780 (1941).

[4] T. F. Anderson and A. B. Burg, J. Chem. Phys. **6**, 586 (1938).

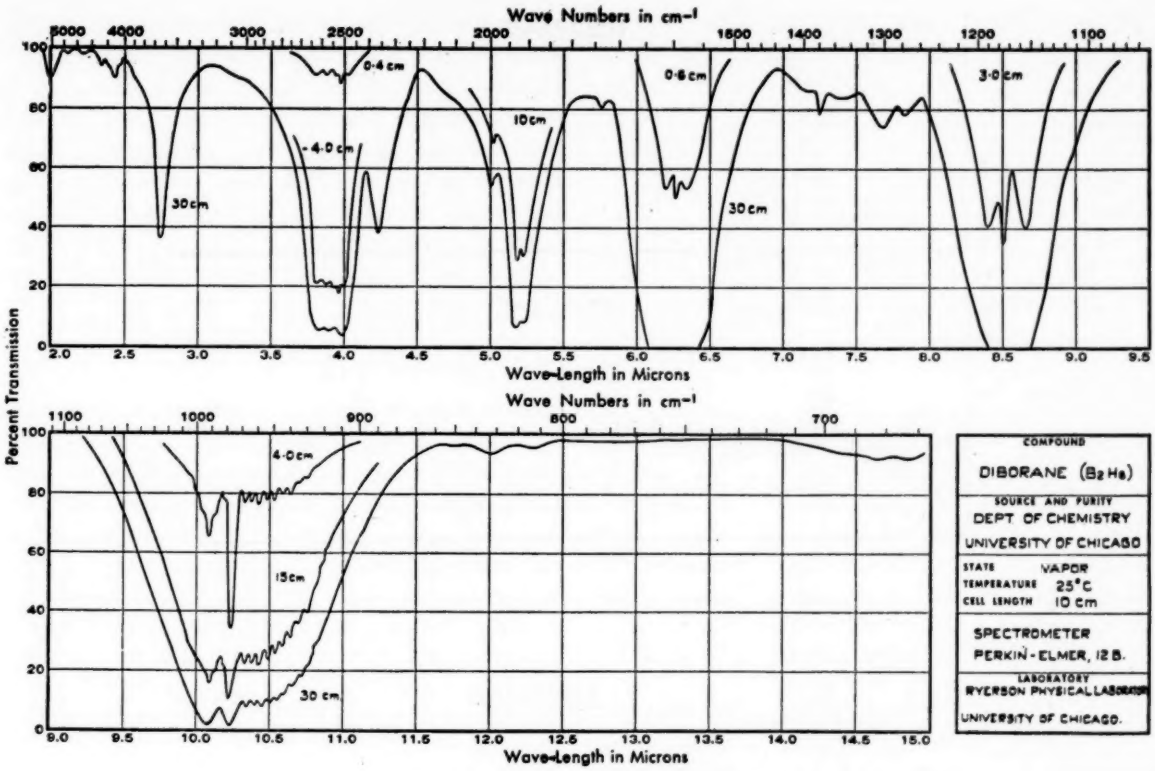

FIG. 1. The spectrum of diborane from 1.5 to 15μ.

Bell and Longuet-Higgins.[2] In our preliminary note[5] the axes of reference in the molecule were taken the same as those used by Herzberg for ethylene[6] (*Ox* axis of smallest moment of inertia, *Oz* axis of largest moment of inertia). However in order to preserve continuity with the treatment of Bell and Longuet-Higgins their axes have been retained—*Ox* axis of smallest moment of inertia, *Oy* axis of largest moment of inertia. While a change to the more conventional axes only affects the symmetry species by interchanging B_1 and B_2, it would involve the renumbering of nine of the fundamental frequencies.

DISCUSSION

The interpretation of the electron diffraction results in terms of a bridge model[7,8] is given in Fig. 3 while Fig. 4 gives the normal vibrations of the bridge model according to Bell and Longuet-Higgins.[2] The factors which eliminate the ethane-type model will be discussed in greater detail as we come to them, but for the sake of convenience they are enumerated here. (1) the alternation of intensity of the rotational structure; (2) the asymmetric top character of the band envelopes; (3) the incompatibility of the magnitude of the rotational separations with the interpretation of the electron diffraction results in terms of an ethane-structure; (4) the comparative success of the normal coordinate treatment of a bridge model in explaining the Raman and infra-red spectra of the molecule.

The rotational structures of the perpendicular bands: The most striking features of the spectrum are exhibited by the perpendicular bands illustrated in Figs. 2a and 2b. The alternation of intensity indicates that the molecule belongs to the symmetry group D_{2h} like ethylene. The alternation to be expected in the perpendicular bands due to the spins of the three pairs of hydrogen nuclei is 9:7.[9] It is, of course, super-

[5] W. C. Price, J. Chem. Phys. **15**, 614 (1947).
[6] G. Herzberg, *Infrared and Raman Spectra* (D. Van Nostrand Company, Inc., New York, 1945), p. 107.
[7] S. H. Bauer, Chem. Rev. **31**, 43 (1942).
[8] R. P. Bell, private communication.
[9] G. Herzberg and E. Teller, private communication.

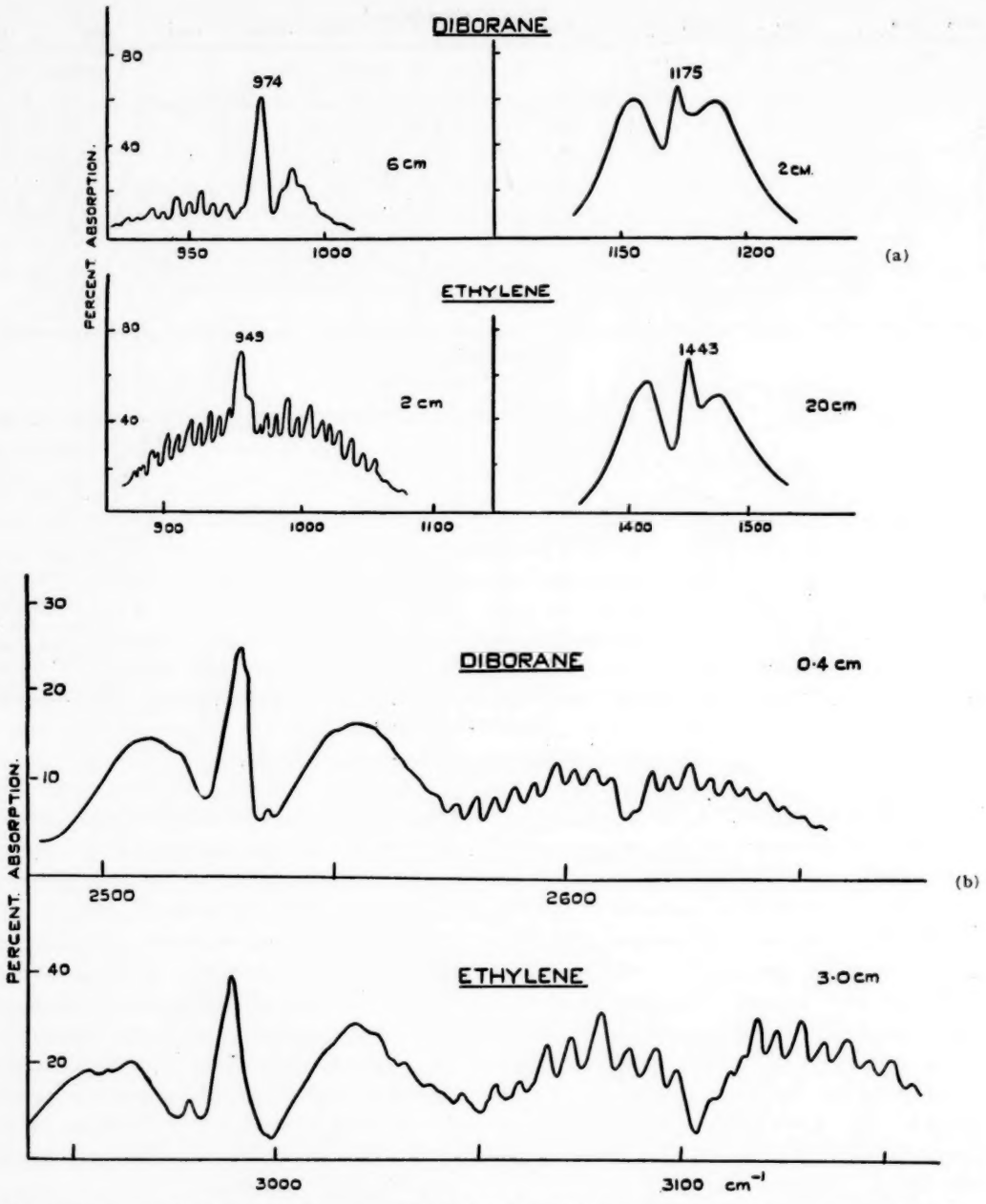

FIG. 2. Corresponding bands in diborane and ethylene in which the terminal XY_2 groups undergo the same bending and stretching motions. The pressure of the gas is given in each case in cm of Hg.

imposed upon a Boltzmann distribution due to the temperature, and is also affected by the finer rotational structures within the Q sub-branches. It is further influenced by the existence of the two isotopes B^{10} and B^{11}, their abundance being such that the relative numbers of $B^{11}-B^{11}$, $B^{11}-B^{10}$, and $B^{10}-B^{10}$ molecules are roughly 2:1:0.125; however, as the vibrations involved are largely in the B—H bands and the borons move but little, the isotope effects are small. In addition, the intensity alternation in polyatomic molecules cannot be expected to be as regular as in diatomic molecules, since the various sub-bands overlap and true integrated intensities cannot be measured. This overlapping, as well as slight differences in the structures of the dif-

ferent sub-bands, may affect the observed intensities of the various Q branches, thus producing apparent anomalies in the intensities of the observed maxima. The intensity alternation is best brought out with only moderate resolution—sufficient to resolve the Q branches of the various sub-bands from each other, but low enough to integrate the intensity of each Q branch—and with the lowest feasible total absorption. (With higher pressures or longer paths, much of the sharp structure may be giving 100 percent absorption even though the apparent absorption with moderate resolution may be much less than this.)

The alternation of intensity shows up clearly in the ${}^{P}Q$ branch of the 974-cm^{-1} diborane band, though slightly inadequate resolving power prevents its being observed distinctly in the ${}^{R}Q$ branch. It is also quite clear in both branches of the 2614-cm^{-1} band. In both bands the alternation is nearly, though not quite, as pronounced as it is in the corresponding bands of ethylene, for which the spin factor is 10:6.[10]

The analysis for the two perpendicular bands in terms of a symmetric top rotator, to which the molecule closely approximates, is given in Table III. In the case of the 2614-cm^{-1} band, the numbering of the Q branches was determined by the fact that the band should be approximately symmetrical about its origin, with the ${}^{P}Q_1$ and ${}^{R}Q_0$ maxima weak or absent as a result of energy level shifts caused by the slight asymmetry of the molecule. This numbering associates odd values of K'' with the strong Q maxima and even values of K'' with the weak maxima, in agreement with theoretical predictions. The numbering in the case of the 974-cm^{-1} band is less unambiguous, but the most reasonable choice (the four central Q maxima missing) also associates odd values of K'' with the strong maxima. (In the case of ethylene, the situation is reversed because of the presence of only two pairs of hydrogen nuclei instead of three, even values of K'' being associated with the strong Q branches.[10])

[10] The intensity alternation in the 949-cm^{-1}-ethylene band is shown in American Petroleum Institute spectrograms, and is shown in both the 3105 and 949-cm^{-1} bands in records made by the present author (Fig. 2). It is not shown in the record of the 949-cm^{-1} band given by Gallaway and Barker [J. Chem. Phys. 10, 88 (1942)], but this may be ascribed to the high resolution and high pressure used. For a theoretical discussion of alternating intensities in the ethylene bands, see G. Herzberg, *Infrared and Raman Spectra* (D. Van Nostrand Company, Inc., New York, 1945), p. 480 and elsewhere.

TABLE I. Table of frequencies of centers of diborane bands and their assignments.

Frequency (Stitt)	Intensity	Frequency (Price)	Intensity	Assignment
393, 412, 431	strong	*ca.* 430	medium	$\pi \times \nu_{10}$
673, 685	* weak	not found	(impurity?)	
—		811	v. weak	
831	weak	831	v. weak	
—		849	v. weak	
981	strong	974 (ps. Q)	strong	ν_{14} ($\perp$ type C)
1154, 1178, 1197	very strong	1175 (ps. Q)	v. strong	ν_{18} ($\parallel$ type A)
1274		1267	fairly weak	ν_9 (1283)
1311	medium	1302	fairly weak	$\perp$ type B?
1377	medium	1377	fairly weak	
1405	medium	*ca.* 1405	v. weak	
1587, 1608, 1626	very strong	1604 (ps. Q)	v. strong	ν_{17} ($\parallel$ type A)
1722	weak	?		
1852, 1874	strong	1850,* −1870	strong	
1993	medium	1984*	weak	ν_{13} ($\perp$ type C)
2134	very weak	2088, 2124, 2143	v. weak	
2217	very weak	2200, 2215, 2230	v. weak	
2353	strong	2345*	medium	$\nu_3+\nu_{18}$ ($\parallel$ type A)
2558	strong	2522 (ps. Q)	strong	ν_{16} ($\parallel$ type A)
2625	strong	2614 (${}^{R}Q(0)$)	strong	ν_8 ($\perp$ type B)
3135	very weak	3135	v. weak	
3670	strong	3600–3700	strong	$\nu_1+\nu_{18}$, $\nu_{11}+\nu_{18}$, $\nu_3+\nu_{16}$, $\nu_3+\nu_8$
4040	weak	4035	v. weak	
4250	weak	4155	weak	$\nu_1+\nu_{17}$
—		4350	weak	$\nu_1+\nu_{13}$, $\nu_2+\nu_3+\nu_{18}$
4550	weak	4473	v. weak	
—		4815	v. weak	
5150	weak	5022	weak	($\parallel$ type A) $\nu_1+\nu_{16}$
—		5140	v. weak	
		5210	v. weak	
		5400	v. weak	
5800	weak	5760	weak	$\nu_1+\nu_2+\nu_{18}$, $\nu_2+\nu_{11}+\nu_{18}$, $\nu_2+\nu_3+\nu_{16}$, $\nu_3+\nu_3+\nu_8$

* These bands have been examined in greater detail by Dr. R. D. Cowan and will be reported by him in a subsequent article.

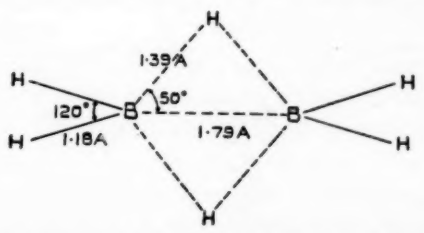

FIG. 3. Structure of diborane molecule according to the interpretation of the electron diffraction results in terms of a bridge model.

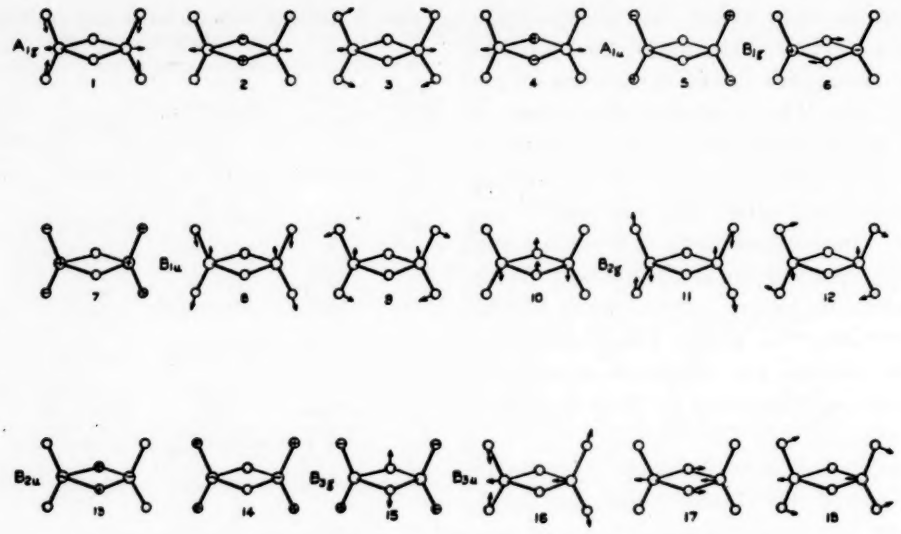

FIG. 4. The character of the normal vibrations of "bridge" diborane. (After Bell and Longuet-Higgins.[2])

The accuracy of the measurements is not much better than 0.5 cm^{-1} and in fact the absolute values in the 2614 band may be out by as much as two wave numbers because of the lack of good wave-length standards in the immediate vicinity of the bands. The convergence of the bands is so small that no separate values of $C-D$ could be derived for the upper and lower states. The value of $C-D$ for the 2614 band is 2.07 cm^{-1}. That for the 974 band is 2.05 cm^{-1}. The expected values for C and D calculated from data based on the bridge model interpretation are $C=2.63$ cm^{-1} and $D=0.58$ cm^{-1} or 0.55 cm^{-1}, according to which of the two larger moments of inertia is taken. This is as good agreement as can be expected, while on the other hand the values calculated using the data obtained by interpreting the electron diffraction results in terms of the ethane-type structure[11] give $C=1.94$ and $D=0.65$ cm^{-1}, i.e., a spacing of consecutive rotational lines by 2.6 cm^{-1}, which is quite incompatible with the value of *ca.* 4.1 cm^{-1} observed. Moreover for an ethane-type molecule it is to be expected that as a result of the influence of nuclear spin every third line should be accentuated as for example in the 12μ band of ethane.[12] In many bands of ethane the rotational structure is quite complicated owing to effects such as Coriolis interaction. It is clear that at least for the bands so far discussed such effects are not operative.

TABLE II. The Raman data of Anderson and Burg* with the assignments of Bell and Longuet-Higgins.**

ν in cm^{-1}	Intensity	Assignment
793	5	$\nu_4(B^{11}-B^{11})$
806	4	$\nu_4(B^{11}-B^{10})$
821	3 (broad)	$\nu_4(B^{10}-B^{10})$, ν_{12}
1008	diffuse	ν_7
1180	2	ν_3
2102	10	ν_2
2489	3	ν_{11}
2523	10	ν_1

* See reference 4.
** See reference 2.

Another perpendicular band at 1980 cm^{-1} has been resolved by Dr. R. D. Cowan[13] who will be discussing it in a later report. It has a rotational structure very similar to the band at 974 cm^{-1} (Fig. 2a). Spectroscopic values for the geometrical parameters of the diborane molecule cannot be calculated until data on the rotational structure of the parallel bands and also on the isotope substituted molecules become available.

The nature of the band envelope of an infrared absorption band depends upon the symmetry of the vibration and the magnitudes of the principal moments of inertia of the molecule. For molecules like ethylene and diborane (bridge model) the deviations from the symmetrical top

[11] S. H. Bauer, J. Am. Chem. Soc. **59**, 1096 (1937).
[12] R. G. Owens and E. F. Barker, J. Chem. Phys. **10**, 146 (1942).
[13] R. D. Cowan, to be published shortly in J. Chem. Phys.

envelope are large for low values of the rotational quantum number (i.e., close to the band center) but rapidly disappear for the higher values. Thus the shape of the center of a band is a very good indication of the degree of asymmetry. It is clear from Figs. 2a and 2b that the asymmetry of ethylene and diborane must not be very different. The ratios of their principal moments of inertia are for ethylene 1:0.825:0.0172 and for diborane 1:0.94:0.022—that is, diborane according to the bridge model interpretation of the electron diffraction data is a somewhat closer approximation to a symmetrical top than ethylene. Slight adjustments such as small increases in the terminal BH_2 angle and diminutions in the internal BH_2 angle would bring the ratios closer. Figure 2 shows the great similarity which also exists in the band envelopes of the corresponding parallel bands of ethylene and diborane. These bands correspond to the vibrations in which the CH_2 and the terminal BH_2 groups undergo the same bending and stretching motions. No similarity of this sort could be established with any bands of ethane.

ASSIGNMENT OF THE BANDS

Apart from minor differences (particularly ν_9 and ν_{13}) and the extension to the overtones, our assignments given in Table I agree with those of Bell and Longuet-Higgins.[2] The more important bands will now be discussed individually and features which support the assignments will be elaborated.

400 cm^{-1}: Definite confirmation of the bands 412 and 393 reported by Stitt[3] has not been obtained in spite of the fact that larger prisms and greater apertures were used in this work. Stitt remarks in his paper that the shape on the long wave-length side of the 412-cm^{-1} band is rather uncertain due to the high percentage of stray radiation and the consequent low sensitivity in this extreme range of the KBr prism. At high pressures (*ca.* 40 cm) we find relatively continuous absorption below 450 cm^{-1} and there appears to be the possibility of a weak diffuse maximum around 430, but the peaks reported at 412 and 391 occur in our background. The absorption is probably not to be associated with a fundamental vibration. It could be the difference band $\nu_{17}-\nu_3$ (1604 − 1180 = 424). Bell[2,14] has assigned it to the 2→3 transition of the rocking vibration ν_{10}. This is a special type of vibration which might be expected to have a low frequency and for which the intensities of the overtones 1→2, 2→3 are comparable with the fundamental. It has been shown by Bell[2] that in this type of ring bending the potential energy is proportional to the fourth power of the displacement and as such it is not subject to the same symmetry restrictions as the other bands. The magnitude of ν_{10}, judging from normal coordinate analysis and specific heat data, appears to be about 266 cm^{-1}.

TABLE III. The line positions in the perpendicular-type bands of diborane.

2614-cm^{-1} band			974-cm^{-1} band		
K''	^PQ	^RQ	K''	^PQ	^RQ
0		2614.0	0		—
1	—	2619.0	1	—	—
2	2608.5	2624.5	2	—	983.9
3	2604.5	2627.8	3	962.7	986.9
4	2599.5	2632.0	4	958.1	990.7
5	2594.5	2635.5	5	954.1	994.5
6	2590.5	2639.5	6	950.0	999.0
7	2587.5	2642.3	7	946.0	1003.4
8	2581.5	2647.5	8	942.0	
9	2577.0		9	937.9	
10	2573.0		10	933.0	
11	2567.0				

974 cm^{-1}: This is a strong perpendicular band of type *C* (ν_{14}). Data on its rotational structure has already been given. While the *P* branch is well resolved and shows clearly the alternation of intensity, the *R* branch owing to its slight convergence is not so well separated. The isotopic $B^{11}B^{10}Q$ branch is not quite resolved from the main $B^{11}B^{11}Q$ branch and this has the effect of making this branch appear shaded slightly towards shorter wave-lengths. The isotopic separation between these two branches cannot be greater than about 3 wave numbers. Its strength relative to the 949 band in ethylene is approximately 1:3.

1175 cm^{-1}: A very strong parallel band type *A* (ν_{18}), i.e. BH_2 deformation. The similarity of the band envelope with the corresponding band of ethylene at 1443 is quite striking. The ratio of their strengths is about 10:1, which is much the same as that of the bands of the BH_2 and CH_2 stretching vibrations, the greater intensities

[14] R. P. Bell, Proc. Roy. Soc. **A183**, 328 (1944).

in diborane resulting from the larger polarities that can be produced in the BH_2 groups. The isotopic separation between the two Q branches which are not resolved cannot be greater than two or three wave numbers. Its closeness to the Raman frequency ν_3 (1180) indicates the almost complete absence of coupling via the BH_2B bridge for this type of vibration. This important point will be referred to again in connection with the 2522-cm^{-1} band.

1267, 1306-cm^{-1} peaks; 1283-cm^{-1} trough: This is tentatively assigned to ν_9 and should be perpendicular type B. Bell and Longuet-Higgins[2] have identified ν_9 with the 1405 frequency given by Stitt.[3] This is a very weak absorption barely perceptible amongst a great deal of water vapor structure and is most likely the R branch of a weak band whose Q branch is at 1375 (see next paragraph). Various factors, the main one of which is inadequate resolution in this region, prevent the observation of the rotational structure of the 1267 and 1306 peaks, though there are some indications that they are resolvable. The weakness of this band is in agreement with its interpretation as a rocking vibration as such distortion does not create appreciable polarity. In fact the analogous band in ethylene at 995 cm^{-1} is also very weak and its strength relative to the 949 ethylene bending vibration is about the same as this diborane band to the corresponding diborane bending mode at 974 cm^{-1}.

1340, 1374, 1405 cm^{-1}: A very weak band with 1374 as the pseudo Q branch. It is not easy to assign any plausible combination to this weak band.

1604 cm^{-1}: This is a very strong parallel band type A, presumably ν_{17} with R and P maxima at 1620 and 1580 cm^{-1}. It is the strongest band in the whole spectrum, being about 3 times as strong as the next strong band (1175). The assignment indicates that it involves a vibration of the bridge hydrogens along the 'protonated' double bond. It is suggested that the great strength of the band is associated with the tendency toward the formation of $BH_2^+BH_4^-$ and $BH_4^-BH_2^+$ at the turning points of the vibration. These structures which are the combination of a linear BH_2^+ and a tetrahedral BH_4^- can no doubt make a considerable contribution to the state of a suitably distorted molecule. The protonated double-bond conception of the bridge would also require the band to be very strong since as the main electron deficiency resides in the bridge any distortion within it will produce large charges. The greater part of this band lies within the water vapor transmission maximum at 6.3μ and an examination of its structure by a grating would seem feasible and worth while.

1850 and 1880 cm^{-1}: This is a very difficult region to work in because of the atmospheric water vapor lines. It has been examined with the lithium fluoride prism by Dr. R. D. Cowan who will be reporting on it in a subsequent article. It appears that the bands present have structures part of which are perpendicular in type and part of which are parallel. Such complications may arise from resonance or Coriolis interactions. If the band is to be ν_{13}, as suggested by Bell and Longuet-Higgins,[2] then it should be a perpendicular type C band similar to that at 974 cm^{-1}. It must be admitted that it has not yet been possible to obtain a satisfactory explanation of this strong absorption. Possibilities such as a combination of the twisting vibrations ν_5 and ν_{15} with intensity borrowed from ν_{17} by Fermi resonance must await a more complete knowledge of the rotational structure. Work at higher dispersion preferably in vacuum will be needed to clear up this region. It is felt unlikely that the assignments of the other bands will require radical alteration to meet the interpretive requirements of this absorption.

1990 cm^{-1}: This has been shown by Dr. Cowan[13] to be a typical type C band and has been assigned by him to ν_{13}. Neither of the combinations suggested by Bell and Longuet-Higgins give the right band type. The isotope separation of the pseudo Q branch is about +4 cm^{-1}.

2345 cm^{-1}: Medium parallel band, type A probably $\nu_3+\nu_{18}$ (1180+1175=2355), isotope shift of Q branch, *ca.* +3 cm^{-1}.

2522 cm^{-1}: Strong parallel band type A (ν_{16}) obviously analogous to the corresponding band in ethylene at 2989.5 cm^{-1} (see Fig. 2b). The absolute intensities of both this and the 2614 band in diborane are greater than the corresponding bands in ethylene by a factor of seven, which is presumably connected with greater

polarity in the BH bond. The isotope effect of the $B^{11}B^{10}Q$ branch is $+2.4$ cm^{-1}. The closeness of the frequency of this band to the Raman frequency ν_1 (2523 cm^{-1}) is very interesting since it indicates the great weakness of the coupling of the terminal BH_2 groups. The frequencies ν_1 and ν_{16} can be regarded as the "in phase" and "out of phase" combinations of the symmetrical valence BH frequency of the terminal BH_2 groups. Thus in diborane the coupling between the two groups is so weak that the two combinations do not have appreciably different frequencies. Exactly the same phenomenon is exhibited by the corresponding combinations of the deformation vibration of the BH_2 groups which results in the close agreement of the Raman frequency ν_3 at 1180 cm^{-1} with the infra-red fundamental ν_{18} at 1175 cm^{-1}. In the case of ethylene the coupling is fairly strong, as can be judged by the differences between the corresponding infra-red and Raman frequencies which are 2989.5 and 3019.3 (CH stretching) and 1443.5 and 1342.4 (CH deformation), respectively.

2614 cm^{-1}: Strong perpendicular band type B (ν_8). The rotational structure of this band has already been described. Although its structure is well resolved it does not show any appreciable vibrational isotope effect which must certainly be less than 1 cm^{-1}. It would not be expected to show any rotational isotope effect. The relative intensities and locations of the 2522 and the 2614-cm^{-1} bands of diborane with respect to one another are very similar to those of the corresponding bands in ethylene, a fact which must be regarded as strong evidence of the analogy drawn between them. This frequency (ν_8) can be regarded as the in-phase combination of the antisymmetrical valence frequency of the BH_2 groups, the out-of phase combination being the Raman frequency (ν_{11}) 2489. The fairly large difference between the two results from the relatively large displacements which the boron atoms undergo in the antisymmetrical valence BH_2 vibration as compared with the symmetrical valence and deformation frequencies of this group. This leads to considerably greater coupling between the two groups for these vibrations. The analogous frequencies in ethylene, *viz.* 3272 and 3105 cm^{-1} show a still larger difference. The apparent absence of vibrational isotope effect in the band may be due to the isotopic shift coinciding with the rotational spacing.

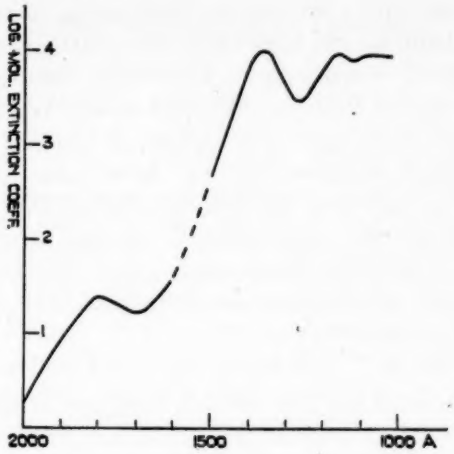

FIG. 5. The absorption of diborane in the region 2000–1000A.

COMBINATION BANDS

The assignments of the combination bands of diborane are governed by the selection rule that since the molecule has a center of symmetry, no combination of two infra-red active frequencies can be infra-red active. This can be broken down if the vibrations are strongly anharmonic or if the molecule loses its center of symmetry by the presence of the two different isotopes in the molecule. However it does not appear likely that combination bands of any appreciable strength could result from either of these causes. The tentative assignments in Table I have therefore been made in conformity with the rule, with the exception of the very weak band at 3135. The only ones which call for comment are the following:

3135 cm^{-1}: This is a very weak band, parallel type A, which it is difficult to interpret.

3660 cm^{-1}, (3600 – 3700): This is quite a strong band, probably parallel type A, though its structure is difficult to determine because of interference from atmospheric absorption. The strength of the absorption is probably due to overlapping due to the many combinations which are possible in this range, *viz.*:

$$\nu_{11}+\nu_{18}\ (2489+1175=3664),$$
$$\nu_1+\nu_{18}\ (2523+1175=3698),$$
$$\nu_3+\nu_{16}\ (1180+2522=3702),$$
$$\nu_3+\nu_8\ (1180+2614=3794),$$

5022 cm^{-1}: An attempt was made to resolve this band on the high dispersion grating spectrograph at Northwestern University through the courtesy of Professor W. S. Huxford. While this failed as a result of a variety of causes it was adequate to show that the band was parallel type *A* and that the isotope shift of the $B^{10}B^{11}$ molecule was about 4 cm^{-1} relative to that of the $B^{11}B^{11}$. The assignment $\nu_1+\nu_{16}$ (2523+2522 =5045), which gives the right band type, seems most probable.

5760 cm^{-1}: This band, which is a well marked band, is of interest since it must correspond to at least three vibrational quanta. It seems likely that it is linked to the strong absorption around 3660 cm^{-1} by the addition of a quantum of the ν_2 (2102) vibration. It can thus correspond to $\nu_2+\nu_{11}+\nu_{18}$ (2102+2489+1175=5766) or $\nu_2+\nu_3+\nu_{16}$ (2102+1180+2522=5804) or both. Its breadth indicates that both combinations are probably present.

ULTRAVIOLET ABSORPTION

The ultraviolet absorption spectrum of diborane has been examined at low pressures down to 1000A using a 1 meter normal incidence grating vacuum spectrograph with the Lyman continuum. The first strong absorption is a broad diffuse band appearing in the region of 1350A at an equivalent thickness of 0.004 mm of the gas at N.T.P. It is followed by further diffuse absorption of similar strength below 1200A. This is compatible with an ionization potential between 11 and 12 electron volts and shows that all the electrons are fairly tightly bound. At higher pressures the bands spread out to longer wave-lengths and presumably merge into the relatively weak band reported by Blum and Herzberg.[15] Figure 5 is a plot of the absorption in which the actual values of absorption have been roughly estimated.

The above work forms part of a program sponsored by the Office of Naval Research. The author is indebted to Dr. George Schaeffer for preparing the sample of diborane and to Professor R. S. Mulliken for suggesting the subject and for much helpful advice. Thanks are also due Professors E. Teller, G. Herzberg, H. I. Schlesinger, and R. P. Bell, for suggestions and discussions. We are also indebted to Dr. R. D. Cowan who is continuing this work and who kindly permitted the author to quote some of the results he has obtained in the 2400−1700-cm^{-1} region. In particular, Professor Mulliken and Dr. Cowan are responsible for revising the numbering in the 2614-cm^{-1} band.

[15] E. Blum and G. Herzberg, J. Phys. Chem. **41**, 91 (1937).

THE JOURNAL OF CHEMICAL PHYSICS VOLUME 16, NUMBER 9 SEPTEMBER, 1948

Countercurrent Gaseous Exchange Method for the Separation of Isotopes*

R. B. BERNSTEIN** AND T. I. TAYLOR
Department of Chemistry, Columbia University, New York, New York

(Received April 19, 1948)

A method is described for isotope enrichment by countercurrent gaseous exchange in a thermal diffusion column. The theory is derived for two cases of interest: diffusion limited and reaction-rate limited. Solutions of the equations are presented for the over-all separation S at the steady state as a function of the following: single stage enrichment factor α; diffusion constant D or exchange rate constant k; length of column Z; and the convective flow L, which in turn depends on pressure, temperature, column dimensions, etc. The results may be expressed in the usual form $S=\alpha^N$. For the diffusion-limited case $N=4\pi D\mathfrak{c}Z/L$, where $\mathfrak{c}$ = moles of gas per cc. For the reaction-rate limited case the number of theoretical plates per unit length is given by the expression $N/Z=k/v$, where v is the convective velocity.

Experiments are described in which C^{13} was concentrated by the exchange reaction $C^{12}O_2+C^{13}O\rightleftarrows C^{13}O_2+C^{12}O$. The observed dependence of the over-all separation upon the operational variables is consistent with the theory.

INTRODUCTION

A CONCENTRATION of the isotopes of several elements has been effected by Urey and his co-workers[1] using two-phase countercurrent systems in which favorable isotopic exchanges existed between the gaseous component and an ion in solution. Favorable isotopic exchanges also exist between two gaseous molecules, as shown by the calculations of Urey and Greiff.[2] Equilibrium constants for many such gaseous exchanges have been tabulated in a convenient form by Urey.[3] The kinetics of a number of these gaseous exchange reactions have been studied by Urey and his co-workers.[4]

A method has been devised by Taylor and Bernstein[5] in which an enrichment of isotopes may be effected in a single fluid phase by establishing countercurrent flow between the exchanging substances in a thermal diffusion column. There appear to be a number of favorable reactions in both the gaseous and the liquid phase for which the method is applicable.

Figure 1 is a diagrammatic representation of the gaseous exchange column and the flow pattern existing in it. Essentially, it consists of a cooled cylindrical column with an axial heated element which produces the desired convective flow. Thermal diffusion causes the downward moving gas stream near the cold wall to be enriched in the heavier component (CO_2, for example, in the case of a mixture of CO and CO_2). If the isotopic exchange at the hot surface favors the transfer of the heavy isotope to the heavier molecule, as is frequently the case, the heavy isotope will concentrate in the cold stream and will be carried by convection toward the bottom of the column. The analogy with a two-phase fractionating column is completed with the introduction of a chemical converter at the bottom of the column. This converts the heavy component to the light one (for example, CO_2 to CO) which then rises in the upward moving stream and undergoes further exchange. A slow stream of an equal molar mixture of the light and the heavy components (both of normal isotopic abundance) is passed across the top end of the column. This acts as an infinite reservoir supplying the heavy isotope to the column.

In order to bring about an enrichment of an isotope that concentrates in the light component, it would, of course, be necessary to place a

* Publication assisted by the Ernest Kempton Adams Fund for Physical Research of Columbia University.

** Eastman Kodak Fellow at Columbia University 1947–48; present address Illinois Institute of Technology, Chicago, Illinois.

[1] H. C. Urey, J. R. Huffman, H. G. Thode, and M. Fox, J. Chem. Phys. **5**, 856 (1937); C. A. Hutchison, D. W. Stewart, and H. C. Urey, *ibid.* **8**, 532 (1940); D. W. Stewart and K. Cohen, *ibid.* **8**, 904 (1940).

[2] H. C. Urey and L. Greiff, J. Am. Chem. Soc. **57**, 321 (1935).

[3] H. C. Urey, J. Chem. Soc. 562 (1947).

[4] J. Brandner and H. C. Urey, J. Chem. Phys. **13**, 351 (1945); E. Leifer, *ibid.* **8**, 301 (1940).

[5] T. I. Taylor and R. B. Bernstein, J. Am. Chem. Soc. **69**, 2076 (1947); T. I. Taylor and W. Spindel, J. Chem. Phys. **16**, 635 (1948).

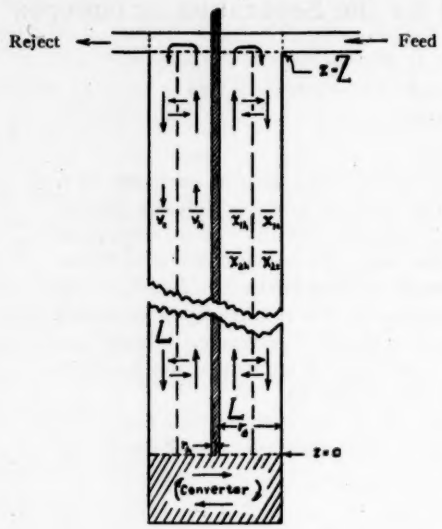

FIG. 1. Schematic representation of the gaseous exchange column. Here L is the convective flow, v is the average convective velocity, x_1 and x_2 represent average mole fractions of the light and heavy components. Subscripts "h" and "c" refer to the "hot" and "cold" streams.

suitable converter at the top of the column and pass the feed mixture across the bottom.

With an infinite reservoir and the condition of total reflux, the number of moles of light component leaving the top of the column per unit time is equal to the number of moles of heavy component entering the column. This method of operation prevents the formation of a vertical concentration gradient of either component. However, a vertical concentration gradient with respect to the isotopic ratio is established. At equilibrium when a steady state is reached, this isotopic gradient does not change with time. The theoretical analysis which follows applies to the above steady-state operation.

The equations already developed for the separation of isotopes in thermal diffusion columns relate the net transport of the isotopes to the operation variables. For the gaseous exchange column it is the total convective flow of the hot and the cold gas streams that is important. This flow corresponds to the throughput in a two-phase exchange column. The equations showing the dependence of the convective flow on the operating variables are given in a later section.

The mechanism of the isotopic separation process is now considered and equations are derived for the over-all separation in two limiting cases: diffusion limited and exchange rate limited.

ISOTOPIC ENRICHMENT IN THE GASEOUS EXCHANGE COLUMN

The first case considered will be the ideal limiting situation where the isotopic exchange rate is very rapid compared to the rate of radial interdiffusion between the two opposing streams. That is, the rate-limiting process is the rate at which reactants are transported into the reaction zone and the rate at which exchange products are removed from this zone. This is analogous to the situation existing in two-phase exchange columns involving rapid exchange reactions and slow interphase transport rates. The second case considered will be one in which the isotopic exchange rate is relatively slow compared to rapid radial mixing by diffusion. In this case there is no radial isotopic gradient. The transition case in which the radial mixing rate is comparable to the isotopic exchange rate will not be treated.

In each case the simplified flow pattern described in the previous section will be assumed. It consists of two rather sharply defined opposing streams: an inner cylindrical hot stream which rises with an average convective flow of L moles/sec. and an outer cold stream descending with an equal and opposite convective flow. The reaction is assumed to take place largely in the hot zone, although not necessarily on the heated surface. Radial gradients in the isotope fractions are simplified in terms of average isotopic fractions in the hot and cold streams. Similar assumptions have often been used in treatments of thermal diffusion columns, packed fractionating towers, and two-phase exchange columns to yield expressions for the dependence of over-all separation on the operating variables. Errors which arise from the use of these simplifying assumptions are primarily errors in *magnitude* rather than in the *form* of the final equations for the over-all separation.

DIFFUSION-LIMITED CASE

At the steady state a material balance for the rare isotope of the light component in the hot zone ($C^{13}O$ in the case of a mixture of CO and

CO_2) may be written as follows:

$$L\bar{x}_{1h}(\partial\bar{\nu}_{1h}/\partial z)dz+Fdz=0, \quad (1)$$

where $\bar{x}_{1h}$ is the average mole fraction of light component in the hot stream, z is the vertical coordinate, and $\bar{\nu}_{1h}$ is the average value of the fraction of rare isotope of light component in the hot stream. The first term of the equation represents the difference in the number of moles of rare isotope of the light component entering and leaving an element of volume as a result of convective flow. In the second term, F represents the outward rate of diffusion of the rare isotope of the heavy component in moles per second per unit length of column ($C^{13}O_2$ in the case of a mixture of CO and CO_2). The rate of loss of rare isotope of the light component in the hot zone because of the exchange reaction is also equal to F since the rate of exchange is limited by the rate of radial outflow of the rare isotope of the heavy component produced by the exchange. This follows from the assumption that the reaction is very rapid so that the single stage equilibrium enrichment factor is always maintained in the hot zone. A term of longitudinal back diffusion caused by the vertical isotopic gradient has been neglected.

F may be evaluated in terms of the radial isotopic gradient, assuming negligible contribution from the thermal diffusion effect for the isotopic molecules. Thus if $\bar{c}$ is the average gas concentration in moles/cc, then for unit length of column:

$$F=-2\pi rD\bar{x}_2\bar{c}(\partial\nu_2/\partial r),$$

where D is the diffusion coefficient of the rare isotope of the heavy component in the presence of the remaining components, $\bar{x}_2\bar{c}$ is the average concentration of the heavy component in the tube, and ν_2 is the mole fraction of rare isotope in the heavy component. It is convenient here to simplify this equation to give a rough estimate of F in terms of mean isotope mole fractions. At the cold wall the approximate value of $r(\partial\nu_2/\partial r)$ is $r_c[(\nu_{2c}-\nu_{2h})/(r_c-r_h)]=r_c[\Delta\nu_2/(r_c-r_h)]\cong\Delta\nu_2$, since r_h is small compared to r_c. Here $\Delta\nu_2$ is the extreme difference in mole fraction of the rare isotope of the heavy component at the wall and at the filament. In terms of the difference in the mean mole fraction of the rare isotope in the two streams, a rough first approximation gives

$$\Delta\nu_2=2(\bar{\nu}_{2c}-\bar{\nu}_{2h}).$$

The expression for the radial term F then becomes:

$$F=-4\pi D\bar{x}_2\bar{c}(\bar{\nu}_{2c}-\bar{\nu}_{2h}).$$

This gives the radial outflow of rare isotope of the heavy component in moles per second per centimeter length of column. The result states that the radial transport rate is proportional to the difference in mean mole fraction of the rare isotope of the heavy component in the two opposing streams. Since $\bar{\nu}_{2h}>\bar{\nu}_{2c}$ due to the isotopic exchange in the hot zone, $F>0$.

Substituting the above value for F in Eq. (1) and solving for the vertical gradient in mole fraction of rare isotope of the light component in the hot stream, the following result is obtained:

$$\partial\bar{\nu}_{1h}/\partial z=(-4\pi D\bar{x}_2\bar{c}/L\bar{x}_{1h})(\bar{\nu}_{2h}-\bar{\nu}_{2c}). \quad (2)$$

In a similar way a consideration of a material balance of the rare isotope of the heavy component in the cold stream leads to

$$\partial\bar{\nu}_{2c}/\partial z=(-4\pi D\bar{x}_2\bar{c}/L\bar{x}_{2c})(\bar{\nu}_{2h}-\bar{\nu}_{2c}). \quad (3)$$

Since the column is operated at total reflux so that $\bar{x}_{1h}=\bar{x}_{2c}$, it follows that the two expressions (2) and (3) are equal.

The single stage equilibrium separation factor α for the exchange reaction at the temperature of the hot filament is defined as $\alpha=\nu_{2h}/\nu_{1h}$. For a predominantly heterogeneous exchange (which is the case for the $CO-CO_2$ exchange) the reaction at the surface may be considered to be responsible for the average enrichment $\bar{\nu}_{2h}/\bar{\nu}_{1h}$ in the hot zone. Thus, roughly, $\alpha=\bar{\nu}_{2h}/\bar{\nu}_{1h}$. Substitution of $\alpha\bar{\nu}_{1h}$ for $\bar{\nu}_{2h}$ in Eqs. (2) and (3) gives two equations with the variables $\bar{\nu}_{1h}$ and $\bar{\nu}_{2c}$ which may be written:

$$\partial\bar{\nu}_{1h}/\partial z=\partial\bar{\nu}_{2c}/\partial z$$
$$=(-4\pi D\bar{x}_2\bar{c}/L\bar{x}_{1h})(\alpha\bar{\nu}_{1h}-\bar{\nu}_{2c}). \quad (4)$$

This shows that the vertical gradient in $\bar{\nu}_{1h}$ must be identical with that of $\bar{\nu}_{2c}$. At the bottom of the column, the converter chemically changes the heavy component into the light one so that $\bar{\nu}_{2c}=\bar{\nu}_{1h}$ at $z=0$. Consequently, at the steady state, $\bar{\nu}_{1h}$ must equal $\bar{\nu}_{2c}$ at every height z in the column. This is analogous to the circumstances existing in a two-phase exchange column where

interphase diffusion is the limiting factor. Here the concentration of the desired isotope in the rising gas phase is equal to that in the downward flowing liquid phase at any height in the column.

Integration of Eq. (4) with the omission of subscripts on ν gives

$$\log\nu=(-4\pi D\bar{x}_2\bar{c}z/L\bar{x}_{1h})(\alpha-1)+\text{const.} \quad (5)$$

The over-all separation S is now defined for separations not too large as the ratio of the concentration of rare isotope at the bottom of the column ($\nu(0)$ at $z=0$) to its concentration at the top of the column ($\nu(Z)$ at $z=Z$) or $S=\nu(0)/\nu(Z)$. It follows that

$$\log S=(4\pi D\bar{x}_2\bar{c}Z/L\bar{x}_{1h})(\alpha-1). \quad (6)$$

This equation gives the maximum over-all separation to be expected for a column of length Z.

NUMBER OF THEORETICAL PLATES

For most isotopic exchanges, α is small and $(\alpha-1)$ can be replaced by $\log\alpha$. Furthermore, $\bar{x}_2\cong\bar{x}_{1h}$ to a fair approximation so that

$$S=\alpha^{4\pi D\bar{c}Z/L}. \quad (7)$$

This is the familiar form of the equation for the over-all separation of fractionating columns and exchange columns:[6]

$$S=\alpha^N,$$

where N is the number of theoretical plates. Consequently, in the diffusion-limited case

$$N=4\pi D\bar{c}Z/L. \quad (8)$$

It will be shown in a later section that L is proportional to P^2r^4. Thus the number of plates should be proportional to the length Z of the column; to $1/P^2$ and to $1/r^4$. Only a slight positive temperature dependence should be expected for L; the over-all separation α^N would therefore be expected to follow the temperature dependence of α.

REACTION-RATE LIMITED CASE

In most actual cases involving gases, the over-all separation will be limited by the rate of the isotope exchange rather than by radial diffusion. This will result in a smaller number of theoretical plates than would be calculated from Eq. (8).

In the reaction-rate limited case a material balance equation is again written for the rare isotope of the light component in the hot stream:

$$L\bar{x}_{1h}(\partial\nu_1/\partial z)dz+Gdz=0. \quad (9)$$

The quantity G is defined as the net rate in moles per second per unit length of column at which the rare isotope of the light component disappears as a result of isotopic exchange. It is assumed here that the radial mixing rate is sufficient to insure the presence of no gradient in the mole fraction of the rare isotope of either component. Subscripts h and c may, therefore, be omitted from the isotopic fractions, ν.

The loss of rare isotope G in Eq. (9) may be written as:

$$G=-A_h(\partial/\partial t)(\bar{x}_{1h}\bar{c}_h\nu_1),$$

where A_h is the cross-sectional area of the hot zone, $\bar{x}_{1h}\bar{c}_h$ is the mean concentration of light component in the hot zone, and ν_1 is the fraction of rare isotope in the light component. Substitution for G in Eq. (9) leads to the following expression for the vertical isotopic gradient:

$$\partial\nu_1/\partial z=(A_h/L)\bar{c}_h(\partial\nu_1/\partial t).$$

It has been shown by McKay[7] that isotopic exchange reactions in general are apparent first order with respect to the rare isotope. This is, of course, true only because the chemical composition of an exchanging mixture is invariant during the exchange process. That is, there is no change in the mole fraction of the heavy and light component as a result of isotopic exchange regardless of the exchange mechanism. This is expressed here in terms of the isotopic exchange rates in the forward and reverse direction:

$$\partial\nu_1/\partial t=-k_1\nu_1+k_2\nu_2, \quad (10)$$

where k_1 and k_2 are the rate constants for the forward and the reverse reactions, respectively. The ratio k_1/k_2 is the equilibrium constant α for the exchange at the temperature of the hot wire.

Hence, substituting $k_2\alpha$ for k_1,

$$\partial\nu_1/\partial t=-k_2(\alpha\nu_1-\nu_2).$$

Combining this with the previous expression for the vertical gradient, one obtains the fol-

[6] K. Cohen, J. Chem. Phys. **8**, 588 (1940).

[7] H. A. McKay, Nature **142**, 997 (1938).

lowing equation:

$$\partial\nu_1/\partial z=(-A_h\bar{c}_hk_2/L)(\alpha\nu_1-\nu_2). \quad (11)$$

In the steady state the rate of accumulation of the rare isotope of the heavy component in the cold stream is equal to the rate of disappearance of the rare isotope of the light component in the hot stream. A material balance equation may be set up for the cold stream as was done in Eq. (9) for the hot stream. The two material balance equations simplify to

$$G=-L\bar{x}_{1h}(\partial\nu_1/\partial z)=-L\bar{x}_{2c}(\partial\nu_2/\partial z). \quad (12)$$

Since $\bar{x}_{1h}=\bar{x}_{2c}$, the two gradients are equal, and

$$\partial\nu_1/\partial z=\partial\nu_2/\partial z=(-A_h\bar{c}_hk_2/L)(\alpha\nu_1-\nu_2). \quad (13)$$

With the two gradients equal and with $\nu_1=\nu_2$ at the bottom of the column, it follows that at the steady state $\nu_1=\nu_2$ at all heights z. Consequently, the subscripts on the isotope fractions may be omitted and Eq. (13) may be integrated with the boundary condition that $S=\nu(0)/\nu(Z)$. The result is

$$\log S=(A_h\bar{c}_hk_2Z/L)(\alpha-1). \quad (14)$$

RELATION OF NUMBER OF THEORETICAL PLATES TO REACTION RATE

Using the logarithmic approximation for $(\alpha-1)$, the over-all separation becomes

$$S=\alpha^N,$$

where N is the number of theoretical plates given by

$$N=k_2A_h\bar{c}_hZ/L. \quad (15)$$

This equation may be simplified further by expressing L in terms of the mean convective velocity of the hot stream, $L=A_h\bar{c}_h\bar{v}_h$. This gives the interesting result that the number of plates per unit length of column is the ratio of the exchange rate constant (sec.$^{-1}$) to the average convective velocity in cm/sec., or

$$N/Z=k/v. \quad (16)$$

In other words the H.E.T.P. for this case is simply v/k.

DEPENDENCE OF OVER-ALL SEPARATION ON EXPERIMENTAL VARIABLES

The number of theoretical plates for a reaction rate limited process is then proportional to the length of the column Z; to $1/p$ (modified by any pressure dependence of k); and to $1/r^2$. Since the predominant temperature dependent term is the rate constant k, the number of plates should be expected to increase rapidly with temperature. However, since α usually decreases with increasing temperature, the over-all separation as given by Eq. (14) should not be expected to increase markedly. Ultimately, at temperatures where α approaches unity no enrichment should be obtained.

CONVECTIVE FLOW FROM THE NET TRANSPORT

It is now necessary to evaluate the dependence of the convective flow upon the operating variables. It is also of interest to obtain an estimate of its magnitude. This is an important quantity in determining the over-all isotope separation.

One method of determining the convective flow is by obtaining a relation between the net transport (a measurable quantity) and the convective flow. The net transport of one component in the gaseous exchange column can be calculated directly from the measured concentration of the light component in the reject stream from the top of the column. Equations for the convective flow are derived for the two major components (CO and CO_2, for example) with no consideration given to the relative isotopic abundance in the two components or to the isotopic exchange process.

Jones and Furry[8] in their review of the theory of thermal diffusion for the separation of isotopes have derived equations for the net transport in the vertical direction for one component of an *isotopic mixture*. For the gaseous exchange column described here it is necessary to estimate the net transport and convective flow for a mixture of the two main components which may differ considerably in molecular weights.

The equation given by Jones and Furry for the net transport τ of light component in grams per second up the column is

$$\tau_1=H\bar{x}_1\bar{x}_2-K(dx_1/dz), \quad (17)$$

where $\bar{x}_1$ and $\bar{x}_2$ are the mean values of the mole fractions of the light and the heavy component,

[8] R. C. Jones and W. H. Furry, Rev. Mod. Phys. **18**, 151 (1947).

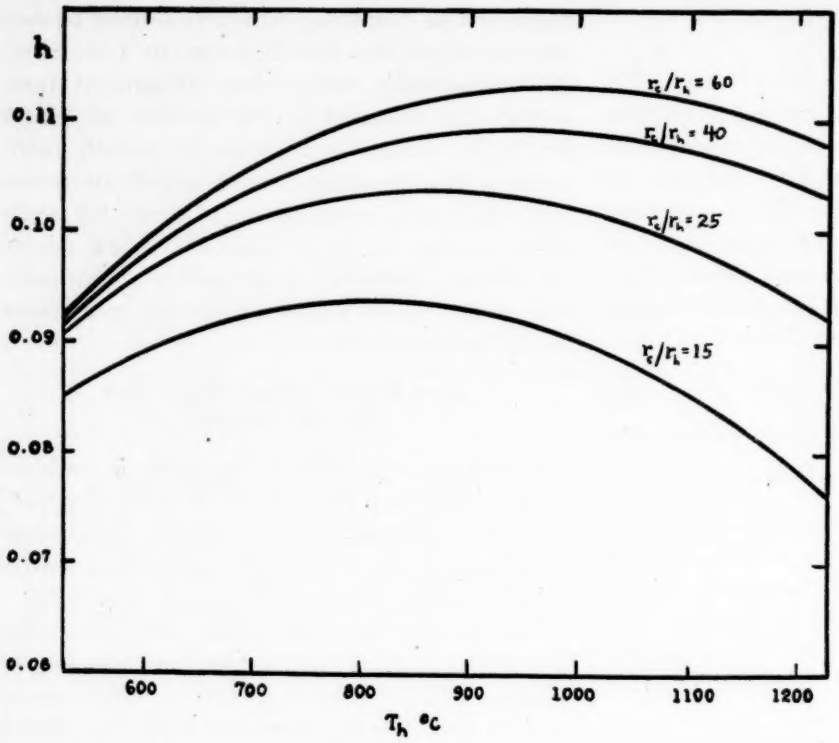

FIG. 2. Dependence of parameter h upon temperature (T_h°C) at different ratios of cylindricity (r_c/r_h), assuming $T_c = 300$°A—from Jones and Furry (reference 8, Table VI) for a "Maxwellian" gas.

respectively, and z is the distance from the bottom of the column. The transport coefficients H and K are constants which have been shown to depend upon the nature of the gas mixture, the dimensions and shape of the apparatus and the temperature difference maintained in the column. K is the sum of coefficients which take into account the various re-mixing effects. However, for the steady-state operation of the gaseous exchange column at total reflux with an infinite reservoir, no concentration gradient of either light or heavy component exists ($dx_1/dz = dx_2/dz = 0$) and the second term of Eq. (17) becomes zero. They evaluate H in terms of the geometry and operating variables of the column as follows:

$$H = (2\pi/6!)\alpha_t(\rho_c^2 g/\eta_c) r_c^4 h(T_h/T_c; r_c/r_h). \quad (18)$$

Here α_t is the thermal diffusion constant, ρ_c and η_c the density and viscosity of the gas mixture at the temperature T_c of the cold wall, g the acceleration of gravity, r_c the radius of the tube, r_h the radius of the hot wire, T_h and T_c the absolute temperature of the hot wire and cold wall, respectively. The function h has been tabulated by Jones and Furry[8] for a Maxwellian gas ($\lambda \propto T$) in the "extreme cylindrical" case where $r_c/r_h \gg 1$ (see Fig. 2).

In order to apply Eqs. (17) and (18) to the gaseous exchange column where a large mass difference may exist between the two main components, a modification appears necessary to satisfy the condition that the net transport of the light component in moles per second equals that of the heavy component in moles per second in the opposite direction. The experimental requirement of constant pressure (no accumulation of material) in the apparatus would not be met by these equations in their present form with τ_1 given in grams per second. For the case under consideration, the revised transport equation after substitution for H becomes:

$$\tau_1 = (2\pi/6!)\alpha_t(\rho_c^2 g/\eta_c) r_c^4 (M_1/\bar{M}) \bar{x}_1 \bar{x}_2 h, \quad (19)$$

where M_1 is the molecular weight of the light component and $\bar{M}$ is the mean molecular weight of the mixture given by $\bar{x}_1 M_1 + \bar{x}_2 M_2$. ρ_c is the mean density of the mixture at the temperature of the cold wall. If the transport τ_2 of the heavy component down the tube is desired, M_1 is replaced by M_2. This equation satisfies the condition of equal molar transport rates of light and heavy components, since now

$$\tau_1/M_1 = \tau_2/M_2 = \tau',$$

where τ' is the net transport rate of either component in moles per second. In the case of two isotopic molecules, Eq. (19) reduces to the usual form since $M_1/\bar{M} \doteq 1$.

The density ρ_c may be expressed in terms of the mean molecular weight by $\rho_c = P\bar{M}/RT_c$ where P is the pressure in atmospheres and R is the gas constant in cc atm./°A mole. Substitution in Eq. (19) gives the following expression for the net transport of either component in moles per second:

$$\tau' = \tau_1/M_1 = \tau_2/M_2 = (2\pi/6!)\alpha_t(P^2\bar{M}/\eta_c R^2 T_c^2) g r_c^4 \bar{x}_1 \bar{x}_2 h. \quad (20)$$

A relation between this quantity and the convective flow may now be obtained by noting that the net upward transport of the light component, for example, is equal to the difference between the total upward and downward flow rates of the light component in the hot and cold streams. Thus,

$$\tau' = \bar{x}_{1h} L_h - \bar{x}_{1c}(-L_c),$$

where $\bar{x}_{1h}$ and $\bar{x}_{1c}$ are the mean mole fractions of light component in the rising hot stream and descending cold stream, respectively. L_h is the convective flow rate in the hot stream in total number of moles of gas per second. It is considered positive since it flows in the positive z direction. L_c is thus negative and for total reflux $L_h = -L_c$. In general, only the positive quantity will be referred to and the subscript will be

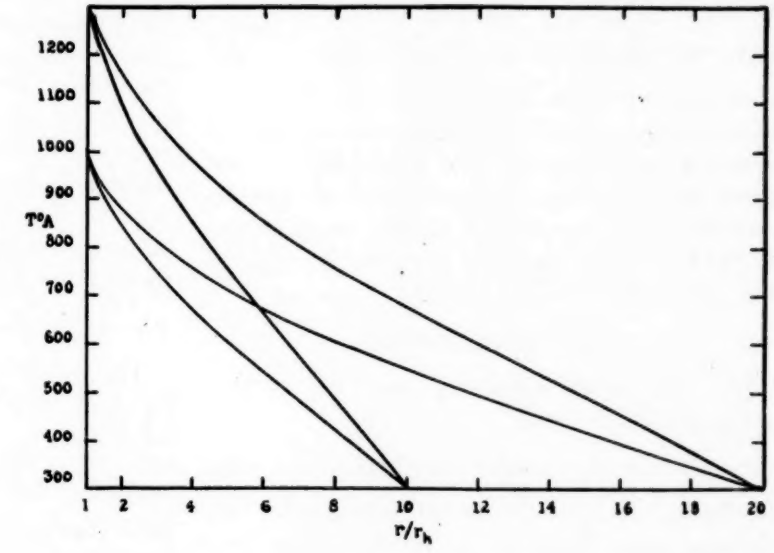

FIG. 3a. Radial temperature distribution calculated for a Maxwellian gas for two values of $T_h = 1000$°A, 1300°A, and for two values of the cylindricity: $r_c/r_h = 10, 20$.

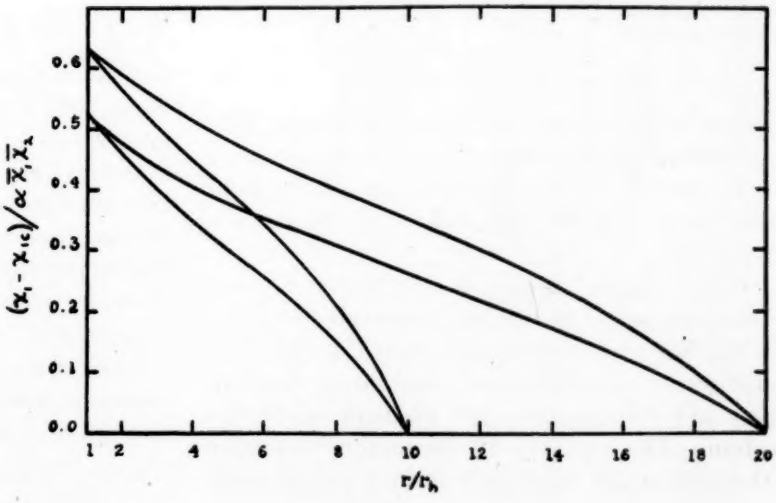

FIG. 3b. Radial concentration distribution due to effect of thermal diffusion. Calculated for the various temperature distributions shown in Fig. 3a.

TABLE I. Equilibrium constant, α, as function of temperature.

Temperature		Equilibrium constant, α
°A	°C	
273	0	1.098
298	25	1.086
600	327	1.029
1000	727	1.012
1400	1127	1.0064

omitted, so that

$$L=\tau'/(\bar{x}_{1h}-\bar{x}_{1c}). \quad (21)$$

The difference in mean concentration $\bar{x}_{1h}-\bar{x}_{1c}$ established between the hot and cold streams as a result of thermal diffusion may be derived from the following equation of diffusion as given by Jones and Furry:[8]

$$x_1(v_1-v)=D_{12}(\alpha_t x_1 x_2 \text{ grad } \log T-\text{grad}x_1). \quad (22)$$

Here (v_1-v) is the net advance velocity of the light component and D_{12} is the ordinary mutual diffusion coefficient of the mixture. For the particular conditions of operation of the gaseous exchange column at the steady state where $dx_1/dz=0$ it can be seen that $(v_1-v)=0$ and Eq. (22) reduces to

$$\text{grad}x_1=\alpha_t x_1 x_2 \text{ grad } \log T.$$

With cylindrical symmetry and no vertical gradient this becomes

$$dx_1/dr=\alpha_t x_1 x_2 (d/dr)(\log T). \quad (23)$$

Replacing x_1x_2 in the usual manner by the average value $\bar{x}_1\bar{x}_2$ across the tube and integrating, the extreme radial concentration difference becomes

$$x_{1h}-x_{1c}=\alpha_t \bar{x}_1\bar{x}_2 \log(T_h/T_c), \quad (24)$$

in which x_{1h} is the concentration of the light component at the hot wire whose temperature is T_h and x_{1c} is the concentration of the light component near the cold wall where the temperature is T_c.

Before approximating the difference in mean concentration of the light component $(\bar{x}_{1h}-\bar{x}_{1c})$ in the hot and cold streams from Eq. (24), it is instructive to examine the temperature distribution and the concentration gradient across the column. The heat loss by conduction through a Maxwellian gas (coefficient of heat conductivity proportional to T) in a concentric cylinder system is given by

$$Q=2\pi r\lambda_0 T(dT/dr),$$

where Q is the heat loss per unit length of heated cylinder and $\lambda_0 T$ is the coefficient of heat conductivity. With the boundary conditions that $T=T_h$ at $r=r_h$ and $T=T_c$ at $r=r_c$, the radial temperature distribution becomes

$$(T_h^2-T^2)/(T_h^2-T_c^2)=(\log r/r_h)/(\log r_c/r_h).$$

Figure 3a shows a set of curves of T as a function of the ratio r/r_h for $T_c=300$°A with T_h at 1000°A and 1300°A at cylindricity ratios r_c/r_h of 10 and 20 for each case. It can be seen that the temperature gradient is greatest in the neighborhood of the wire. In Fig. 3b a quantity proportional to the concentration difference (x_1-x_{1c}) is plotted against the ratio r/r_h for each of the above conditions. This shows the concentration gradient to be approximately linear, as has been assumed in most simplified treatments of the thermal diffusion column.

From the above result, the desired difference in mean concentrations of light component in the hot and cold streams is approximated as

$$\bar{x}_{1h}-\bar{x}_{1c}\cong\tfrac{1}{2}(x_{1h}-x_{1c})=\tfrac{1}{2}\alpha_t\bar{x}_1\bar{x}_2\log(T_h/T_c). \quad (25)$$

The convective flow L may now be obtained by combining Eqs. (20), (21), and (25) with the result that

$$L=(4\pi/6!)[P^2\bar{M}gr_c^4h/\eta_c R^2T_c^2\log(T_h/T_c)]. \quad (26)$$

Substituting for the constants, the convective flow in moles/sec. becomes

$$L=2.5\times10^{-3}[P^2\bar{M}r_c^4h/\eta_c T_c^2\log(T_h/T_c)]. \quad (27)$$

Values of the function h for different ratios of T_h/T_c and r_c/r_h are plotted in Fig. 2 from the table given by Jones and Furry.[8] It can be seen that h is rather insensitive to the temperature and cylindricity. Consequently, the convective flow is proportional to the square of the pressure and to the fourth power of the tube radius. It is inversely proportional to $\log(T_h/T_c)$ but is not a function of the thermal diffusion constant α_t.

The convective flow L may also be evaluated from the experimentally determined values of τ' and α_t by means of Eqs. (21) and (25). Thus

$$L=\tau'/\tfrac{1}{2}\alpha_t\bar{x}_1\bar{x}_2\log(T_h/T_c). \quad (28)$$

Approximate agreement of these experimental values with the values calculated from Eq. (27) will be shown in a later section.

EXPERIMENTAL TESTS OF THE THEORY

The isotopic exchange reaction $C^{13}O+C^{12}O_2 \rightleftharpoons C^{12}O+C^{13}O_2$ was selected for an investigation of the countercurrent gaseous exchange method of isotope separation. The equilibrium constant for this exchange at several temperatures has been calculated by Urey and Greiff.[2] Their values along with those calculated for the higher temperatures using the method of Bigeleisen and Mayer[9] are summarized in Table I.

The kinetics of the exchange in the region of 900°C have been studied by Brandner and Urey.[4] They found the reaction to be primarily heterogeneous and surface-catalyzed. The rate of the exchange was markedly increased by the presence of H_2 or H_2O. The rate constants were shown to be independent of the pressure and of the composition of the mixture in the ranges studied. Values varied, for example, from 2×10^{-5} sec.$^{-1}$ in a quartz vessel at 898°C to 1×10^{-3} sec.$^{-1}$ in the presence of gold at 898°C where the total pressure was about 11 mm Hg.

Apparatus

A small gaseous exchange column was constructed, as illustrated in Fig. 4. It consisted of a water-jacketed glass tube 1.0 cm in diameter and 110 cm long. A number of filaments were tested; a platinum wire (B. and S. No. 22) 0.64 mm in diameter seemed to be most satisfactory. Small cross pieces of platinum wire were spot-welded onto the filament to center it in the column. A 100-g weight attached to the lower end of the filament was used to keep the filament taut. Electrical contact was made to a pool of mercury in a glass well at the bottom of the column. The temperature of the filament was estimated to within ±50°C from measurements of the resistance of the wire. In one set of experiments CO_2 was supplied to the top of the column from a 20-liter reservoir. Convection, produced by heating one of the tubes leading from the tank to the column, served to circulate gas across the top of the column. Provision was made for withdrawing samples periodically from the reservoir. Microanalyses of these samples were performed to measure the rate at which the concentration of CO increased in the tank.

In other sets of experiments CO_2 was metered across the top of the column. For analysis, the reject gas was passed into an Orsat analysis unit. From the CO_2 flow (measured by a capillary flowmeter) and the concentration of CO in the exit gases, the net CO transport was calculated.

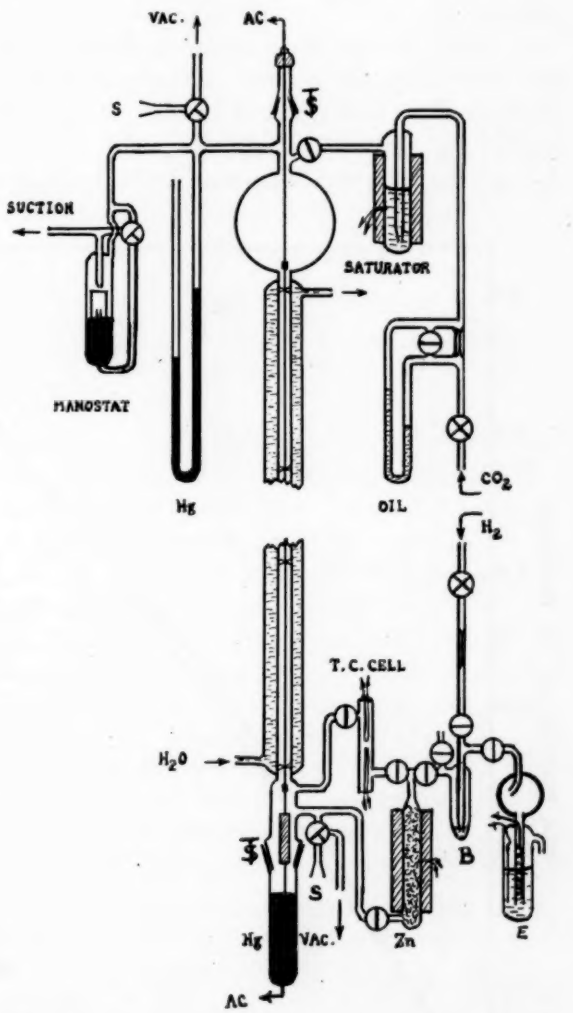

FIG. 4. Experimental apparatus (glass column). The column is shown with filament, spacers, weight, and Hg pool. Ground joints allow for removal of the filament. The standard taper joints "*S*" for sample withdrawal are indicated at top and bottom. The Zn converter and thermal conductivity cell are shown. The bubbler flowmeter "*B*" and the auxiliary electrolysis unit "*E*" for calibration are indicated. The CO_2 may be saturated with H_2O before passing across the top of the column. The manostat leading to the rough vacuum line is shown.

[9] J. Bigeleisen and M. G. Mayer, J. Chem. Phys. **15**, 261 (1947).

A cartesian manostat in the reject line maintained constant pressure.

At the bottom of the column, zinc at 400°C was used to convert CO_2 to CO.[10] With the converter in a vertical position the convective circulation rate was several times greater than the net transport of CO_2 to the bottom of the column. This insured a condition of total reflux. A small thermal conductivity cell in series with the converter gave a continuous indication of the conversion efficiency, usually greater than 95 percent.

In some of the experiments hydrogen was introduced into the bottom of the column as a catalyst. This was done by means of a small electrolysis unit. By adjusting the current through the cell a small constant flow of hydrogen could be admitted to the exchange column. For the experiments at other than atmospheric pressure it was found more convenient to supply hydrogen from a tank through a small metal capillary leak. Flow rates were measured by means of a special bubbler flowmeter previously calibrated with the electrolysis unit.

Water instead of hydrogen was introduced as a catalyst in a number of experiments. This was done by means of a water saturator in the carbon dioxide inlet line at the top of the column. The temperature of the saturator was high enough to insure condensation of a small amount of water on the cold tube. This water then covered the walls of the column, thereby maintaining in the column a partial pressure of water vapor. The existence of the water gas reaction, $CO+H_2O \rightleftharpoons$

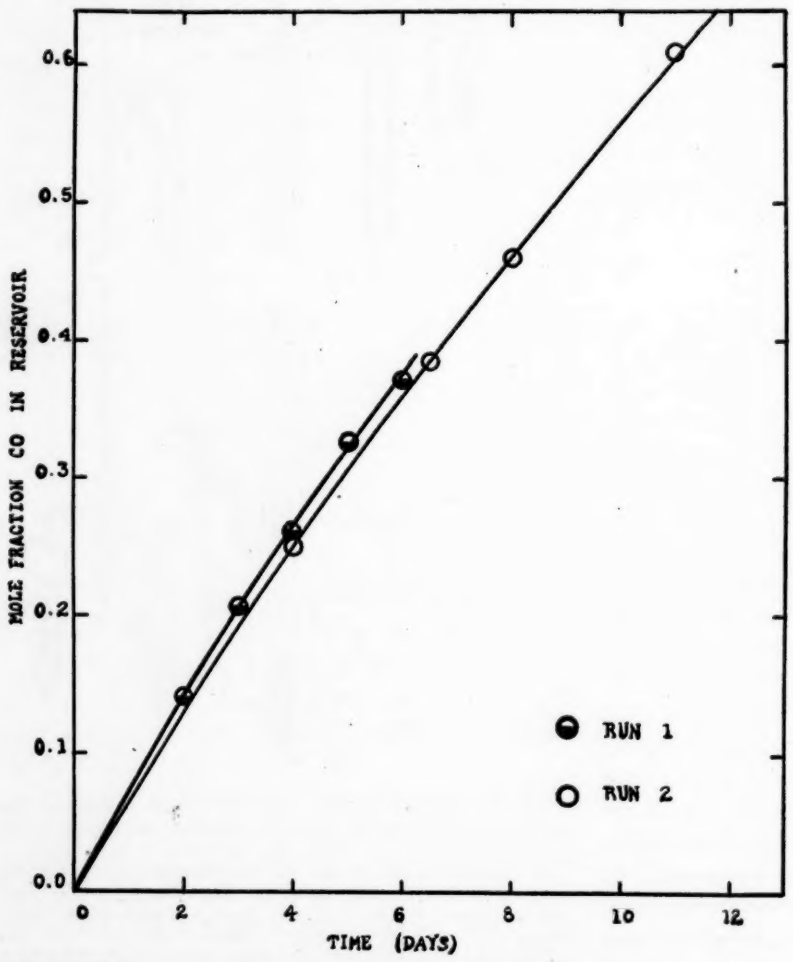

FIG. 5. Time dependence of CO concentration in the 20-liter reservoir at top of gaseous exchange column for two runs. Run 1, $T_h = 700°C$; run 2, $T_h = 800°C$.

[10] R. B. Bernstein and T. I. Taylor, Science **106**, 498(1947).

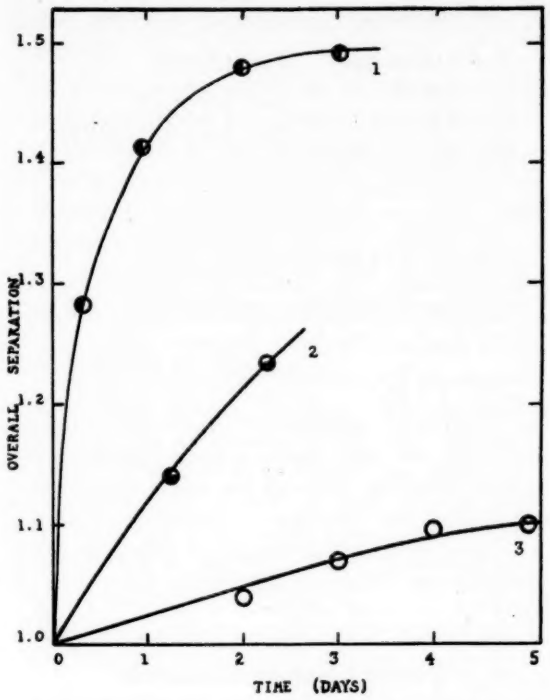

FIG. 6. Dependence of over-all separation at 1.0 atmos. upon time. Three runs under different conditions of temperature, catalyst, and filament. Curve 1: platinum filament, $T_h = 1150°C$; presence of H_2O vapor (run 11). Curve 2: platinum filament, $T_h = 800°C$; presence of H_2O vapor (run 7). Curve 3: nichrome filament, $T_h = 700°C$; no H_2O (run 1).

$CO_2 + H_2$ with an equilibrium constant of unity at about 800°[11] insures the presence of hydrogen which may also aid in catalyzing the exchange.

Convective Flow

The rate of increase in concentration of CO in the 20-liter reservoir attached to the top of the column was determined by analysis with a Blacet microgas analysis unit (A. H. Thomas Company). Figure 5 shows the results of two such experiments. Net transport rates of CO were calculated from the initial slopes of each curve. Thus:

$$\text{net transport (cc/min.)} = V(dx/dt)_0,$$

where V is the volume of the reservoir (2×10^4 cc) and $(dx/dt)_0$ is the initial rate of increase in mole fraction of CO in the reservoir. In those experiments in which CO_2 was passed across the top of the column the net transport of CO was obtained from the product of the mole fraction of CO in the reject gas stream and the total flow rate in cc/min. The results of these experiments are given in Table II to show the dependence of net transport on the temperature of the filament and on the pressure. The small decrease in net transport of CO with increase in temperature is in qualitative agreement with the temperature variation of the parameter h (Fig. 2). The increase of the net transport with the pressure agrees quite well with that expected from Eq. (20) in which τ' is seen to be proportional to P^2. The experiments of Clusius and Dickel[12] with the

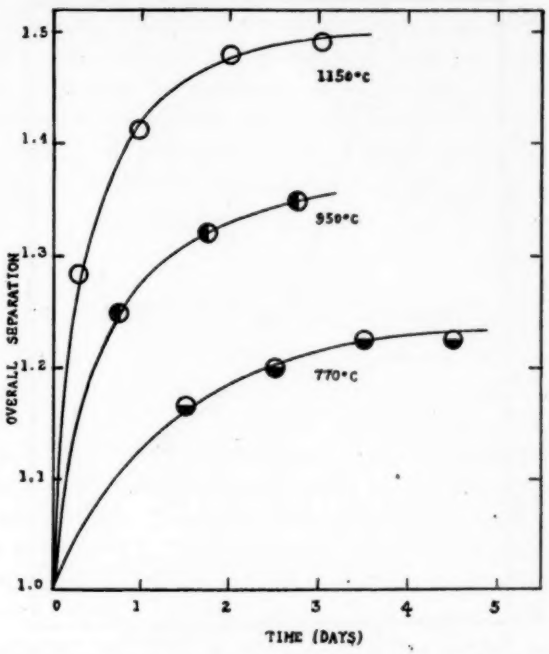

FIG. 7. Dependence of over-all separation on time and filament temperature at 1 atmos. total pressure with constant H_2O vapor pressure. Pt filament 0.64 mm in diameter. Column length, 1.1 meter. Data from runs 9, 10, and 11.

TABLE II. Determinations of the net transport of CO.

Filament	Diameter (mm)	Temperature °C(±50°)	Pressure (atmos.)	Net transport (std. cc/min.)
Nichrome	0.30	700	1.00	0.97
Nichrome	0.30	800	1.00	0.93
Platinum	0.64	770	1.00	0.88
Platinum	0.64	950	1.00	0.62(?)
Platinum	0.64	1150	1.00	0.79
Platinum	0.64	1150	1.48	1.47

[11] D. D. Wagman, J. E. Kilpatrick, W. J. Taylor, K. S. Pitzer, and F. D. Rossini, J. Research Nat. Bur. Stand. 34, 143 (1945).

[12] K. Clusius and G. Dickel, Zeits. f. physik. Chemie B44, 397, 451 (1939).

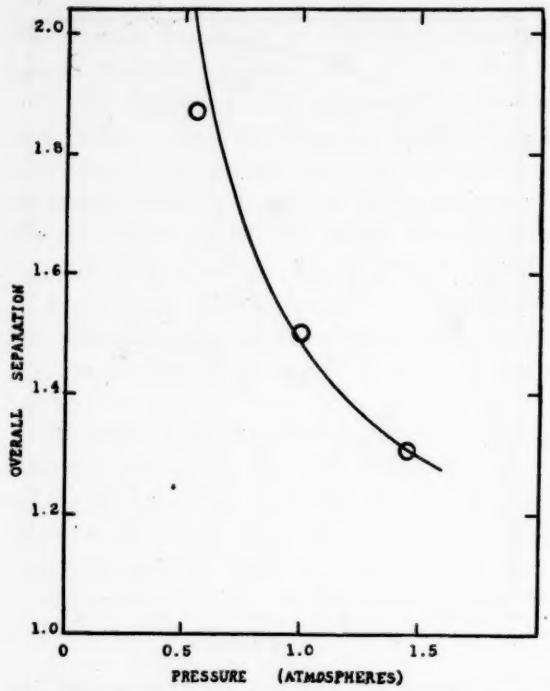

FIG. 8. Dependence of over-all separation on pressure (atmospheres) at about 1100°C. Solid curve calculated from expected pressure dependence (theoretical). Data from runs 11, 12b, and 13b.

mixture O_2 and N_2 have amply verified the pressure dependence given by the theoretical equations of Jones and Furry.[8]

The convective flow L, which is an important quantity in determining over-all isotope separation, may be calculated from Eq. (28) using the experimental net transport along with the thermal diffusion constant α_t. A value of $\alpha_t=0.10$ was obtained by extrapolating the data of Kitagawa and Wakao[13] for a mixture of CO_2 and CO to 1000°C. Substitution of $\tau'=0.8$ cc/min. at $T_h=1000$°C and $P=1.0$ atmos. into Eq. (28) leads to the following value for the convective flow L:

$$L=\frac{0.8}{(0.5)(0.10)(0.5)(0.5)\log_e(1273/298)}$$

$$=43.5 \text{ cc/min.}=3.0\times10^{-5} \text{ mole/sec.}$$

This result may be compared with the theoretical value obtained by substituting into Eq. (27) the following:

$P=1.00$ atmos.; $T_h=1273$°A;
$T_c=298$°A; $r_h=0.032$ cm;
$r_c=0.50$ cm; $\eta_c=1.7\times10^{-4}$ poise;
$\bar{M}=36$; $h=0.09$

Thus,

$$L=\frac{(2.5\times10^{-3})(1.00)^2(36)(0.5)^4(0.09)}{(1.7\times10^{-4})(298)^2\log_e(1273/298)}$$

$$=2.3\times10^{-5} \text{ mole/sec.}$$

The numerical agreement with the previous value from the experimental data may be somewhat fortuitous in view of the approximations in the theory, but it seems reasonable to expect that the correct dependence of the convective flow upon the variables is given by Eqs. (27) and (28).

Over-All Isotope Separation

Carbon isotope abundance ratios of the samples withdrawn periodically from the column were determined to a precision of about 1 percent by measurement of the 44 and 45 peaks of the CO_2 with a Nier-type mass spectrometer.

The effect of the presence of water or hydrogen and the effect of change in filament temperature are shown in Fig. 6 where the over-all isotope separation is plotted against time. The upper curves, 1 and 2, show qualitatively that the over-all separation is increased by the presence of the catalyst and by the temperature increase. In curve 1, H_2 was admitted at a rate of about 0.2 cc/min., which appeared to be equivalent to the addition of water vapor. This is, of course, expected from the equilibria involved in the water gas reaction. Brandner and Urey[4] had previously shown this catalytic effect in their kinetic measurements.

The effect of filament temperature is more clearly illustrated by the experiments shown in Fig. 7. Here the total pressure was maintained at 1.00 atmosphere with a constant flow of H_2 into the column. The over-all separation increases with T_h even though α decreases with increasing temperature (Table I). This is attributed to the increase in exchange rate with temperature. In principle, however, temperatures would be

[13] H. Kitagawa and M. Wakao, J. Chem. Soc. Japan **62**, 100 (1941).

reached where α approaches 1, resulting in no separation.

The effect of the variation in pressure on the over-all separation is illustrated by the data plotted in Fig. 8. Here, the values for the over-all separation are those taken from the end points of curves of separation against time at three pressures. The temperature was maintained at approximately 1100°C and the water vapor pressure was about 20 mm Hg. This dependence on pressure is expected from an analysis of Eq. (14), where it was previously shown that the over-all separation should increase with decreasing pressure. This agreement with the theory is demonstrated by the solid curve calculated from the pressure dependence of the terms in the relation $N/Z=k/v$. Here the convective velocity is proportional to the first power of the pressure and k is assumed to be independent of pressure as was demonstrated by Brandner and Urey.[4]

An interesting application of Eq. (16), $N/Z=k/v$, is its use in determining experimentally rather fast exchange rates from a knowledge of the convective flow and the equilibrium constant for the exchange. In the experiment at 1150°C at 1 atmos. of pressure, for example, the measured net transport of CO (0.79 cc/min.) corresponds to a convective flow rate of 43.5 cc/min. or to a convective velocity of about 1.9 cm/sec. (This might be measured more precisely by the use of an added trace of radioactive isotopes.) At 1150°C the value of α is 1.006 and with an over-all separation S of 1.5, the number of plates in the 1.1 meter column is 68. The height equivalent to each theoretical plate (H.E.T.P.) is thus 1.6 cm. This corresponds to a reaction velocity constant of $k=vN/Z=1.9\times(68/110)=1.2$ sec.$^{-1}$. Because of the large temperautre uncertainty, it was not possible to obtain a reliable value for the apparent activation energy of the exchange. However, the results indicate a considerably lower value than that reported by Brandner and Urey.[4]

As the reaction rate increases, the H.E.T.P. will approach that for the diffusion-limited case. Substituting in Eq. (8) $L=3\times10^{-5}$ mole/sec. and evaluating the quantity $\bar{c}D$ at the mean temperature of about 800°K as $(4.1\times10^{-5})\times(0.2)\times(800/300)^{0.8}=1.8\times10^{-5}$ mole cm sec.$^{-1}$, the estimated limiting value of the H.E.T.P. is 1.3 mm. This implies that if the rate constant could be increased by catalysis or by an increase in surface, a greater isotope concentration could be achieved in a given column. Such conditions might also allow operation at lower temperatures where the isotopic exchange equilibrium constant is larger.

Comparison with Other Methods

It is of interest to compare the results of these experiments with isotope separations obtained by other methods. For the separation of $C^{13}H_4$ by ordinary thermal diffusion of methane, Nier[14] used a concentric tube column 730 cm long with a spacing of 0.71 cm and a temperature difference of about 300°C. At a pressure of 46 cm approximately 4.5×10^{-8} g/sec. of C^{13} was transported and collected as 4.5 percent $C^{13}H_4$ gas. The transport of isotope in the gaseous exchange column as measured by the initial increase in concentration of C^{13} in the bottom assembly of the column (180 cc) is about 1×10^{-8} g/sec. A value of 3×10^{-8} g/sec. may be calculated from the simple transport equation $Lv_0(\alpha-1)$. This transport rate is less than that obtained in the ordinary thermal diffusion column, but it might be pointed out that the area of the annular space was 9.4 cm^2 for Nier's column compared to 0.8 cm^2 for the gaseous exchange column. A comparison of separations can be made by calculating the over-all separation obtainable in a 1.1-meter length of Nier's thermal diffusion column. The constant A (reference 8, p. 177, Eq. (149)) for the column was 0.81×10^{-3} cm^{-1} (reference 8, p. 207, Eq. (363)) so that the over-all separation at equilibrium (reference 8, p. 178, Eq. (150)) would be 1.2 at one atmosphere. An over-all separation of 1.5 was obtained with the exchange column (Fig. 7). Consequently, for a given length of column a higher separation may be achieved in the exchange column.

The power required for the gaseous exchange column was approximately 0.2 kw/meter as compared with 0.38 kw/meter for Nier's column. Considering the differences in the transport rates and lengths of columns required, it can be seen that the power required to produce C^{13} at a

[14] A. O. Nier, Phys. Rev. **57**, 30 (1940).

given concentration is approximately the same as for the thermal diffusion column.

The two-phase counter-current exchange methods developed by Urey and his co-workers[1] have been used to produce concentrations as high as 25 percent C^{13} at high transport rates of 2×10^{-6} g/sec. of C^{13}. The power requirements with these methods are low; they are therefore much more economical.

The authors wish to thank Mr. E. H. Musbach for assistance in assembling the mass spectrometer for the isotope analysis. Thanks are due Professors G. E. Kimball and K. S. Halford for reviewing the manuscript.

THE JOURNAL OF CHEMICAL PHYSICS VOLUME 16, NUMBER 9 SEPTEMBER, 1948

The Mercury Photosensitized Hydrogenation of Propylene*

WALTER J. MOORE
Department of Chemistry, Catholic University of America, Washington, D. C.
(Received May 24, 1948)

The mercury photosensitized hydrogenation of propylene has been investigated at 30°, 110°, and 200°, using an 8/1 ratio of hydrogen to propylene. The hydrocarbon products were analyzed with a mass spectrometer. The occurrence of 2,3-dimethylbutane as the principal C_6 product indicates that a hydrogen atom adds preferentially to the terminal carbon atom of propylene to form the isopropyl radical. Analyses of the C_6 and C_9 products suggests that the isopropyl radical adds preferentially to the middle carbon atom of propylene.

A CONVENIENT source of hydrogen atoms in low concentrations is provided by the reaction of excited mercury atoms with molecular hydrogen:

$$Hg(^1S_0)+h\nu(2537\text{ A.U.})=Hg(^3P_1)$$
$$Hg(^3P_1)+H_2=Hg(^1S_0)+2H.$$

If hydrogen atoms are produced in this way in a mixture of hydrogen and an olefin, the subsequent addition of a hydrogen atom to the olefinic double bond will yield an aliphatic free radical. For example:

$$H+C_2H_4=C_2H_5.$$

The reaction products from the mercury photosensitized hydrogenation at 25°C of ethylene, propylene, and butene-2 were analyzed by Moore and Taylor,[1] who found a considerable formation of the radical recombination products, butane, hexane, and octane, respectively. Thus,

$$2C_2H_5=C_4H_{10};\quad 2C_3H_7=C_6H_{14};\quad 2C_4H_9=C_8H_{18}.$$

These reactions were carried out with a high (about 8 to 1) ratio of hydrogen to olefin. This has the effect of minimizing photosensitized reactions of the olefins themselves, which might otherwise obscure the simple atomic hydrogen reactions. The quenching cross section of propylene is probably around ten times[2] that of hydrogen for $Hg(^3P_1)$. In the absence of hydrogen excited ethylene or propylene molecules are readily deactivated without undergoing chemical reaction.[3] It is probable, however, that some formation of hydrogen atoms and propyl radicals occurs through the reaction of excited propylene with molecular hydrogen:

$$C_3H_6^*+H_2=C_3H_7+H.$$

The quenching cross sections of the saturated hydrocarbons are much lower than those of the olefins. With the excess of hydrogen used it is therefore possible to study the hydrogenation reactions of the olefins without undue complications from the mercury photosensitized reactions of the hydrocarbon reactants and products.

The present work is a more extended investigation of the mercury photosensitized hydrogenation of propylene over a range of tempera-

* Presented at the 113th Meeting, American Chemical Society, Chicago, April 19, 1948.

[1] W. J. Moore and H. S. Taylor, J. Chem. Phys. **8**, 504 (1940).

[2] K. J. Laidler, J. Chem. Phys. **15**, 718 (1947).

[3] H. E. Gunning and E. W. R. Steacie, J. Chem. Phys. **14**, 57 (1946).

tures from 30° to 200°. The reaction products were analyzed by means of a mass spectrometer, so that the isomeric hydrocarbons could be identified precisely even with samples amounting to around 10 cc of vapor.

EXPERIMENTAL

Purified hydrogen and propylene were introduced into a cylindrical quartz reaction vessel, 40 mm in diameter and 40 cm long. Mercury vapor was provided by a pool of mercury maintained at 25°C in a short length of tubing at the bottom of the reaction vessel. The vessel was surrounded by a furnace, except for a narrow slit into which was fitted the ultraviolet lamp, a Hanovia SC-2537 mercury-resonance discharge tube providing an intense source of 2537 A.U. resonance radiation. Temperature was measured by means of a thermometer suspended inside the reaction vessel.

When the arc was turned on the photosensitized reaction proceeded very rapidly; it was followed by the accompanying fall in pressure. In a typical run at 30°C with 32 mm propylene and 249 mm hydrogen, the pressure fall amounted to a practically linear drop of 18 mm in 8 minutes, after which time there was no further decline in pressure. The arc was turned off about two minutes after the pressure fall ceased.

Then the products condensable at liquid nitrogen temperature (−195°C) were frozen out by repeated passage of the product gases back and forth through a chilled trap. The non-condensable gases, presumed to be almost entirely methane and residual hydrogen, were withdrawn with a Töpler pump. The hydrogen was burned on cupric oxide at 300°C, the water vapor condensed in a −78°C cold trap, and the residual gas recorded as methane. The fraction condensed at −195°C was analyzed by means of a Consolidated mass spectrometer. These analyses were provided through the kind cooperation of the mass spectrometer section of the National Bureau of Standards.

EXPERIMENTAL RESULTS

The course of the pressure-time curves is illustrated by the examples in Fig. 1. Not much kinetic information can be derived from these curves. They appear to indicate a constant reaction rate determined solely by the rate of production of hydrogen atoms.

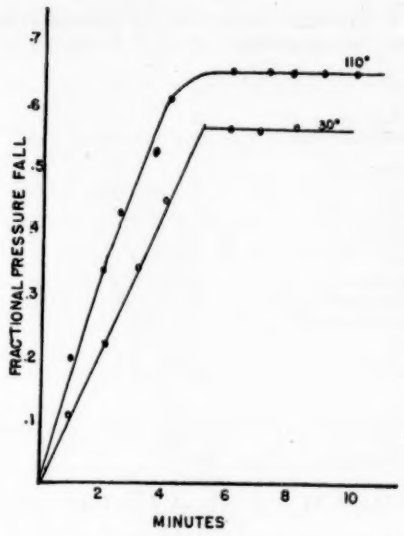

FIG. 1. Pressure-time curve.

It was found that some of the propylene remained unreacted at the end of the run, and the analytical results have been calculated on the basis of the portion of propylene that was consumed. These analyses are summarized in Table I.

It was not possible to identify exactly the nonane found. Mass spectrometer patterns for 15 out of the total of 35 different nonanes were compared with the unknowns. This inability to identify the C_9 component introduces a small uncertainty into the reported analyses, perhaps of the order of ±1 percent.

CONCLUSIONS AND DISCUSSION

A. The Addition of Hydrogen Atoms to Propylene

It is evident that, except for a trace of 2,2-dimethyl-butane, the only hexane formed in these reactions is 2,3-dimethylbutane (di-isopropyl). This fact leads to the conclusion that when a hydrogen atom adds to propylene it does so exclusively at the terminal carbon atom, yielding the isopropyl radical:

$$H+CH_3—CH=CH_2 = CH_3—CH—CH_3. \quad (1)$$

The addition to the middle carbon atom does not occur:

$$H+CH_3—CH=CH_2 = CH_3\cdot CH_2\cdot CH_2. \quad (2)$$

TABLE I. Products from mercury photosensitized hydrogenation of propylene with 8:1 hydrogen/propylene ratio.

Run No. Temperature, °C	1 30	2 30	3 110	4 200
Methane	6	6	17	32
Ethane	4	2	2	5
Propane	46	55	40	28
n-Butane	4	4	3	4
Butenes	2	0	4	5
Pentanes	1	1	3	6
2,3-Dimethylbutane	35	30	27	13
2,2-Dimethylbutane	1	—	1	1
Nonane	2	1	1	3

Two isopropyl radicals may then recombine to yield 2,3-dimethylbutane:

$$2(CH_3)_2CH\cdot = (CH_3)_2CH{-}CH(CH_3)_2. \quad (3)$$

An alternative mechanism for the formation of hexane is the addition of an isopropyl radical to propylene, followed by addition of a hydrogen atom to the hexyl radical so formed.

$$(CH_3)_2CH\cdot + CH_3{-}CH{=}CH_2 = (CH_3)_2CH{-}\underset{\displaystyle CH_3}{\underset{|}{CH}}{-}CH_2\cdot, \quad (4)$$

$$(+H) = (CH_3)_2CH{-}CH(CH_3)_2. \quad (5)$$

The product of these steps is again 2,3-dimethylbutane.

The failure to obtain any evidence for the occurrence of a normal propyl radical probably is due to a difference in the activation energies, E_2-E_1, for the addition of a hydrogen atom to the middle and the terminal carbon in propylene, since there is little reason to suppose that there is any considerable activation entropy difference. An estimate of the minimum value of E_2-E_1 can be obtained from the analytical data. Let us assume that at 110°, at which temperature 2,3-dimethyl butane constituted 27 percent of the products, not more than 1 percent of 2-methylpentane was formed. This is approximately equivalent to assuming that the rate of reaction (1) is 27 times that of reaction (2). It then follows that $E_2-E_1=\Delta E=2400$ calories.

It is interesting to note that Steacie, LeRoy, and Potvin[4] found no evidence for *n*-propyl in the cadmium photosensitized reaction of propane. It therefore appears that both in the addition of a hydrogen atom to propylene and in the removal of a hydrogen atom from propane, the sole product is the isopropyl radical, at least at temperatures up to around 300°C.

[4] E. W. R. Steacie, D. J. LeRoy, and R. Potvin, J. Chem. Phys. 9, 306 (1941).

B. Polymerization Reactions: The Addition of Isopropyl to Propylene

The occurrence of nonane among the reaction products can be explained by a polymerization process initiated by the addition of isopropyl to propylene. The following reaction sequence may be postulated:

$$(CH_3)_2CH\cdot + CH_3{-}CH{=}CH_2 \rightarrow CH_3{-}\underset{\displaystyle CH(CH_3)_2}{\underset{|}{CH}}{-}CH_2{-}, \quad (6)$$

$$CH_3{-}\underset{\displaystyle CH(CH_3)_2}{\underset{|}{CH}}{-}CH_2\cdot + CH_3{-}CH{=}CH_2 \rightarrow CH_3{-}\underset{\displaystyle CH(CH_3)_2}{\underset{|}{CH}}{-}CH_2\cdot CH_2\cdot \underset{\displaystyle CH(CH_3)_2}{\underset{|}{CH}}{-}CH_3, \quad (7)$$

(R_9)

$R_9+H\rightarrow$2,3-dimethylheptane.

If the hexyl radical formed in reaction (6) picked up a hydrogen atom, the product would be 2,3-dimethylbutane, which is the experimentally found hexane. It is expected that this mechanism for its formation would be almost as favorable as that involving the combination of two isopropyl radicals. Reaction (6) indicates that when isopropyl adds to propylene it does so preferentially at the central carbon atom. It therefore differs in this respect from the hydrogen atom which adds only at the terminal carbon atom. If isopropyl added at the terminal carbon, one would expect to find 2-methylpentane among the reaction products, but this is not in fact observed.

It was not possible to identify the nonane formed, for out of the 35 possible isomeric nonanes, only 15 were available as pure samples for matching the mass spectrometer patterns. Most of these 15 were highly branched isomers. Unfortunately 2,3-dimethylheptane was not available. The nonane 2,3,5-trimethylhexane was among those tested and its absence was indicated. This lends further support to the hypothesis that isopropyl adds to the central carbon of propylene, for addition to the terminal carbon fol-

lowed by combination of the hexyl radical so formed with an isopropyl would have yielded 2,3,5-trimethylhexane. More detailed analysis of the free radical polymerization mechanisms should be postponed until additional mass spectrometer data are available, but the possibility of working out definite reaction sequences from the observed isomeric constitution of the products appears quite promising.

C. Cracking Reactions

In this investigation the hydrogen atom concentration was considerably higher than that used in the earlier work of Moore and Taylor,[1] since a greater intensity of ultraviolet radiation was used. Therefore, cracking reactions occurred to a greater extent. This effect of an increased hydrogen atom concentration is shown very clearly in the study by Rabinowitch, Davis, and Winkler[5] of the reaction of propylene with hydrogen atoms produced by the discharge tube method. The products found in this case were methane, ethane, and propane. It is evident that high concentrations of atomic hydrogen favor cracking reactions such as the following:

$$H+C_3H_7=CH_3+C_2H_5. \quad (8)$$

It is probably less likely that cracking occurs according to:

$$H+C_3H_7=C_2H_4+CH_4. \quad (9)$$

[5] B. S. Rabinowitch, S. G. Davis, and C. A. Winkler, Can. J. Research **B21**, 251 (1943).

Once methyl and ethyl radicals are formed, the production of the observed methane, ethane, butane, and pentane is readily explained.

D. The Occurrence of 2,2-Dimethylbutane

The small amount of 2,2-dimethylbutane reported in the analysis is rather difficult to explain. Although other mechanisms might be devised to account for it, the following rather unusual reaction may be possible:

$$2(CH_3)_2CH=(CH_3)_3—C—CH_2—CH_3. \quad (10)$$

This involves a shift in the methyl group and may proceed through the intermediate formation of the tertiary butyl radical by a methyl-hydrogen atom disproportionation. On the other hand, the 2,2-dimethylbutane may be a secondary product arising from reaction of the primary saturated products with excited mercury, since irradiation was continued for several minutes after the cessation of the hydrogenation reactions. It would be preferable in future work of this kind to stop irradiation the moment the pressure fall ceases.

ACKNOWLEDGMENT

I wish to thank Mr. C. E. Wise, Mr. R. M. Reese and Miss Laura Williamson for the hydrocarbon analyses, Dr. Leo Wall for helpful discussions, and the American Philosophical Society for a grant used in the purchase of eqiupment.

THE JOURNAL OF CHEMICAL PHYSICS VOLUME 16, NUMBER 9 SEPTEMBER, 1948

The Magnetic Susceptibilities of Some Uranium (IV) Compounds

CLYDE A. HUTCHISON, JR. AND NORMAN ELLIOTT*
Institute for Nuclear Studies, University of Chicago, Chicago, Illinois
(Received May 27, 1948)

The magnetic susceptibilities of $U(SO_4)_2 \cdot 3.26H_2O$, $U(C_2O_4)_2 \cdot 5H_2O$ and $U(C_5H_7O_2)_4$ have been determined at a series of temperatures from the boiling point of liquid N_2 to 60°C. The Weiss-Curie law is obeyed at temperatures above 195°K. The data indicate the presence of two 5*f* electrons in the ground state. The susceptibility of $Th(C_5H_7O_2)_4$ at room temperature has also been determined.

INTRODUCTION

IT is now clear that somewhere near atomic number 90, 5*f* orbitals become prominent in the ground state electronic configurations of the atoms and ions of the elements. The calculations of Wu and Goudsmit,[1] followed by those of Mayer,[2] show that as one increases the atomic number the sum of the Fermi-Thomas and the centrifugal potentials for *f* electrons in a central field develops in addition to the usual hydrogen-like minimum at a radius of about 6A a second minimum at a few tenths of an A. This minimum is so deep by the time atomic number 58 is reached that 4*f* orbitals of low energy and relatively small radius are filled in the ground state configuration. It is certain that in the vicinity of atomic number 90 the inner minimum is so much deeper still that 5*f* electrons will occur in the ground state structures.**,[3]

Spectroscopic observations[4–7] have confirmed these calculations, particularly in the case of U.

On the other hand, reported magnetic studies[8–14] on U compounds have consistently indicated "spin only" moments and have been interpreted as indicating the presence of *d* electrons and quenching of the orbital angular momentum contribution to the magnetic moment.

For the case of the ion U^{+4}, if both the unpaired electrons are 5*f*, application of Hund's rules gives a $^3H_4$ ground state for Russell-Saunders coupling and a magnetic moment of 3.58 Bohr magnetons for a free gaseous ion with such a structure. *jj* coupling would result in a moment of 3.84 Bohr magnetons. In each case the figure given neglects contributions of excited electronic states to the moment. On the other hand, two 6*d* electrons would result in a LS ground state of configuration $^3F_2$ with a free gaseous ion moment of 1.63, or a *jj* coupling moment of 1.96 Bohr magnetons.

The "spin only" moment would be 2.83 Bohr magnetons, corresponding to just complete quenching of the orbital contribution to the moment.

Magnetic measurements are consequently of interest in connection with the problem of determining at what point in the periodic table 5*f* orbitals become prominent in the ground state configurations.

PREPARATION AND ANALYSIS OF COMPOUNDS

Uranium (IV) Sulfate

Merck's "Reagent" $UO_2(NO_3)_2 \cdot 6H_2O$ was converted to UO_3 by heating in an open evaporating dish in a muffle furnace at 450°C. On reduction of samples of this UO_3 to UO_2 with H_2 at 700°C the

* Now at Brookhaven National Laboratory, Associated Universities, Inc., Upton, Long Island, New York.

[1] Wu and Goudsmit, Phys. Rev. **43**, 496 (1933); Wu, *ibid.* **44**, 727 (1933).

[2] M. Goeppert Mayer, Phys. Rev. **60**, 184 (1941).

** These considerations are also in agreement with the older work of Sugiura and Urey (see reference 3) employing the old quantum theory.

[3] Sugiura and Urey, Kgl. Danske Vid. Sels. Math-fys. Medd. **7**, 13 (1926).

[4] Kiess, Humphreys and Laun, J. Res. Bur. Stands. **37**, 57 (1946).

[5] McNally, Harrison and Park, J. Opt. Soc. Am. **32**, 334 (1942).

[6] de Bruin, Schuurmans and Klinkenberg, Z. Physik. **121**, 667 (1943); *ibid.* **122**, 23 (1944).

[7] Schuurmans, Physica **11**, 419 (1946).

[8] Bose and Bhar, Z. Physik. **48**, 716 (1928).

[9] Sucksmith, Phil. Mag. [7] **14**, 1115 (1932).

[10] Henckel and Klemm, Zeits. Anorg Allg. Chem. **222**, 70 (1935).

[11] Tilk and Klemm, Zeits. Anorg Allg. Chem. **240**, 355 (1939).

[12] Haraldsen and Bakken, Naturwiss. **28**, 127 (1940).

[13] Bommer, Zeits. Anorg Allg. Chem. **247**, 249 (1941).

[14] Lawrence, J. Am. Chem. Soc. **56**, 776 (1934).

average value of the expression

$$\frac{\text{wt. of product}}{\text{wt. of initial sample}} \times \frac{\text{at. wt. U}}{\text{mole wt. } UO_2}$$

was found to be 82.91±0.38 percent as a result of four determinations. The theoretical value is 83.22. The 1947 International Atomic Weight of U, 238.07, is employed throughout this paper.

$U(SO_4)_2 \cdot 3.26H_2O$ was prepared from this UO_3 by the photochemical reduction of UO_2SO_4 prepared from it.[15] As an example of a typical procedure, 30 g of UO_3 was triturated with 35 ml of concentrated H_2SO_4. The UO_3 was added in small portions and the mixture was cooled by an ice bath. The mixture was dissolved in 200 ml of 95 percent C_2H_5OH, giving a clear solution, and irradiated 8 to 10 hours with a General Electric AH-6 mercury vapor lamp. The relatively insoluble $U(SO_4)_2$ was filtered, washed with C_2H_5OH, and dried in air at 80°C. The product was analyzed by ignition to U_3O_8 at 750°C. The average value of percent U so found was 48.72±0.15 percent. Gravimetric sulfate determinations gave 39.28±0.20 percent as the average percent sulfate. These values correspond to an average value of the mol ratio of SO_4 to U of 1.999. The mol ratio of H_2O to U is calculated from these data to be 3.26. Spectrographic analytical results are given in Table I.

TABLE I. Spectrographic analytical results: The parts per million by weight of various elements in samples of U_3O_8 prepared from the compounds studied were found by spectrographic analysis to be as shown.

Element	$U(SO_4)_2 \cdot 3.26H_2O$	$U(C_2O_4)_2 \cdot 5H_2O$	$U(C_5H_7O_2)_4$
Ag	2	2	<1
Al	<20	<20	<20
B	2	2	30
Ba	<2	<2	<2
Be	2	<1	<1
Ca	20	20	<20
Co	<5	<5	<5
Cr	<5	<5	<5
Cu	20	20	40
Fe	300	100	<5
K	<10	<10	<10
Li	<1	<1	<1
Mg	200	50	<1
Mn	20	<1	20
Na	200	<1	<1
Ni	<10		<10
Pb	400	100	10
Sb	<5	<5	<5
Si	200	200	400
Sn	10	10	20

Uranium (IV) Oxalate

$U(C_2O_4)_2 \cdot 5H_2O$ was precipitated from an aqueous solution of $U(SO_4)_2 \cdot 3.26H_2O$ prepared as described above by the addition of $(CO_2H)_2 \cdot 2H_2O$. There are two oxalates, a neutral and an acid salt.[16] The neutral salt, obtained by precipitation at elevated temperatures, was the one employed in our work.

20 g of $U(SO_4)_2 \cdot 3.26H_2O$ was dissolved in 300 ml of 0.1N H_2SO_4 and heated to 60°C in a nitrogen atmosphere. To this solution was added a solution of 20 g of $(CO_2H)_2 \cdot 2H_2O$ in 100 ml of H_2O. The mixture was then heated with stirring to 90°C and held at that temperature for 1 hour. The $U(C_2O_4)_2 \cdot 5H_2O$ which precipitated was filtered, washed with H_2O, C_2H_5OH, and $(C_2H_5)_2O$ and dried in vacuum at room temperature.

The product was analyzed for U by ignition to U_3O_8. Total oxidizing power of the product was determined by titration with ceric ion. The mol ratio of C_2O_4 to U was calculated from these two determinations. The total C and H_2O contents were determined by combustion. The results are summarized below.

Quantity	Found	Calculated for $U(C_2O_4)_2 \cdot 5H_2O$
Percent U	47.57±0.07%	47.22%
Mol ratio of C_2O_4 to U	2.004	2.000
Percent CO_2	35.44±0.06%	34.92%
Percent H_2O	17.77±0.07%	17.87%

Spectrographic analytical results are given in Table I.

Uranium (IV) Acetylacetonate

$U(C_5H_7O_2)_4$ was prepared from a 0.4N aqueous H_2SO_4 solution of $U(SO_4)_2 \cdot 3.26H_2O$ prepared as described above by adding excess $CH_3COCH_2COCH_3$ (Kahlbaum redistilled) and neutralizing the mixture with 2N KOH.

In a typical preparation 5 g of $U(SO_4)_2 \cdot 3.26H_2O$ was dissolved in 60 ml of 0.4N H_2SO_4. 10 ml of $CH_3COCH_2COCH_3$ was added to this solution. The solution was then slowly neutralized with 2N KOH (~50 ml was required). During the neutralization the solution was maintained at

[15] F. Gioliti and G. Liberi, Gazz. Chim. Ital. **36** II, 443 (1906).

[16] Gmelin, Handbuch der Anorganische Chemie, **55**, 166, 167 (1936).

~0°C and was protected from air oxidation by an atmosphere of N_2.

The precipitated $U(C_5H_7O_2)_4$ was filtered, washed with H_2O and dried in a vacuum desiccator at room temperature. The yield of this crude product was 92 percent of the theoretical value. The product was purified by dissolving in $(C_2H_5)_2O$ and recrystallizing at solid CO_2 temperature.

The product was analyzed for U by ignition to U_3O_8. C and H were determined by combustion. It was found necessary to dilute with N_2 the O_2 used in the combustion to prevent minor explosions of the $U(C_5H_7O_2)_4$ at ~200°C. The results are summarized below.

Quantity	Found	Calculated for $U(C_5H_7O_2)_4$
Percent U	37.31±0.03%	37.52%
Percent CO_2	135.4 ±0.3%	138.72%
Percent H_2O	38.8 ±0.5%	39.75%

In the case of another sample used analysis showed 37.48±0.05 percent U. Spectrographic analytical results are given in Table I.

TABLE II. Summary of measurements.

Compound	ρ, g cm^{-3}	Ammeter reading, amp[a]	Temperature °K	$\chi_{U^{+4}}$ ×10^6	$\chi_{U^{+4}}^{-1}$ molal
$U(SO_4)_2 \cdot 3.26H_2O$	1.504	4.00	328.1	14.72	285.4*
		4.00	318.7	15.11	278.0*
		4.00	297.5	15.92	263.9*
		4.00	273.9	16.83	249.6*
		4.00	239.5	18.47	227.4*
		2.78	74.8	37.45	112.2*
	1.465	4.00	294.2	16.17	259.7*
		4.00	238.7	18.60	225.8*
		4.00	195.4	21.51	195.3*
		4.00	75.4	38.46	109.2*
$U(C_2O_4)_2 \cdot 5H_2O$	0.877	5.17	295.6	15.96	263.2*
		5.17	239.6	18.15	231.4*
		2.78	195.2	20.39	206.0*
		2.78	74.6	25.91	162.1*
	0.840	5.17	296.8	15.80	265.8
		2.78	296.8	15.95	263.4
		5.17	239.2	18.08	232.3
		5.17	195.2	20.17	208.2
$U(C_5H_7O_2)_4$	0.725	8.83	328.3	12.59	333.7*
		8.83	298.1	13.51	310.9*
		8.83	297.4	13.56	309.8*
		8.83	273.9	14.37	292.3*
		8.83	239.5	15.79	266.0*
		8.83	237.9	15.89	264.3*
		8.83	221.0	16.78	250.3*
		8.83	195.2	18.29	229.7*
		8.83	76.0	33.97	123.7*
		5.17	74.2	34.37	122.2*
	0.727	8.83	294.4	13.89	302.4
		5.17	76.2	28.39	148.0
		2.78	76.0	37.17	113.0
	0.745	8.83	293.7	13.72	306.2
		5.17	293.7	13.70	306.6
		2.78	75.2	36.78	114.2
		5.17	75.2	36.07	116.5

[a] See section on magnetic measurements for approximate values of the field strengths corresponding to the tabulated ammeter readings.
* Employed in the construction of Figs. 1–3.

Thorium Acetylacetonate

$Th(C_5H_7O_2)_4$ was prepared and purified by a procedure similar to that described above for $U(C_5H_7O_2)_4$.

For example, 50 g of McKay $Th(SO_4)_2$ was added to a mixture of 500 ml of H_2O and 100 ml of 2N H_2SO_4. A 10 g residue remaining after standing overnight at room temperature was removed by filtration. 100 ml of redistilled Eastman $CH_3COCH_2COCH_3$ was added to the solution. The mixture was made slightly alkaline with 2N KOH. The precipitate was filtered, dried and purified by recrystallization from $(C_2H_5)_2O$ at solid CO_2 temperature.

The product was analyzed for Th by dissolving in 6N H_2SO_4 and fuming. The residue was ignited at 800–900°C. The average value of four determinations of Th was 37.20±0.10 percent. The theoretical value is 36.93 percent. The product was free of sulfate as indicated by the absence of any visible precipitate when $BaCl_2$ was added to a solution of the material in aqueous HCl. The product dissolved completely in C_2H_5OH indicating the absence of ThO_2 and $Th(OH)_4$.

Spectrographic analytical results are given in Table I.

MAGNETIC MEASUREMENTS

The Gouy method was employed for making the magnetic measurements. The apparatus used was similar to that employed by Freed.[17] The sample tube was made of Pyrex and evacuated below the partition. The sample tube was suspended in a Pyrex jacket through which dry N_2 or He was passed. The jacket was immersed in a Dewar flask which fitted between the pole pieces of a Weiss magnet and contained the fluid necessary for maintenance of constant temperature.

[17] Freed, J. Am. Chem. Soc. 52, 2702 (1930).

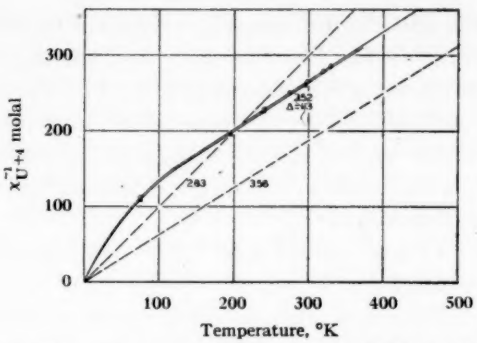

FIG. 1. $\chi^{-1}_{U^{+4}}$ molal *vs.* temperature for $U(SO_4)_2 \cdot 3.26H_2O$.

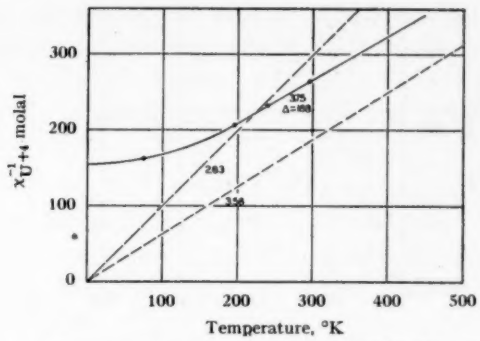

FIG. 2. $\chi^{-1}_{U^{+4}}$ molal *vs.* temperature for $U(C_2O_4)_2 \cdot 5H_2O$.

During the period over which weighings were being made the gas stream was stopped from flowing around the sample and passed through an upper section of the jacket only. This upper section was separated from the lower by a partition with a hole just large enough to allow passage of the suspension chain.

The current in the magnet was regulated through automatic thermionic control of the field of the generator supplying the magnet.

Measurements were made at the boiling point of N_2, at the triple point and boiling point of NH_3, at temperatures between these latter two, slightly above the ice point, at room temperature, and at temperatures somewhat above room temperature. Pumping on the liquid NH_3 was employed to produce temperatures down to its triple point. Circulating water was employed to maintain temperatures above the ice point.

Temperatures were measured by means of copper-constantan thermocouples, made from calibrated spools of wire, and were reliable to $\pm 0.1°$ at 0°C and $\pm 0.3°$ at the boiling point of N_2. Couples were located at several points along the jacket.

The sample tube had an inside mean cross-sectional area of 0.3229 cm² with a ~2 percent variation over the length of the tube, as determined by weighing cathetometrically measured lengths of H_2O at 25°C. The length of sample used was ~16 cm, the value being determined in each case by cathetometric measurements.

The tube was calibrated magnetically by weighing it filled with H_2O, $NiSO_4$ solution and $Fe(NH_4)_2(SO_4)_2 \cdot 6H_2O$. When the calibration of the tube with water was employed in calculating the gram susceptibility of Ni^{++} in a solution containing 0.03500 g Ni^{++} per g of solution (determined electrolytically and checked by $CH_3C(:NOH)C(:NOH)CH_3$ (dimethylglyoxime) precipitations) the value obtained was 75.13×10^{-6} at 26.4°C compared with the value 75.12×10^{-6} interpolated from the results of Nicolau.[18] In the calibrations and other measurements the measured magnetic forces were corrected for the force exerted on the tube which was found to be -0.000042 g when the upper half was filled with N_2. The values of Auer[19] for the susceptibility of H_2O were employed. Measurements of the magnetic force on the tube when filled with the Ni^{++} solution were made over the range of field strengths employed for the U salts. The molal susceptibility of a sample of $Fe(NH_4)_2(SO_4)_2 \cdot 6H_2O$ which contained 100.0 percent of the theoretical amount of Fe was calculated on the basis of weighings in the calibrated tube to be 0.01223 at 22.2°C. The value found by Jackson[20] was 0.01255 and by Onnes and Oosterhuis[20] was 0.01228 (~5° extrapolation from their tables of values).

In the case of the U salts the gram susceptibilities were calculated from the weighings of the U compound and of the standard substances by use of the following expression:

$$\chi_{U^{+4}} = \frac{1}{m_{U^{+4}}}\left\{\frac{1}{\rho_{UD_1D_2\cdots}}\left[\frac{F_{UD_1D_2\cdots\kappa_{Ni^{++}}}}{F_{Ni^{++}}} - \frac{6.48\times10^{-6}}{T}\right] - \chi_{D_1}m_{D_1} - \chi_{D_2}m_{D_2} - \cdots - \mu_{U^{+4}}m_{U^{+4}}\right\}$$

[18] Nicolau, Comptes rendus **205**, 557 (1937).
[19] E. C. Stoner, *Magnetism and Matter* (Methuen and Company, Ltd., London, 1934), p. 552.
[20] Jackson, Phil. Trans. Roy. Soc. London **A224**, 1 (1924).

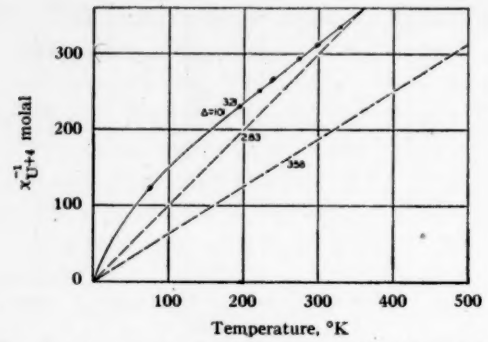

FIG. 3. $\chi^{-1}U^{+4}$ molal *vs.* temperature for $U(C_5H_7O_2)_4$.

where the meanings of the symbols are as follows:

χ	g susceptibility.
κ	cm³ susceptibility.
m_i	g *i*th constituent per g salt.
F_i	force on the substance, *i* (this is the force exerted by the magnetic field minus the force exerted on the empty sample tube).
$\mu_{U^{+4}}$	diamagnetic g susceptibility of U^{+4}.
ρ	density.
Ni^{++}	standard Ni^{++} solution.
$UD_1D_2\cdots$	U salt, the anions and water of crystallization being denoted by D_1, D_2, $\cdots$.

The second term in the square brackets is a correction for the air mixed with the sample in the tube.

$$(6.48\times10^{-6})/T=(1-(\rho/\rho'))\frac{0.029\times298\times10^{-6}}{T}$$

when $\rho=0.25\rho'$, ρ' is the theoretical crystalline density, and 0.029×10^{-6} is the cm³ susceptibility of air at 298°K and 1 atm. The value of $\kappa_{Ni^{++}}$ as calculated from the measurements previously described is 2.138×10^{-6} at 26.4°C. The values used for $F_{Ni^{++}}$ were either directly measured as previously described at the same magnet current as used for the measurement of $F_{UD_1D_2}$..., or calculated from a directly measured value using measurements on $Fe(NH_4)_2(SO_4)_2\cdot6H_2O$ made at the same magnet currents. (Small temperature corrections were applied to the results of these standard weighings to bring them all to the weight that would be exerted at 26.4°C and these latter values were used in the calculations.) The densities were calculated from the area and length measurements made as previously described, and the difference in weights of the filled and empty tube. The $F_{UD_1D_2}$... were the directly measured changes in weight produced by the field after correction for the tube effect mentioned above. The χ_D and $\mu_{U^{+4}}$ were obtained as follows:

(a) $\chi_{SO_4^-}$ and $\mu_{U^{+4}}$ were calculated by the method of Angus.[21]

The values -0.482×10^{-6} and -0.122×10^{-6} were obtained:

(b) $\chi_{C_2O_4^-}$ was taken as equal to the measured value for $H_2C_2O_4$ as determined by Selwood.[22] The value is -0.6×10^{-6}. χ_{H_2O} was taken as -0.722×10^{-6} based on the measurements of Auer.[19] $\chi_{C_5H_7O_2^-}$ was taken as equal to the measured value for $Th(C_5H_7O_2)_4$ described in this paper corrected for the value of $\chi_{Th^{+4}}$ as calculated by the method of Angus[21] (-0.112×10^{-6}). The value obtained is -0.499×10^{-6}.

The m_i were calculated as follows:

(a) $m_{U^{+4}}$ was taken as equal to the average results of chemical analysis;

(b) all other m_i with the exception of m_{H_2O} were calculated from the $m_{U^{+4}}$ assuming the theoretical composition of the salts;

(c) m_{H_2O} was calculated assuming it to be equal to the difference between 1 and the sum of (a) and (b) above.

The forces exerted on the U salts were in general in the vicinity of 0.1 or 0.2 g. The approximate values of the field for various magnet currents as determined from tube geometry and measured forces on standard substances, and checked by fluxmeter measurements, were 1.24, 1.09, 0.84, 0.66 and 0.46 in units of 10^4 oersted for ammeter readings of 8.83, 7.15, 5.17, 4.00 and 2.78 amperes respectively.

RESULTS

The results of the measurements made on the three compounds $U(SO_4)_2\cdot3.26H_2O$, $U(C_2O_4)_2\cdot5H_2O$ and $U(C_5H_7O_2)_4$, are summarized in Table II. The variations in density are the result of repacking the tube with different samples of powder. The values of $\chi_{U^{+4}}$, the g susceptibilities, were calculated as previously described. Values of the quantity $(\chi_{U^{+4}}\times238.07)^{-1}$ are entered in the column headed $\chi^{-1}U^{+4}$ molal.

[21] W. R. Angus, Proc. Roy. Soc. London **A136**, 569 (1932).
[22] P. W. Selwood, J. Am. Chem. Soc. **55**, 3161 (1933).

The values of $\chi^{-1}{}_{U^{+4}\ molal}$ were plotted against the entries in the temperature column on a scale of 4 units per cm for each quantity. For measurements made above 195.0°K the sets of points corresponding to each separate packing of the tube were found to lie on straight lines. A best straight line was drawn through each such set of points and for a given compound these lines were found to differ only by a small displacement along the χ^{-1} axis. See Fig. 1 for an example.

Figures 1, 2, and 3 show such plots for points marked with an asterisk in Table II. At liquid N_2 temperatures the deviation from straight line behavior is marked. The extrapolation to the axis is made quite arbitrarily. In each figure the Curie law behavior for a moment of 3.58 Bohr magnetons and for 2.83 Bohr magnetons is shown using broken lines.

The Weiss-Curie law

$$\chi_{molal} = C/(T+\Delta)$$

is obeyed above 195.0°K by all three compounds. The value of Δ was calculated in each case by means of the expression

$$\Delta = \frac{\chi_{300}{}^{-1}}{S} - 300$$

where $\chi_{300}{}^{-1}$ is the value of the ordinate at 300°K and S is the slope of the best straight line through the experimental points above 195.0°K as determined graphically. Only those points plotted in the figures were employed for the calculation of Δ. In the case of Fig. 1 the upper line was employed.

Values of the quantity,

$$[(3k/\beta^2 N)S^{-1}]^{\frac{1}{2}} = (7.997/\text{slope})^{\frac{1}{2}}$$

where k is the Boltzmann constant, β the Bohr magneton and N the Avogadro number, were calculated and are listed in each figure near the solid line through the experimental points.

The susceptibility of $Th(C_5H_7O_2)_4$ was measured for the purpose of determining whether or not the chelated groups made any abnormal contribution to the diamagnetic corrections to be applied in the case of such compounds. The measured value of $\chi_{Th(C_5H_7O_2)_4}$ at 296.3°K was -0.356×10^{-6}. The molal susceptibility is -223.6×10^{-6}. The calculated molal susceptibility employing the set of values of atomic susceptibilities listed by Angus and Farquharson,[23] and a value of the molal susceptibility of Th^{+4} calculated by the method of Angus (-25.9×10^{-6}) is -227.1×10^{-6}, in good agreement with our measured value.

DISCUSSION

The Weiss-Curie law is very closely obeyed at temperatures above 195.0°K. If one attaches to the constant C (see previous section) the significance

$$C = \mu^2\beta^2 N/3k$$

where μ is the magnetic moment in units of Bohr magnetons and the other symbols have the meanings previously given, then our data lead to values of

$$\mu = (3kC/\beta^2 N)^{\frac{1}{2}} = (7.997/S)^{\frac{1}{2}}$$

which are interpretable only on the assumption of the existence of two $5f$ electrons in the ground state. In fact for the compounds $U(SO_4)_2\cdot 3.26H_2O$ and $U(C_2O_4)_2\cdot 5H_2O$ the values of μ obtained are 3.52 and 3.75 respectively. These are in agreement with the values 3.58 or 3.84 which one calculates for a free gaseous ion in the LS state, $^3H_4$, or for a ground state involving two $5f$ electrons in a jj coupling scheme respectively. In the case of the $U(C_5H_7O_2)_4$ the value obtained for μ is much too high to be accounted for by ground states containing no f electrons.

On the other hand, the values of Δ obtained are very large relative to those found, for instance, in the case of rare earth compounds, indicating large interactions of some kind. Consequently, the meaning of the Weiss-Curie law in such cases may not be too clear and it may be regarded as somewhat remarkable that values in such close agreement with the theory for free gaseous ions are obtained. In any case, the susceptibility values are such as to indicate clearly the existence of $5f$ electrons in the ground state configurations.

At low temperatures the departures from the Weiss-Curie law are relatively large. It should be noted that these anomalies are (on the basis of the single points obtained) in the case of the oxalate, of the same sort as have been observed in the case of the hydrated sulfate of the analogous rare earth element Pr(III) which has two $4f$ electrons. The departure from the Weiss-Curie

[23] Angus and Farquharson, Proc. Roy. Soc. **A136**, 580 (1932).

law in the other two cases is in the opposite direction, as has been observed for the anhydrous sulfate of Pr.[24]

The disagreements of our data on the sulfate with those obtained by Sucksmith[9] should be pointed out.

[24] See reference 19, pp. 306–309.

ACKNOWLEDGMENTS

The authors express their thanks to L. S. Myers Jr. for the preparation of the $Th(C_5H_7O_2)_4$ and one of the samples of $U(C_5H_7O_2)_4$ used in the experiments and to the Argonne National Laboratory, Division of Chemistry, for the spectrographic chemical analyses.

THE JOURNAL OF CHEMICAL PHYSICS VOLUME 16, NUMBER 9 SEPTEMBER, 1948

A Further Investigation of the Mercury Photosensitized Polymerization of Propylene

H. E. GUNNING* AND E. W. R. STEACIE
Division of Chemistry, National Research Laboratories, Ottawa, Canada

(Received June 10, 1948)

A reinvestigation has been made of the authors' earlier work on the reaction of propylene with mercury ($^3P_1$) atoms at 30°C in a static system, with special concentration on the products of the reaction.

The mechanism

$$C_3H_6+Hg(^3P_1)\rightarrow C_3H_6^*+Hg(^1S_0)$$
$$C_3H_6^*+C_3H_6\rightarrow 2C_3H_6$$
$$C_3H_6^*\rightarrow C_3H_5+H$$

which was proposed in the earlier work has been confirmed. Some twenty-two different products were identified at low pressures, all of which, with the exception of acetylene, can be explained as the result of interactions of the free radicals present.

The quantum yield of the reaction reaches a maximum of 0.18 at 6.5 mm, and falls to 0.04 at 72 mm.

INTRODUCTION

IN an earlier publication,[1] the authors came to the conclusion that propylene reacted with mercury ($^3P_1$) atoms at 30°C by an activated molecule mechanism according to the sequence:

$$C_3H_6+Hg(^3P_1)\rightarrow C_3H_6^*+Hg(^1S_0) \quad (1)$$

$$C_3H_6^*+C_3H_6\rightarrow 2C_3H_6 \quad (2)$$

$$C_3H_6^*\rightarrow C_3H_5+H \quad (3)$$

followed by polymerization reactions of the type

$$C_3H_5+C_3H_6\rightarrow C_6H_{11}. \quad (4)$$

In the investigation reported below, the previous work has been repeated, and a much more detailed analysis of the products of the reaction has been made.

EXPERIMENTAL

A general description of the apparatus and experimental technique has already been given in a previous publication.[2]

The measurements were made in a static system at 30.00±0.01°C. The cylindrical quartz cell had a volume of 240 cc. The total volume of the system was 1050 cc.

The analyses of the condensible products of the reaction were made on a mass spectrometer through arrangement with the National Bureau of Standards. The sampling technique employed, as well as the method of analysis of the products, non-condensible in liquid air, have been previously described.[3]

The propylene used was obtained from the Ohio Chemical and Manufacturing Company.

* Department of Chemistry, University of Rochester, Rochester, N. Y.

[1] H. E. Gunning and E. W. R. Steacie, J. Chem. Phys. **14**, 57 (1946).

[2] H. E. Gunning and E. W. R. Steacie, J. Chem. Phys. **12**, 484 (1944).

[3] H. E. Gunning and E. W. R. Steacie, J. Chem. Phys. **14**, 544 (1946).

TABLE I. Composition of original propylene.

Component	Mole percent
Propylene	99.6
Propane	0.1
Butenes	0.15
Methyl pentenes	0.02
Dimethyl butanes	0.08
Trimethyl butanes	0.03

After several trap-to-trap distillations, the middle fraction was collected and stored in a two-liter flask provided with a Warrick-Fugassi valve.[4] The composition of the propylene used, as determined on the mass spectrometer is shown in Table I.

RESULTS

In the present investigation the linearity of the pressure *vs.* time curves, which we had found previously,[1] was confirmed. The pressure rates are given in Table II and Fig. 1 together with the actual rates of consumption of propylene. By referring to Fig. 1, it can be seen that, at higher pressures, polymerization is practically the only reaction occurring. The rapid decrease in the rate of propylene consumption with increasing pressure in the complete quenching region is compelling evidence in favor of collisional deactivation. The maximum rate of consumption of propylene seems to occur at an initial pressure of 6.5 mm. In our previous publication[1] this maximum occurred at about 9 mm and since the same source and electrical characteristics were used in both series of measurements, the difference must be attributed to experimental error.

The products of the reaction are shown in Table III. It is interesting, first of all, to note that the rate of formation of hydrogen is five times greater than that of methane, in the complete quenching region. This is in complete agreement with our earlier work.[1] The enormous number of products formed at low initial pressures serves to show very pointedly the tremendous complexity of free radical reactions in hydrocarbons. The over-all reaction becomes considerably simpler at higher pressures, where the interactions of free radicals with each other become less important than the disappearance of these radicals in the propagation of polymer chains. The data presented in Table III are to be regarded only as rough semi-quantitative indications of the minor products of the reaction.

[4] E. Warrick and P. Fugassi, Ind. Eng. Chem. (Anal. Ed.) **15**, 13 (1943).

TABLE II.

P_0 mm	$-\Delta P/\Delta t$ mm/min. $\times 10^2$	$-d(C_3H_6)/dt$ mm/min. $\times 10^2$	$-d(C_3H_6)/dt$ moles/min. $\times 10^6$	φ (Propylene)
1.70	1.62	1.93	1.08	0.10_8
3.83	2.18	2.90	1.61	0.16_1
6.32	2.40	3.23	1.80	0.18_0
9.67	2.18	2.82	1.57	0.15_7
20.4_9	1.87	2.18	1.22	0.12_2
33.4_9	1.70	1.90	1.06	0.10_6
39.7_1	1.67			
53.2_5	1.33			
59.8_7	1.07	1.03	0.58	0.05_8
72.2_6	0.68	0.70	0.39	0.03_9

The C_2 hydrocarbon which we found in our earlier work[1] to correspond by combustion analysis to C_2H_4, was apparently, from Table III, a roughly equimolar mixture of acetylene and ethane. It is also evident from Table III that the liquid which we isolated in our earlier runs must be a complex mixture of saturated and unsaturated hydrocarbons in the C_5 to C_8 range.

The polymer formed in the reaction has already been adequately described.[1]

QUANTUM YIELD

The incident light intensity was determined indirectly by filling the cell with ethylene, at an initial pressure of 13 mm, and determining the initial rate of formation of hydrogen. The hydrogen was determined by oxidation over copper oxide at 250°C. The average of eight runs gave $dH_2/dt = 2.5 \pm 0.1 \times 10^{-6}$ moles/min. Allen and

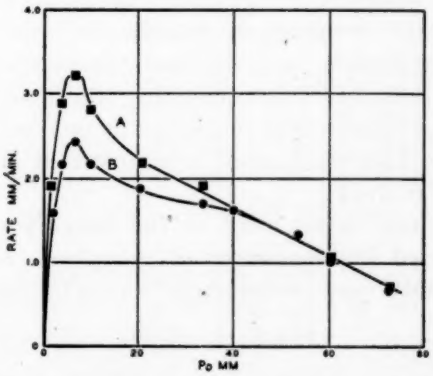

FIG. 1. Squares: rate of consumption of propylene *vs.* initial pressure. Circles: rate of pressure decrease *vs.* initial pressure.

TABLE III. The products of the reaction.

Initial pressure mm Product	1.70	3.83	6.32	9.67	20.4	33.4	53.2	59.8	72.2
	All rates are in moles per minute $\times 10^8$.								
Hydrogen	0.015	0.056	0.066	0.060	0.044	0.031	0.027	0.021	0.020
Methane	0.056	0.040	0.031	0.019	0.011	0.006	0.005	0.004	0.004
Acetylene	0.005	0.022	0.041	0.031					
Ethane	0.016	0.013	0.009	0.015					
Propane	0.044	0.091	0.076	0.052	0.018				
Butenes		0.020	0.041	0.040	0.043	0.043	0.020	0.018	0.033
Butanes	0.010	0.047	0.050	0.031					
Pentadienes		0.005	0.014						
Pentenes	0.005	0.025	0.050	0.015					
Pentanes	0.011								
Benzene		0.001							
Cyclohexadienes			0.003						
Hexadienes		0.006	0.040	0.022	0.018				
Methyl Pentadienes				0.005					
Methyl Pentenes	0.003	0.024	0.067	0.029	0.010	0.020			
Dimethyl Butanes	0.004	0.022	0.059	0.031	0.001				
Heptynes	0.001			0.007					
Trimethyl Butanes	0.006			0.013	0.006	0.008			
Dimethyl Pentanes		0.022	0.035						
Ethyl Cyclohexenes		0.001	0.003						
Ethyl Cyclohexanes		0.002	0.004						
Trimethyl Pentenes	0.001			0.004					

Gunning[5] have recently shown that the initial quantum yield of hydrogen formation in the ethylene reaction is 0.25. And therefore, $I_{abs}=1.0\times10^{-5}$ einsteins/min. The quantum yields of propylene disappearance for each run are shown in the last column of Table II. In our previous work[1] we found that $\varphi_{C_3H_6}=0.15\pm0.05$ at 14 mm. On the basis of our present data $\varphi_{C_3H_6}=0.14$ at 14 mm, in agreement, within experimental error, with our earlier value. The effect of collisional deactivation is strikingly evident in the fact that the quantum yield decreases from its maximum value of 0.18 at 6.5 mm to 0.04 at 72 mm.

DISCUSSION

The results of the present investigation seem to show fairly conclusively that the activated molecule mechanism, proposed in our previous publication,[1] describes very adequately the kinetics of the decomposition of propylene by mercury ($^3P_1$) atoms. This mechanism is summarized in reactions (1) to (4).

In some recent work on the mercury photosensitized hydrogenation of propylene, Moore[6] has shown very convincingly that in the reaction

$$H+C_3H_6\rightarrow C_3H_7 \qquad (5)$$

the radical formed is isopropyl, since he found that di-isopropyl was the only important hexane formed. Our results tend to confirm Moore's findings, in view of the fact that dimethyl butane is the only hexane found in our products. Of course, in our case dimethyl butane is only an important product at low pressures where radical recombination would assume a significant role in the reaction.

It would seem unwise, without more extensive data, to attempt to write reactions to account for the large number of products found at lower pressures. It is important to note, however, that, with the exception of acetylene, all the significant products found at lower pressures could quite naturally arise by the interaction of the free radicals already postulated in reactions (3) to (5), together with methyl and ethyl radicals formed by an "atomic cracking" reaction of the type

$$C_3H_7+H\rightarrow C_2H_5+CH_3. \qquad (6)$$

The marked rise in the rate of formation of methane at very low pressures, as recorded in Table III suggests that the reaction

$$H+CH_3\rightarrow CH_4 \qquad (7)$$

might be occurring to a major extent under these conditions at the wall. As a matter of fact it is quite possible that the wall plays a very important part as a third body for radical recombi-

[5] G. A. Allen and H. E. Gunning, J. Chem. Phys., in press.

[6] W. J. Moore, paper presented at the Chicago meeting of the American Chemical Society, April, 1948.

nation in the formation of many of the products found at low pressures.

CONCLUSIONS

The investigations which the authors have made on the alkyl-substituted alkenes and alkadienes[1,3,7] offer fairly unequivocal evidence for the initial formation of an activated molecule by the reaction

$$RH+Hg(^3P_1)\rightarrow RH^*+Hg(^1S_0). \quad (8)$$

The low quantum yields of the reaction, together with the decreasing rate with increasing pressure follow from the collisional deactivation of the activated molecule formed in (8) by

$$RH^*+RH\rightarrow 2RH. \quad (9)$$

Reaction (9) is somewhat different in the case of butene-1,[7] owing to its ease of isomerization to butene-2, with the result that in butene-1, collisional deactivation seems to proceed in the main by

$$1-C_4H_8^*+1-C_4H_8\rightarrow 2-C_4H_8+1-C_4H_8. \quad (10)$$

On the basis of the authors' work[3] isobutene seems to be excluded from this generalization, since the evidence for activated molecule formation with isobutene was by no means compelling. However, recently the isobutene reaction has been reinvestigated by Allen and Gunning[5] up to initial pressures of 250 mm. The results of this investigation definitely bring isobutene into line with the other alkyl-substituted olefins, which react with mercury ($^3P_1$) atoms by reactions (8) and (9).

The actual chemical reaction in these compounds results from the unimolecular decomposition of the activated hydrocarbon molecule formed in (8), by the reaction

$$RH^*\rightarrow R+H \quad (11)$$

as we pointed out in our previous paper on propylene,[1] this bond split would likely occur at one of the C−H bonds in a position once-removed from the double bond. Polymerization would then proceed by the successive addition of olefin molecules to the radicals generated in (11).

Laidler[8] has recently discussed the electronic configuration of activated molecules of the type postulated in reaction (8). He has suggested that the Wigner Spin Conservation Principle may apply to collisions between photo-excited atoms and molecules. And since the mercury atom in reaction (8) undergoes a triplet-to-singlet transition in reverting to the ground state, the hydrocarbon, which is normally in a singlet state, must be in a triplet state after collision with the mercury ($^3P_1$) atom, in order that spin angular momentum be conserved in the over-all process. Laidler's explanation of the large quenching cross sections of the unsaturated hydrocarbons in comparison with the alkanes, and of the tendency in the former to form activated molecules, derives its strength from its plausibility, rather than from any direct evidence for the existence of such triplet states in hydrocarbons. However, Lewis and Kasha,[9] on the basis of their phosphorescence studies, have concluded that there is a triplet state in ethylene at 72–74 kcal. above the ground (singlet) state. Theoretical calculations of the singlet-triplet separation in ethylene were made by Hartmann[10] who obtained the rather low value of 70 kcal. Craig[11] has recently repeated Hartmann's calculation and obtained a value of 95 kcal. or greater. Now the transition $Hg(6^3P_1)\rightarrow Hg(6^1S_0)$ in reaction (8) corresponds to a transfer of 112 kcal. per mole to the hydrocarbon molecule, and if Craig's calculation is correct, it is quite possible that the resonance for the energy exchange in reaction (8) might be very satisfactory, leaving only a small amount of residual energy to be imparted to the vibrational degrees of freedom of the hydrocarbon molecule.

ACKNOWLEDGMENT

The authors would like to express their gratitude to Dr. Fred L. Mohler of the Mass Spectrometry Section of the National Bureau of Standards for his kindness in performing the mass spectrometric analyses reported in this paper.

Our thanks are also due to Mr. Yves Lupien for assistance in performing some of the measurements.

[7] H. E. Gunning and E. W. R. Steacie, J. Chem. Phys. 14, 581 (1946).
[8] K. J. Laidler, J. Chem. Phys. 15, 712 (1947).
[9] G. N. Lewis and M. Kasha, J. Am. Chem. Soc. 66, 2100 (1944).
[10] H. Hartmann, Zeits. f. physik. Chemie **B53**, 96 (1943).
[11] D. P. Craig, J. Chem. Phys. 16, 158 (1948).

Letter to the Editor

THIS section will accept reports of new work, provided these are terse and contain few figures, and especially few halftone cuts. The Editorial Board will not hold itself responsible for opinions expressed by the correspondents. Contributions to this section should not exceed 600 words in length and must reach the office of the Managing Editor not later than the first of the month preceding that of the issue in which the letter is to appear. No proof will be sent to the authors. The usual publication charge ($4.00 per page) will not be made and no reprints will be furnished free.

Dipole Moments and Internal Rotation in Some Substituted Hydrocarbons

RICHARD A. ORIANI AND CHARLES P. SMYTH
Frick Chemical Laboratory, Princeton University, Princeton, New Jersey
July 9, 1948

IT has long been recognized that one of the best methods of studying internal rotation is by means of the variation of dipole moments with temperature. However, this is applicable only to molecules having dipoles on each of the internally rotating groups; moreover, for vapor measurements, the compounds must be stable over relatively large ranges of temperature. Solution measurements of dipole moment *vs.* temperature are of interest and have been carried out,[1] but the evaluation of the internal rotation is vitiated by our lack of knowledge as to the effect of the solvent on the measured dipole moment.

The dipole moment method applied to such molecules in the vapor state is unique among means of investigating internal rotation in that it yields an isolated quantity which is a direct function of the rotation. This is in contrast to the thermodynamic method, the results of which depend on the small difference between two large numbers, and to the method of electron diffraction, in which the resulting pattern is a function of much more than the parameters pertaining to the internal rotation. Since only relatively little experimental data on vapor measurements of moment *vs.* temperature exist in the literature,[2] it was considered worth while to investigate other cases of interest with respect to internal rotation.

TABLE I.

Molecule	Temp. range, °C	Moment $\times 10^{18}$	V_0 cal./mole
1,2-dichloropropane	70–235	1.45–1.68	2500
2,3-dichloropropene	125–245	1.74–1.77	2075
1,1,2-trichloroethane*	105–258	1.45–1.47	2820
1,3-dichloropropene			
104° isomer	120–208	1.78	—
112° isomer	120–230	1.81	—
1,4-dichlorobutane	160–235	2.22	—

* This compound displays a flat though definite minimum of 1.40 at 170°.

Table I presents a brief resume of our measurements to date. By far the most interesting result is that for 1,1,2-trichloroethane, for which the moment first decreases then increases with temperature; this behavior is in qualitative agreement with the electron diffraction results of Turkevich and Beach.[3] As a preliminary analysis, the potential energy barrier V_0 has been calculated for several of the compounds by the method of Beach and Stevenson,[4] who apply the function

$$V(\varphi) = (V_0/2)(1-\cos\varphi)$$

to the internal rotation; in these calculations we have used 1.85 as the group moment of CH_2Cl.

A complete description and fuller analysis is in process of preparation.

[1] Smyth, Dornte, and Wilson, J. Am. Chem. Soc. **53**, 4242 (1931); C. P. Smyth and W. S. Walls, J. Chem. Phys. **1**, 200 (1933); Penney and Sutherland, Trans. Faraday Soc. **30**, 898 (1934); Hampson and Weissberger, J. Am. Chem. Soc. **58**, 2111 (1936); G. L. Lewis and C. P. Smyth, J. Chem. Phys. **7**, 1085 (1939); Mizushima, Morino, Miyahara, Tomura, and Okamoto, Sci. Pap. Inst. Phys. & Chem. Research No. 1088, **39**, 387 (1942).

[2] C. T. Zahn, Phys. Rev. **40**, 291 (1932); **38**, 521 (1931); E. W. Greene and J. W. Williams, Phys. Rev. **42**, 119 (1932); Smyth and McAlpine, J. Am. Chem. Soc. **57**, 979 (1935); R. H. Wiswall and C. P. Smyth, J. Chem. Phys. **9**, 356 (1941); Maryott, Nobbs, and Gross, J. Am. Chem. Soc. **63**, 659 (1941); Watanabe, Mizushima, and Morino, Sci. Pap. Inst. Phys. & Chem. Research No. 1090, **39**, 401 (1942).

[3] Turkevich and Beach, J. Am. Chem. Soc. **61**, 3127 (1939).

[4] J. Y. Beach and D. F. Stevenson, J. Chem. Phys. **6**, 635 (1938).